

**Synthesis and characterization of Tellurium oxide
glasses for photonic applications**

*Thesis submitted to
Cochin University of Science and Technology
In partial fulfillment of the requirements for the degree of
Doctor of Philosophy*

By

Rose Leena Thomas



**International School of Photonics
Cochin University of Science and Technology
Cochin-682022, Kerala, India.**

April 2013

Synthesis and characterization of Tellurium oxide glasses for photonic applications

Ph D Thesis in the field of Photonics

Author

Rose Leena Thomas

Research Fellow

International School of Photonics,

Cochin University of Science and Technology,

Cochin – 682 022, India.

Email: roseleenat@gmail.com

Research Advisor

Dr. Sheenu Thomas

Assistant Professor

Cochin University College of Engineering Kuttanad

Cochin University of Science & Technology

Cochin -682022, Kerala, India

Ph: + 91 9349405537

sheenuthomas29@gmail.com, st @cusat.ac.in

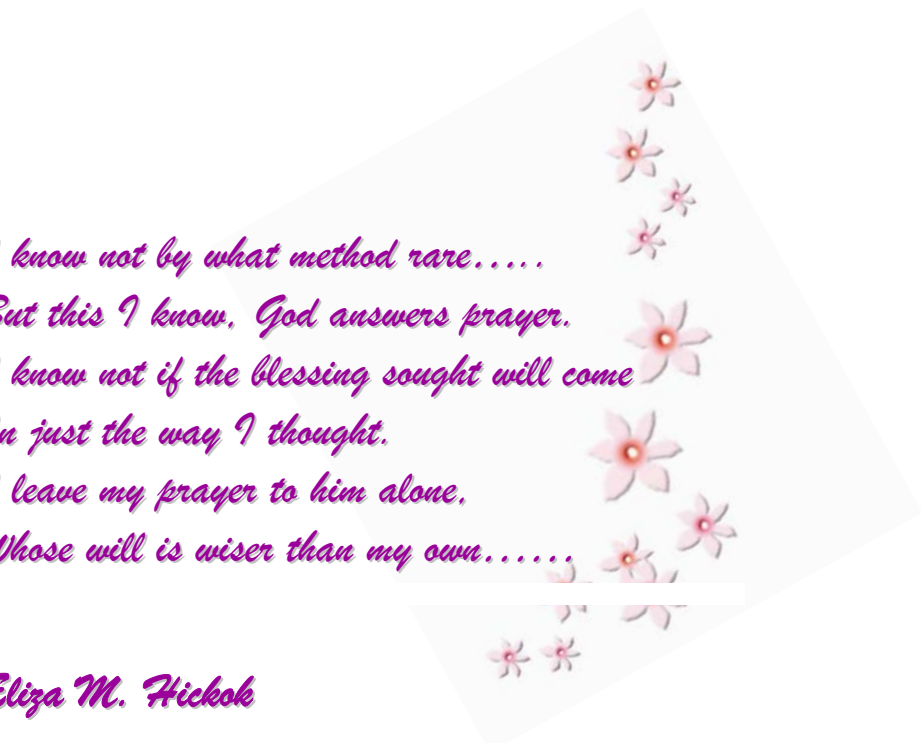
International School of Photonics

Cochin University of Science & Technology

Cochin – 682 022, INDIA

www.photonics.cusat.edu

April 2013



*I know not by what method rare.....
But this I know, God answers prayer.
I know not if the blessing sought will come
In just the way I thought.
I leave my prayer to him alone,
Whose will is wiser than my own.....*

Eliza M. Hickok

*Dedicated to my loving husband
and children...*



Dr. Sheenu Thomas

Assistant Professor

Cochin University College of Engineering Kuttanad

Cochin University of Science & Technology

Cochin -682022, Kerala, India

Phone: Ph: + 91 9349405537

Email: sheenuthomas29@gmail.com, st@cusat.ac.in

Certificate

Certified that the research work proposed in the thesis entitled **“Synthesis and characterization of Tellurium oxide glasses for photonic applications”** is based on the original work done by Mrs. **Rose Leena Thomas** under my guidance at International School of Photonics, Cochin University of Science and Technology, Cochin, India and has not been included in any other thesis submitted previously for the award of any degree.

Cochin-22

Dr. Sheenu Thomas
(Supervising guide)

Declaration

I hereby declare that the work presented in this thesis entitled “**Synthesis and characterization of Tellurium oxide glasses for photonic applications**” is based on the original research work done by me under the supervision of **Dr. Sheenu Thomas**, Assistant Professor, Cochin University College of Engineering Kuttanad, Cochin University of Science and Technology, Cochin, India and has not been included in any other thesis submitted previously for the award of any degree.

Cochin-22

Rose Leena Thomas

Acknowledgements

Glory to GOD the almighty, who provided me with such a superb opportunity. He protected me with good health and intellectual ability and patience althrough, providing favorable circumstances, guiding me towards accomplishing this research work,

It is my proud privilege to express a deep concern at gratitude to my guide Dr. Sheenu Thomas for her inspiration, sustained encouragement, constructive criticisms, concrete suggestions and profound guidance in the course of this dissertation.

It gives me immense pleasure to express my deep sense of gratitude to Prof. VPN Nampoori, ISP CUSAT for his judicious guidance and attention amidst of his numerous activities during the course of this study.

I would like to express my sincere gratitude to Prof. P Radhakrishnan, for all his valuable comments and evaluation at every stage of the thesis. I am very thankful to Prof. C P Girija Vallabhan, Prof. Nandakumaran and Dr. Kailasnath for their apt advices and support.

I am very thankful to Annie teacher, Reethama teacher, Priyamvada teacher and other teaching and non teaching staff for their timely help.

I am much grateful to the teachers and friends at Dept. of Instrumentation, CUSAT, to let me use the furnace, to prepare glass samples used for my study.

I would gteatefully acknowledge the financial support of the University Grants Commission, through RFSMS and DST.

I express my sincere thanks to Dr. Geetha and Dr. Sony for their advices and earnest desire to keep me on track. Special thanks go to Subin, Dr. Anu, Nisha, Misha, Libish sir, Bejoy, Bobby sir, Dr. Nithyaja, Mathew, Rajeena, Sreeja.S, Pradeep, Rejimol and Saritha, for their liberal help whenever I was in need. The cheerful company given by my friends Dr. Lyjo, Dr. Manu, Dr. Rajesh, Dr. Santhi, Thomas Chettan, Dr. Tintu, Sreelekha, Vasuja, Linessh, Indu, Divya, Musfir, Rethesh, Sabitha, Sreeja thampi, Aparna, Bini, Mintu, Lincelal, Sr. Rosmin, Roopa, Manju, Jaison and Suneetha, will ever be green in my memories.

Mere words would not suffice to express my gratitude to my husband, who is my strength and support, always standing by me in every step of my life and our loving kids, who make our life ever cheerful and meaningful. From the bottom of my heart, I thank my parents and In laws for their love and affection. Special mention is worth towards all my family members for their support and prayer, to complete my PhD.

Rose Leena Thomas

Preface

Tellurite glasses are photonic materials of special interest to the branch of optoelectronic and communication, due to its important optical properties such as high refractive index, broad IR transmittance, low phonon energy etc. Tellurite glasses are solutions to the search of potential candidates for nonlinear optical devices. Low phonon energy makes it an efficient host for dopant ions like rare earths, allowing a better environment for radiative transitions. The dopant ions maintain majority of their individual properties in the glass matrix. Tellurites are less toxic than chalcogenides, more chemically and thermally stable which makes them a highly suitable fiber material for nonlinear applications in the midinfrared and they are of increased research interest in applications like laser, amplifier, sensor etc. Low melting point and glass transition temperature helps tellurite glass preparation easier than other glass families.

In order to probe into the versatility of tellurite glasses in optoelectronic industry; we have synthesized and undertaken various optical studies on tellurite glasses. We have proved that the highly nonlinear tellurite glasses are suitable candidates in optical limiting, with comparatively lower optical limiting threshold. Tuning the optical properties of glasses is an important factor in the optoelectronic research. We have found that thermal poling is an efficient mechanism in tuning the optical properties of these materials. Another important nonlinear phenomenon found in zinc tellurite glasses is their ability to switch from reverse saturable absorption to saturable absorption in the presence of lanthanide ions. The proposed thesis to be submitted will have seven chapters.

Chapter 1 is an introduction to glasses focusing on tellurite glasses for nonlinear photonic applications. It opens to the world of amorphous materials, beginning from glass transition, which is one of the mysteries regarding glasses yet to be solved. Tellurium dioxide is not a conditional glass former, but when it forms a glass with other oxides it exhibits

astonishing optical properties. Trigonal bipyramid is the structural unit of tellurite glasses and they vary in number with different combinations of glass and hence determine its optical properties. Optical properties vary with different glass compositions because the bond angle and bond length gets changed with different dopant ions. This enables one to tune the material properties of tellurite glasses for different photonic applications.

Chapter 2 deals with the description of various characterization techniques used in the present research work. First part of this chapter describes formation of glasses by melt quench method, emphasizing the fact that fast cooling is required from the glass melt in order to avoid crystallization. Structural characterization techniques such as X-ray Diffraction technique (XRD), Fourier Transform Infrared spectroscopy (FTIR); thermal characterizations such as Differential Scanning Calorimetric (DSC) and optical characterizations such as optical absorption spectroscopy, fluorescence spectroscopy etc. is described in detail. Experimental techniques such as thermal poling and Z-scan technique are discussed in this chapter. The former allow structural modifications in the glass network and the latter is a simple experimental set up to study the third order susceptibility of a material medium.

Chapter 3 focuses on the structural, thermal, linear and nonlinear optical studies of zinc tellurite glasses. Structural study using XRD reveals that the prepared material is amorphous in nature due to the absence of crystallization peaks. FTIR also contains information regarding the structural units TeO_4 and TeO_3 in the zinc tellurite glass network. From fluorescence studies we have observed a blue fluorescence emission, where the intensity was found to be proportional to the tellurium content. Tellurite glasses are in the category of highly nonlinear optical materials, due to their large refractive index. Our results also support this idea indicating the Two Photon Absorption behavior of zinc tellurite glasses. The reverse saturable absorption exhibited by these glasses proves them to be a good optical limiter.

Chapter 4 discusses on the thermal poling technique, which is found to be an effective tool in modifying the structure of the material of glass and tuning its linear and nonlinear optical properties. Thermal poling is done by heating the sample and applying a potential across it. The voltage is removed only after the sample has been cooled down to room temperature in order to create a change in the dipole arrangement in the glass. The modification of dipoles allows the glass to increase the density and allows tuning of its optical properties. The astonishing results are that thermal poling leads to the tuning of optical properties such as band gap, refractive index and enhancement of Two Photon Absorption in the glass.

Chapter 5 focuses the influence of lanthanide ions in the zinc tellurite glass matrix. We have incorporated oxides of lanthanum, samarium, europium and holmium in the study because of their capability in modifying the linear and nonlinear optical properties in the tellurite vitreous network. All of the lanthanide ions doped in the zinc tellurite glasses, exhibit their characteristic absorption bands in the absorption spectra. The major result we report in this chapter is the observed switching of optical nonlinearities from Reverse Saturable Absorption to Saturable Absorption in zinc tellurite glasses without and with rare earth content. Our studies reveal that the Two Photon Absorption is getting enhanced in the rare earth doped zinc tellurite glasses in the decreasing order of atomic number.

Chapter 6 reports the laser induced fluorescence spectroscopy of europium doped zinc tellurite glasses. The low phonon energy based emission spectroscopy is an important field in various applications like optical amplifiers, phosphors, fibers, lasers etc. Europium oxide is found to be efficient in fluorescing in the visible wavelength with laser excitation. The present chapter also gives some space to explain the concentration effect of europium and glass former (tellurium dioxide)/ modifier (zinc oxide) on fluorescence.

Chapter 7 concludes the major findings of the thesis and give details of the future works that can be done based on the results obtained.

Contents

Chapter 1

Introduction to Tellurium oxide glasses..... 01 - 34

1.1	Introduction -----	01
1.2	The glass transition and vitreous state -----	03
1.3	Oxide glasses -----	05
1.4	TeO ₂ -based bulk glasses -----	11
1.4.1	Tellurium -----	11
1.4.2	Literature Review on Tellurite glasses-----	13
1.4.3	Structure of Tellurite glasses -----	16
1.4.4	Properties of Tellurite glasses-----	19
1.4.5	Applications of Tellurite glasses-----	28
1.5	Scope of the thesis-----	29
1.6	Summary and conclusions -----	31
	References-----	32

Chapter 2

Essence of characterization techniques 35 - 68

2.1	Introduction -----	35
2.2	Glass preparation -----	36
2.2.1	Melt quench method to prepare bulk Tellurite glasses -----	36
2.3	Structural analysis -----	37
2.3.1	X-ray diffraction spectroscopy -----	37
2.3.2	Fourier transform infrared spectroscopy-----	38
2.4	Thermal characterization -----	40
2.4.1	Thermal Annealing -----	40
2.4.2	Glass transition temperature measurement-DSC -----	41
2.5	Linear Optical characterization -----	42
2.5.1	Absorption spectroscopy-----	42
2.5.2	Refractive index measurement-----	44
2.5.3	Fluorescence spectroscopy -----	45
2.5.4	Laser Induced Fluorescence spectroscopy-----	45
2.6	Nonlinear optical characterization -----	47
2.6.1	Non-linear optics -----	47
2.6.2	Open/Closed aperture Z-scan -----	48
2.6.3	Two Photon Absorption (TPA) -----	55
2.6.4	Free Carrier Absorption (FCA) -----	55
2.6.5	Excited State Absorption (ESA)-----	56
2.6.6	Saturable and Reverse Saturable Absorption (SA & RSA)-----	57
2.6.7	Optical Limiting -----	58

2.6.8	Nonlinear refraction	59
2.6.9	Merits and Demerits of Z scan technique	60
2.7	Thermal poling	61
2.8	Summary and conclusions	63
	References	64

Chapter 3

Structural, Thermal, Linear and Nonlinear

Optical Spectroscopy of Zinc Tellurite glasses 69 - 98

3.1	Introduction	69
3.2	Structural properties of Zinc Tellurite glasses	71
3.3	Thermal characterization of Zinc Tellurite glasses	76
3.4	Linear Optical properties of Zinc Tellurite glasses	78
3.5	Fluorescence spectroscopy of Zinc Tellurite glasses	81
3.6	Nonlinear optical properties of Zinc Tellurite glasses	86
3.6.1	Nonlinear optical properties of 80 TeO ₂ :20 ZnO glass	87
3.6.2	Nonlinear optical properties of 75 TeO ₂ :25 ZnO glass	88
3.6.3	Nonlinear optical properties of 70 TeO ₂ :30 ZnO glass	89
3.6.4	Nonlinear refraction	93
3.7	Summary and conclusions	94
	References	96

Chapter 4

Band gap tuning and enhancement of two photon absorption

coefficient in Zinc Tellurite glasses via thermal poling..... 99 - 121

4.1	Introduction	99
4.2	Experiment	101
4.3	Theory	102
4.4	Results	107
4.4.1	Thermal poling on 80 TeO ₂ :20 ZnO glass	107
4.4.1.1	Linear optical properties	108
4.4.1.2	Nonlinear optical properties	109
4.4.2	Thermal poling on 75 TeO ₂ :25 ZnO glass	110
4.4.2.1	Linear optical properties	110
4.4.2.2	Nonlinear optical properties	111
4.4.3	Thermal poling on 70 TeO ₂ :30 ZnO glass	112
4.4.3.1	Linear optical properties	112
4.4.3.2	Nonlinear optical properties	113
4.5	Discussion	114
4.6	Summary and Conclusions	117
	References	118

Chapter 5

Influence of Lanthanides on structural, thermal, linear and nonlinear optical properties of Zinc Tellurite glasses 123 - 154

5.1	Introduction	123
5.2	Influence of rare earth ions on structure of Zinc Tellurite glasses	125
5.3	Influence of rare earth ions on thermal properties of Zinc Tellurite glasses	131
5.4	Influence of rare earth ions on linear optical properties of Zinc Tellurite glasses.....	134
5.5	Influence of rare earth ions on linear fluorescence of Zinc Tellurite glasses	140
5.6	Influence of rare earth ions on TPA of Zinc Tellurite glasses.....	143
5.7	Summary and Conclusions.....	150
	References.....	152

Chapter 6

Laser induced fluorescence studies on europium doped Zinc Tellurite glasses 155 - 176

6.1	Introduction	155
6.2	Fluorescence spectroscopy of europium doped Zinc Tellurite glasses	156
6.3	Laser induced fluorescence spectroscopy of Zinc Tellurite glasses	159
6.3.1	Introduction	159
6.3.2	Experiment	160
6.3.3	Results	161
6.3.3.1	Laser induced fluorescence spectroscopy of 80 TeO ₂ :15 ZnO: 5 Eu ₂ O ₃ glass	161
6.3.3.2	Laser induced fluorescence spectroscopy of 75 TeO ₂ :20 ZnO: 5 Eu ₂ O ₃ glass	163
6.3.3.3	Laser induced fluorescence spectroscopy of 70 TeO ₂ :25 ZnO: 5 Eu ₂ O ₃ glass	165
6.3.4	Discussion	166
6.4	Concentration effect of europium on Laser induced fluorescence spectroscopy of Zinc Tellurite glasses.....	171
6.5	Summary and Conclusions.....	174
	References.....	175

Chapter 7

Future work and Conclusions 177 - 182

List of Publications

Journal Papers:

- [1] **Optical Non-linearity in ZnO Doped TeO₂ Glasses**, Rose Leena Thomas, Vasuja, Misha Hari, V. P.N. Nampoore, P. Radhakrishnan, Sheenu Thomas, *Journal Of Optoelectronics and advanced Materials*, Vol. 13, Issue 5, May 2011, pp. 523-527.
- [2] **Optical Limiting In TeO₂-ZnO Glass From Z-Scan Technique**, Rose Leena Thomas, Vasuja, Misha Hari, B. Nithyaja, S. Mathew, I.Rejeena, Sheenu Thomas, V. P. N. Nampoore and P. Radhakrishnan, *Journal of Nonlinear Optical Physics & Materials (JNOPM)*, Volume: 20, Issue: 3, DOI no: 10.1142/S0218863511006133, Page: 351-356
- [3] **Optical spectroscopy and visible fluorescence of TeO₂- ZnO glasses**, Rose Leena Thomas, Rejimole P.R., V P N Nampoore, P Radhakrishnan and Sheenu Thomas, *Optics and Photonics Journal(In Press)*
- [4] **Bandgap tuning and enhancement of Two Photon Absorption in Zinc Tellurite glasses via thermal poling**, Rose Leena Thomas, V P N Nampoore, P Radhakrishnan, Sheenu Thomas (communicated)
- [5] **Laser induced fluorescence in europium doped zinc tellurite glasses**, Rose Leena Thomas, V P N Nampoore, P Radhakrishnan and Sheenu Thomas, (communicated)
- [6] **Optical Nonlinear Switching from RSA to SA in Europium Doped Zinc Tellurite Glasses**, Rose Leena Thomas, V P N Nampoore, P Radhakrishnan, Sheenu Thomas(communicated)
- [7] **Optical Nonlinearity in Lead Iodide Di Hydrate grown with UV and IR radiations using Z-scan Technique**, I.Rejeena, B.Lillibai, Rose Leena Thomas, V.P.N.Nampoore, P.Radhakrishnan, *Optics: Phenomena, Materials, Devices, and Characterization*, AIP Conf. Proc. 1391, 691-693 (2011); doi: 10.1063/1.3643651

Conference Papers:

- [1] **Two photon absorption in TeO₂-ZnO glass at different laser irradiances**, Rose Leena Thomas, Vasuja, Misha Hari, V P N Nampoori, P Radhakrishnan, Sheenu Thomas, ICMST 2012, St.Thomas College, Pala.
- [2] **Optical non-linearity in ZnO-TeO₂ glass from z-scan technique**, Rose Leena Thomas, Vasuja, Rajeena, Misha Hari, Nityaja B, V. P. N. Nampoori, P. Radhakrishnan and Sheenu Thomas. *International Conference on Contemporary trends in Optics and Optoelectronics, XXXV Optical Society of India Symposium, Thiruvananthapuram, India, 17-19, Jan 2011.*
- [3] **Enhancement Of Two Photon Absorption In Zinc Tellurite Glasses Via Thermal Poling**, Rose Leena Thomas, V P N Nampoori, P Radhakrishnan, Sheenu Thomas, International Conference on Fiber Optics and Photonics, 09-12, December in Chennai, India
- [4] **Bandgap Tuning in Zinc Tellurite Glasses Via Thermal Poling**, Rose Leena Thomas, V P N Nampoori, P Radhakrishnan, Sheenu Thomas, Functional Glasses 2013, ITALY .
- [5] **Nonlinear Optical Switching from RSA to SA in Europium Doped Zinc Tellurite Glasses**, Rose Leena Thomas, V P N Nampoori, P Radhakrishnan, Sheenu Thomas, National Laser Symposium, 2012
- [6] **Nonlinear Optical Investigation on Lead Iodide Di Hydrate grown with UV and IR radiations using Open aperture Z-scan Measurement**, G.Lillibai, I.Rejeena, Rose Leena Thomas, V.P.N.Nampoori, P.Radhakrishnan. International conference on optics, NIT, Calicut, 2010.
- [7] **Green Fluorescence in Europium Doped Zinc Tellurite Glasses**, Rose Leena Thomas, V P N Nampoori, P Radhakrishnan, Sheenu Thomas, National Seminar on Smart Materials For a Smarter World, 27-28 September 2012, Department of Physics, St. Berchmans College, Changanassery, Kerala.



INTRODUCTION TO TELLURIUM OXIDE GLASSES

This chapter is an introduction to glasses focusing on Tellurium oxide (tellurite) glasses for nonlinear photonic applications. It opens to the world of amorphous materials, beginning from glass transition, which is one of the mysteries regarding glasses yet to be solved. Tellurium dioxide is not a conditional glass former, but when it forms a glass with other oxides it exhibits astonishing optical properties. Trigonal bipyramid is the structural unit of tellurite glasses and they vary in number with different combinations of glass and hence determine its optical properties. Optical properties vary with different glass compositions because the bond angle and bond length gets changed with different dopant ions. This enables one to tune the material properties of tellurite glasses for different photonic applications.

1.1 Introduction

Amorphous solids are no crystalline solids in which the atoms and molecules are not organized in periodic lattice pattern. The atomic arrangements of solids and liquids are in close proximity to each other, but their properties are, entirely different. A solid material has both a well-defined volume and a well-defined shape; a liquid has a well-defined volume but a shape that depends on the shape of the container. This means that a solid exhibits resistance to shear stress while a liquid does not. On an atomic level, these macroscopic distinctions arise due to the nature of the atomic

motion. Atoms in a solid are not stationary, but instead oscillate rapidly about this fixed point and it can be viewed as a time-averaged centre of gravity of the rapidly jiggling atom. The spatial arrangement of these fixed points constitutes the solid's durable atomic-scale structure, but a liquid possesses no enduring arrangement of atoms and are mobile and continually wandering throughout the material.

There are two main classes of solids: crystalline and amorphous. The major characteristics of both the classes are listed in a table[Table 1.1] below.

Table 1.1: Classification of crystalline and amorphous solids.

Crystalline	Amorphous
Lattice/unit cell can be defined	No lattice/unit cell can be defined
Atomic positions in a crystal exhibit a property called long-range order or translational periodicity; positions repeat in space in a regular array	No long range order in their atomic arrangement ,but short range order/medium range order
Crystal formation is by slow cooling in order to keep the atomic order of arrangement	Amorphous formation by fast cooling from a melt in order to avoid crystallization
Crystallization is a thermodynamically favored process below melting temperature	Glass transition is believed to be a kinetic process, rather than a thermodynamic one
Crystallization by nucleation and growth	No nucleation and growth in the formation of a glass

1.2 The glass transition and vitreous state

Glass formation is a matter of bypassing the process of crystallization^[1-5] and almost all materials can, be prepared as amorphous solids by quick cooling. The rate of cooling varies enormously from material to material. When glass is made, the material is quickly cooled from a supercooled liquid, an intermediate state between liquid and glass. To become an amorphous solid, the material is cooled, below a critical temperature called the glass-transition temperature. Past this point, the molecular movement of the material's atoms has slowed and the material forms a glass^[1-5]. The newly formed amorphous structure is not as organized as a crystal, but it is more organized than a liquid.

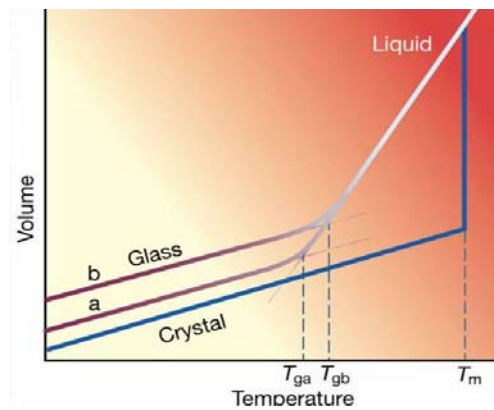


Figure 1.1: V-T Diagram showing glass formation

In the process of glass transition, it is important to plot the behavior of amorphous materials, from the super cooled state to glass, in a **V-T** diagram [Figure 1.1]. Here, temperature is plotted in the x-axis and the volume/enthalpy occupied by the material is plotted along the y-axis, where temperature T_m is the melting point, and T_g is the glass transition

temperature. The glass transition occurs when the supercooled liquid freezes into an amorphous solid with no abrupt discontinuity in volume, near the glass transition temperature^[1-5].

The glass transition temperature T_g is not as sharply defined as T_m ; T_g shifts towards lower temperature when the cooling rate is reduced. The reason for this phenomenon is the steep temperature dependence of the molecular response with time. T_g also varies with the composition of raw materials selected for preparation of glass. When the temperature is lowered below T_g , the response time for molecular rearrangement becomes much larger than experimentally accessible times, so that liquid like mobility disappears and the atomic configuration becomes frozen into a set of fixed positions to which the atoms are tied. Possible range of glass formation is represented by temperatures T_{ga} and T_{gb} . T_{ga} is the glass transition temperature for a glass formed when the cooling rate is reduced and T_{gb} is that of increased rate of cooling.

The slopes of crystal and glass lines in a V-T diagram are small, compared to the high slope of the liquid section which reflect the fact that the coefficient of thermal expansion of a solid is small in comparison with that of the liquid. An important change, the jump of heat capacity, also happens during liquid-glass transition, which is why physicists thought there is some sort of a phase transition, between the liquid phase and the glass phase.

The following are the major ideas regarding glass transition:

- Cooling rate is higher for glass formation to avoid nucleation and crystal growth
- As temperature decreases viscosity increases

- Free energy is higher for glasses, which is clear from the V-T diagram
- Glass is a Metastable state

Glasses/the vitrified solids show structural disorder like liquids, but their mechanical properties are typical of brittle solids. Various combinations of glasses are being prepared, with enormous properties using various families of the periodic table like oxide, chalcogenide, halide etc.

1.3 Oxide glasses

Oxide glasses are prepared from various oxides commonly SiO₂, P₂O₅, B₂O₃, GeO₂, TeO₂ etc. One of the advantages of oxide glasses is that they can be easily prepared by melt quench technique, with competing properties compared to chalcogenide glasses. The following paragraphs of the thesis give a general description of the structure, structural models, optical and thermal properties and some of the applications of oxide glasses.

In determining the structure of amorphous solids, researchers commonly use the information obtained from structure-probing experiments that is, the curve of Radial Distribution Function (RDF) ^[1]. The significance of the RDF is that it gives the probability of neighbouring atoms being located at various distances from an average atom. Amorphous solids, like crystalline solids, exhibit a wide variety of atomic-scale structures. Most of these can be recognized as falling within one or another of three broad classes of structure associated with the following models:

- The continuous random-network model (CRN), applicable to covalently bonded glasses, such as amorphous silicon and the oxide glasses

- The random-coil model (RC), applicable to the many polymer-chain organic glasses, such as polystyrene glasses
- The random close-packing model (RCP), applicable to metallic glasses.

We would like to confine ourselves on CRN model, since we are focusing on oxide glasses.

Continuous Random Network model

In his classic paper of glass science, Zachariasen^[6] argued that since the mechanical properties of glasses are similar to those of the corresponding crystals and the atomic forces in both must be of the same order but with a variation in the number of structural units and the periodicity of lattice. The diffuseness of the X-ray diffraction spectra for glasses clearly indicated that glass itself has an infinitely large unit cell. A direct consequence of the randomness would result in glass having higher internal energy than the crystal. Zachariasen believed that this difference in internal energy from that of the corresponding crystal must be small and also the resulting glass should require an open and flexible structure.

Note that both crystalline and glassy forms are composed of AO_3 triangles joined to each other at corners, except that the glassy form has disorder introduced by changes in the A-O-A angles called bond angle and slight changes in the A-O bond length. Zachariasen laid down four rules for glass formation in a compound AmOn .

- 1) An oxygen atom is linked to no more than two atoms of A.
- 2) The oxygen coordination around A is small, say 3 or 4.
- 3) The cation polyhedral share corners, not edges, not faces.
- 4) At least three corners are shared.

Zachariasen therefore defined a glass as a “substance that can form extended three-dimensional networks lacking periodicity with energy content comparable with that of the corresponding crystal network”.

Band structure of oxide glasses

According to D.L. Wood and J Tauc^[7] absorption edge of amorphous semiconductors are of same energy range as that of crystalline form and below this edge^[8], the transparency of amorphous materials can be remarkably high. Also the absorption edges of semi conducting glasses are sensitive to glass preparation conditions, thermal history and purity of materials used. Figure 1.2 is a schematic diagram of the density of states for amorphous semiconductors.

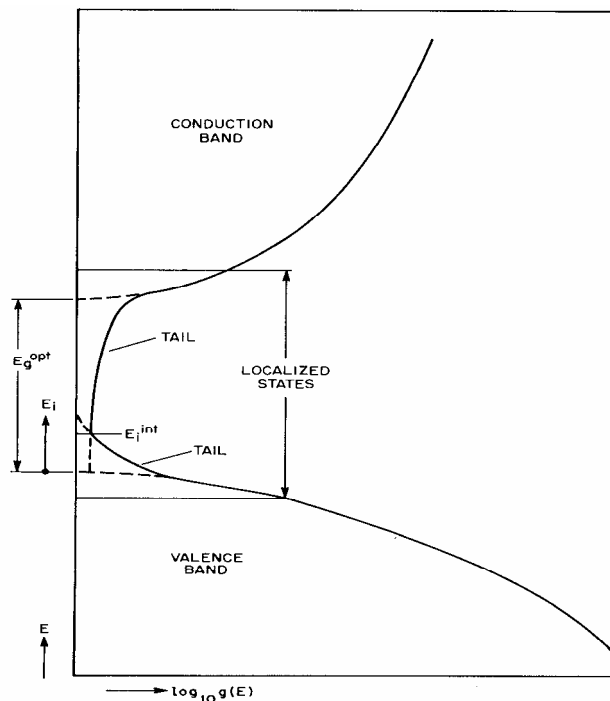


Figure 1.2: Schematic diagram of the density of states for amorphous semiconductors. [Taken from: D.L.Wood, J. Tauc, “Weak absorption tails in amorphous semiconductors”, Physical review B, 5, 8, (1972)]

According to Mott ^[9], in any non-crystalline system the lowest states in the conduction band are “localized”, that is to say traps, and that on the energy scale there is a continuous range of such localized states leading from the bottom of the band up to a critical energy E_c , called the mobility edge, where states become non-localized or extended. The deep levels in glasses are due to defect states, due to charged or uncharged dangling bonds.

There exist band states and tail states based on the form of the energy dependence on their densities. According to Wood et al ^[7], the band states correspond to the bonding states in the valence band and the antibonding states in the conduction band and also the tail states correspond to the defects such as dangling bonds. The band states are localized below the mobility edge and extended at energies above it. The optical transitions take place from localized states with state density $N(E_i)$ to the extended states of opposite band with state density $g(E)$, with only energy conservation. The maximum energy in the optical absorption associated with the tail is the band gap of the material of glass.

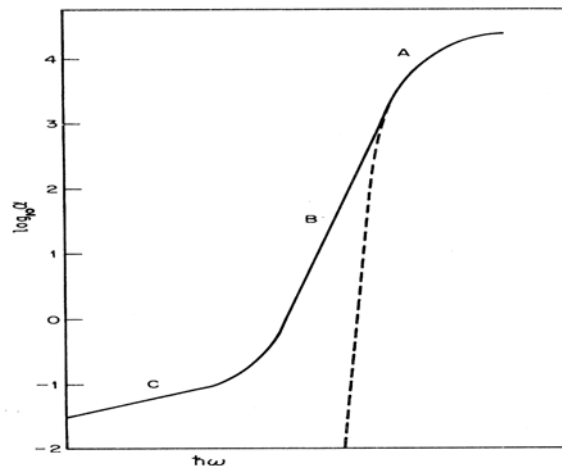


Figure 1.3: The three major absorption regions in glasses [Taken from: D.L.Wood, J. Tauc, “Weak absorption tails in amorphous semiconductors”, Physical review B, 5, 8, (1972)]

Thus there are three absorption regions found in amorphous solids as shown in figure 1.3. Region A is due to transitions between the band states and B,C are associated with the tail states. Transitions between localized states are less probable than transitions between extended states or between a localized state and extended states.

Characteristics and applications of oxide glasses

To understand processes that occur in glasses, it is necessary to understand their structure. The most common network inorganic glasses are silicates and the most common example is window glass. The basic structural unit of the silicate glass network is a tetrahedron, in which a silicon atom is surrounded by four oxygens. The tetrahedra, connected by bridging oxygens, are randomly oriented in space because they have been “frozen” into place by rapid quenching. The silicon atoms are the network formers and some of the other well known network formers are such as tellurium, boron, and phosphorus.

Atoms called network modifiers mainly alkali and alkaline earth ions, when added to the glass, they depolymerize the network, forming ionic bonds with oxygens. These oxygen that are covalently bonded to one network former and ionically bonded to one network modifier are called nonbridging oxygen (NBOs) ^[10]. The properties of oxide glasses rely on their composition, and some others result from the presence of various modifiers agents in certain basic glass-forming materials. Some of the technological applications of amorphous solids and the properties that make those applications possible are gathered and presented below.

The most common example of glass is a window glass that has blossomed during the second half of the 20th century. The first electronic

application of amorphous semiconductors was in xerography or electrostatic imaging. The electrical conductivity of glasses are lower than that of the corresponding crystalline material, because the structural disorder impedes the motion of the mobile electrons that make up the electrical current. The photoconductor, which is an electrical insulator in the absence of light but which conducts electricity when illuminated, is exposed to an image of the document to be copied. This process is also widely used in laser printers, in which the photoconductor is exposed to a digitally controlled on-and-off laser beam that is raster scanned (like the electron beam in a television tube) over the photoconductor surface.

Thermal conductivity of a glass is also lower than that of the corresponding crystalline insulator; glasses thus make good thermal insulators. The continuous liquid-to-solid transition near T_g , the glass transition, has a profound significance in connection with classical applications of glasses. The ability to tune the viscosity of the melt (viscosity steeply increases with decreasing temperature) allows glass to be conveniently processed and worked into desired shapes; glass blowing is a classic example of the usefulness of this widely exploited property.

Applications of amorphous silicon thin films include^[11] solar cells based calculators, image sensor in fax machines, photoreceptor in some xerographic copiers etc. All these applications exploit the ability of amorphous silicon to be vapour-deposited in the form of large-area thin films. A silicon-hydrogen alloy containing 10 percent hydrogen eliminates the electronic defects that are intrinsic to pure amorphous silicon and is used in high-resolution flat-panel displays for computer monitors and for television screens.

1.4 TeO₂-based bulk glasses

1.4.1 Tellurium

Chalcogens are one of the families of interest among glass researchers and Tellurium is one among them, along with O, S, and Se from group VI A of the periodic table.

Tellurium was discovered in 1782 by Austrian mineralogist Baron Franz Joseph Muller von Reichenstein. It seldom occurs in its pure state and usually found as a compound in ores of gold, silver, copper, lead, mercury or bismuth. The most common uses of tellurium today are in specialized alloys in making chemicals and electrical equipment etc. Muller discovered tellurium while studying gold taken from a mine in the Borzsony Mountains of Hungary. He had received the gold from a colleague who thought that it contained an impurity. The colleague was unable to identify the impurity, but thought it might be unripe gold. This concept is reflected in its names like aurum paradoxum, means paradoxical gold, something that acts like gold and metallum problematum, means the problem metal. After three years of experiments by Muller on the new element, it is named tellurium, from the Latin word tellus, meaning "Earth". Tellurium is often found with another element, selenium and is one of the rarest elements in the earths crust; about one part per billion, implying it is less common than gold, silver or platinum.

The properties of tellurium^[12] include

- Tellurium is a grayish-white solid with a shiny surface
- Melting point of 449.8°C (841.6°F) and a boiling point of 989.9°C (1,814°F)
- Density is 6.24 grams per cubic centimeter

- It has many metal-like properties; it breaks apart rather easily and does not conduct an electric current very well.
- Tellurium does not dissolve in water
- Tellurium also has the unusual property of combining with gold. Gold normally combines with very few elements. The compound formed between gold and tellurium is called gold telluride (Au_2Te_3)
- Its abundance places it about number 75 in abundance of the elements in the earth
- The most common mineral of tellurium is sylvanite. Sylvanite is a complex combination of gold, silver, and tellurium.
- Tellurium is obtained commercially today as a by-product in copper and lead refining
- Eight naturally occurring isotopes of tellurium are known. They are tellurium-120, tellurium-122, tellurium-123, tellurium-124, tellurium-125, tellurium-126, tellurium-128, and tellurium-130.
- Tellurium improves machinability of steel when added to it.
- It is important in the vulcanization of rubber.
- It improves picture quality in photocopiers and printers.
- A compound of tellurium, cadmium, and mercury is also used in infrared detection systems in satellites.
- Very small amount of tellurium is used for minor applications, such as a coloring agent in glass and ceramics

1.4.2 Review of early research

Tellurium dioxide (TeO_2) is the most stable oxide of tellurium (Te). From the viewpoint of fundamental chemistry, the transitional position of Te between metals and nonmetals has got special significance. The stability of tellurium oxide is one of the properties that originally attracted researchers, to tellurite glasses^[1]. The properties of tellurium oxides that give them their stability proved to be transferrable to their glass derivatives. Tellurite glasses are of special interest to glass researchers from 1980 onwards, when glass research started to focus on various properties of glasses to be utilized in various applications.

The first reports on tellurite glass were by Barady^[1,13,14]. He prepared tellurite glasses by fusing TeO_2 with a small amount of Li_2O and used X-ray analysis to investigate the structure and radial distribution of electrons within this glass. The distribution function Barady obtained consists of two well-resolved peaks, one at about 1.95 Å and the other at about 2.55 Å, with areas 2220 and 1340 electrons respectively. The interatomic distances and areas of the peaks were consistent only with Te–O nearest-neighbor coordinations and so the basic coordination scheme of the crystal was closely reproduced in the glass. Later on he could obtain better separation of the peaks of the distribution function at larger radial distances and he concluded that tellurite glass is unusual because it is octahedral, with faces that exhibit a close-order configuration such that four oxygen atoms are found uniformly at a distance of 1.95 Å and two others are at 2.75 Å. Barady observed that the minimum mole ratio of modifier actually required is approximately 1:10 and concluded that only a fraction of the edges are opened and, therefore, that the glass cannot be made up completely of octahedrals linked together only by their corners.

Barady concluded that the SRO structure in tellurite glass differs little from that of the crystal and that this close order does not have to be tetrahedral.

At the same time, Winter^[15] studied the ability to form bonds leading to a vitreous network, to the periodic table of the elements focusing on group VI A elements, the chalcogen elements, easily form vitreous network with elements from groups III, IV, or V of the periodic table. Winter prepared many new glasses and his structural studies are the following:

- Self vitrifying elements are elements from group VII and either an element from group II,III or IV or a transition element
- Tellurite glasses are comparable to that of the crystalline form. TeO_2 is covalent and has a highly deformed octahedron in its structure, because the valence characteristic of Te results in two sets of Te-O distances.
- Each oxygen atom must be shared with three tellurium atoms, symmetry requirements force a distortion of the octahedral
- There are 6 different Te–O bond lengths, 4 Te–Te distances, and 12 O–O distances. It is possible that this distortion produces a structure energetically similar to that of the vitreous state, in which there is only Short-Range Order (SRO).
- Preparation of TeO_2 glass from the pure material is by breaking one edge in TeO_2 however, an oxygen atom must be supplied to complete the octets of the two cations involved. The addition of modifier oxide supplies ions for this process. When modifier ions are introduced, the disrupted-edge (O) ions may coordinate around them in much the same way as in the silicate system, in which modifier ions find positions in the holes in the network.

- Modifier ions are surrounded by the O ions, which are bonded only to one Si. The only difference for TeO₂ is that the O atom from the added oxide plays a more essential role, that of breaking an edge.
- In crystalline TeO₂, four octahedrals share three edges. If the glass consists of a network of octahedrals in which all the shared edges are broken, the minimum molecular-mass ratio (mole ratio) of modifier to TeO₂ would be 3:4.

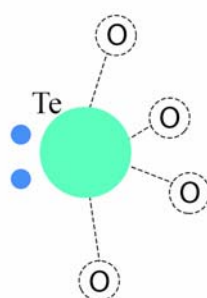
In 1975 Wells^[16] presented his research findings that, there are two crystalline forms of TeO₂, including a yellow orthorhombic form (the mineral tellurite) and a colorless tetragonal form (paratellurite).

- There is four coordination of Te in both forms, the nearest neighbors being arranged at four of the vertices of a trigonal bipyramid, which suggests a considerable covalent character to the Te–O bonds.
- Tellurite has a layered structure in which TeO₄ groups form edge-sharing pairs that then form a layer by sharing their remaining vertices.
- The short Te–Te distance, 3.17 Å (compare with the shortest in paratellurite, 3.47 Å) may account for its color.
- In paratellurite, very similar TeO₄ groups share all vertices to form a 3D structure with 4:2 coordination in which the O-bond angle is 140°, distances of the two axial bonds are 2.08 Å, and distances of the two equatorial bonds are 1.9 Å

Following the basic researches presented here, the accepted structural descriptions and how it determines the glass properties are presented below, even though the basic structural research is ongoing still on tellurite glasses.

1.4.3 Structure of tellurite glasses

Earlier studies of glasses have focused on silicates because they have been technologically most useful. The studies in the present thesis focus on understanding dynamical processes that occur in zinc oxide- tellurium oxide glasses. In order to accomplish this, the molecular structure of tellurium oxide glass must be understood. Supporting Zachariasen random network theory, tellurite structural units are similar to that of tellurite crystal. Tellurites differ from silicates in that their structure that they are not tetrahedral but a distorted octahedron/trigonal bipyramid. The basic unit of a tellurium oxide is a trigonal bipyramidal structure^[17-22], composed of two long bonds to oxygens called Bridging Oxygens(BO) and two short bonds with an electron pair occupying the fifth place, as shown in Figure below.



trigonal bipyramid (tbp)

Figure 1.4: TeO₂ Trigonal Bipyramidal Structure

Tellurium oxide glass is composed of a three-dimensional network structure in which these trigonal bipyramid [Figure 1.4] units are connected edge sharingly with random orientations. The connectivity of this structure, which is the number of other tellurium atoms that are directly bonded via an oxygen atom, is four. The addition of modifier oxides generally creates Non

Bridging Oxygen's (NBOs), which are bonded ionically to the modifier ions. Breaking up the covalent network structure (depolymerization) creates mobile ion species in the material and tellurite structural units of the form $\text{TeO}_3 / \text{TeO}_{3+1}$ [Figure 1.5] are created^[17-22].

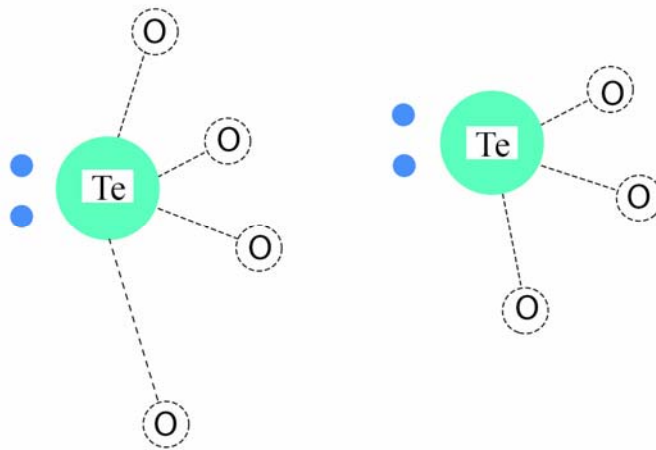


Figure 1.5: TeO_{3+1} and TeO_3 Structures

This greatly reduces its ability to form a three-dimensional covalently bonded network and the Te- Te reduced connectivity also increases the ability of the local network to relax because of the increased mobility of non-bridging oxygens, increasing the ratio of TeO_3 to TeO_4 arrangements. The dynamic processes present in inorganic glasses are intimately related to the connectivity and structure around the tellurium atoms. The primary relaxation of network glasses involves long range cooperative movements and the breaking and reforming of covalent bonds (locally) and so the network modifiers are free to move between sites near non bridging oxygen ions in the tellurite glass matrix, due to the weak and non-directional ionic bonds^[10].

The modifications and so the properties of glass depend on the type of modifier ions used, the amount of modifiers and also the thermal history

(cooling rate) of the prepared glass sample. Change in the NBO ions will reflect in the X-ray diffraction, band gap from the optical absorption spectrum and the glass transition temperature from the Differential scanning calorimetry spectrum. Thus in a more modified glass structure more NBOs and lower T_g are observed [23]. A schematic of the variation of the fraction of BO/NBO with the mole fraction of the modifier content is shown in figure 1.6 below.

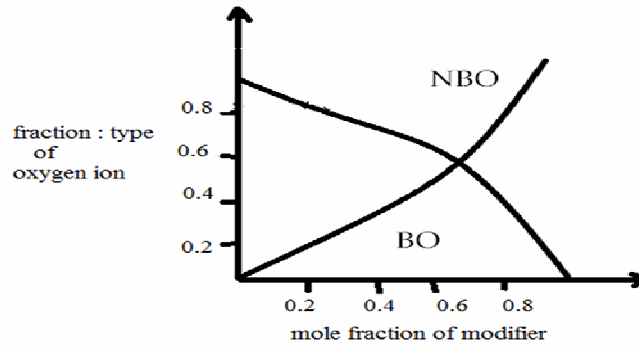


Figure 1.6: A schematic of the variation of the fraction of BO/NBO with the mole fraction of the modifier content

Structural modifications in the glass network with the addition of modifier ions are explained in terms of the field intensity of the cations, which quantifies the polarization of the surrounding anions due to the charge and size of each cation. It can be estimated from the electrostatic force between the cation and the anion [24]. For a cation with charge Z_c , bonded to an anion with charge Z_a , that force F is:

$$F = (Cons \tan t) \cdot \frac{Z_c Z_a e^2}{a^2} \quad (1.1)$$

where e is the electron charge and the distance between the cation and the anion, i.e. the sum of their ionic radii. Since in the present work the anion is

O^{2-} in all cases, $Z_a e^2$ is considered constant. We can define then the field intensity, F , as:

$$F = \frac{Z_c}{a^2} \quad (1.2)$$

It is empirically known that oxides of cations having high field intensities are network formers while low values of F correspond to network modifiers^[24] and thus, it is possible to relate F of the different cations to the fraction of NBO induced in the network by their presence.

1.4.4 Properties of tellurite glasses

a) Thermal properties

The physical properties of tellurite glasses have attracted the attention of many researchers, not only because of the numerous potential and realized technical applications for these properties but because of a fundamental interest in their microscopic mechanisms. Thermal properties of glasses depend on the network structure, since they depend on connectivity of structural units and strength of interatomic bonds. It is necessary to design glasses having better thermal properties in order to realize better nonlinear devices for various applications. Thermal stability is also a factor deciding, whether the glass is suitable for various applications. Modifier influence in determining the structure of glass and its properties are important to be considered in the preparation of glasses. For to study the thermal behavior of an amorphous solid, the first thing to be referred is its V-T diagram, which says its thermal history and is important in determining its properties. The V-T diagram gives information regarding the glass transition of the material. Below glass transition, the viscosity of a material increases to a sufficiently high value, typically about 10^{13} poise and the slope of the $V-T$ curve

becomes smaller than that of the liquid. The important terms ^[1] to be considered while studying the V-T diagram are the following:

- Stabilization (*S*) is the slowest process of glass formation, where if the *T* of the glass is held constant just below *T_g* and the cooling is stopped, the glass will slowly contract further until its *V* returns to a point on the smooth continuation of the construction curve of the super-cooled liquid ^[1]. *S* is an indicator of stability against crystallization.

$$S = (T_c - T_g) \quad (1.3)$$

- The glass-forming tendency

$$K_g = (T_c - T_g) / (T_m - T_c), \quad (1.4)$$

- Viscosity ; $P = Fd/vA$, (1.5)

where, *F* is the shearing force applied to a liquid of plane area *A*, *d* is the distance apart, *v* is the resultant relative velocity of flow, and *P* is viscosity in poise. Viscosity varies with *temperature* and determines the melting conditions.

- Heat capacity is given by $C_p = \Delta Q / \Delta T$. The conduction process for heat-energy transfer under the influence of a *temperature* gradient depends on the energy concentration present per unit *volume* of movement, and its rate of dissipation with the surroundings. The conduction of heat in dielectric solids can be considered as either the propagation of anharmonic elastic waves through a continuum or the interaction between quanta of thermal energy called phonons.
- Thermodynamically, structure energy increases as entropy decreases. The DSC curves are used to record the differential

heat input to a sample, expressed as the heating rate (dH/dT) in meters per joule per second or meters per calorie per second on the ordinate against T or time (t) on the abscissa.

- The observed thermal behavior of tellurite glasses according to references ^[1,10] are the following:
 - Low melting point
 - Low glass transition
 - Decrease in molar *volume* are attributed to changes in structure caused by the decrease in interatomic spacing, which can in turn be attributed to an increase in the stretching-force constant of the bonds inside the glassy network, resulting in a more compact, denser glass.
 - When tellurite glasses are added with some modifiers it decreases/increases the molar volume allowing a corresponding change in the bridging of structural units in the glass matrix.
 - The increase in the T_g induced by addition of the modifier could be explained by the increased degree of polymerization, for binary tellurite glasses which are produced by breaks in the network of the tellurium chains, which was confirmed from the calculated molar *volume* of these binary glasses.
 - As the *temperature* increased, there was increased chain alignment to reduce the internal energy of the system, and this self-alignment gave rise to nucleation and crystal growth.
 - As the percentage of TeO_2 oxide increased, the *temperature* of viscosity decreased, while entropy increased and the specific

heat capacity is decreased. Although the structural units of TeO_4 and TeO_3 are connected weakly with each other, and thus the intermediate structure varies with increasing *temperature*, the rearrangement kinetic of TeO_4 and TeO_3 during heating is affected by modifier mixing^[25,26].

- Increase in the C_p value at the glass transition, because Te–O–Te bonds are weak and bond-breaking occurs easily in the glass transition region, leading to large configuration entropy changes and thus large ΔC_p values. Measurements of the *temperature* variation of the C_p have been a rich source of information on electronic, atomic, and molecular dynamics of solids.
- The addition of modifier oxides produces complimentary effects on the magnitude of C_p . Because modifier oxides degrade the network structure, the melt viscosity decreases. Glasses formed in such systems tend to become more “ideal” in the sense that they have a lower magnitude of entropy and hence of frozen configuration C_p . At the same time, the degraded units produce defects in which the oxygen is more tightly bound to the central cation; therefore, the number of independent oscillators and the C_p are increased.

b) Linear optical properties

All the properties are determined by the basic combination and the so formed structure. Refractive index is a measure of the distortion of atomic electron clouds by the electromagnetic field of an external incident light beam. The electron cloud distortion by this field is reflected in a

parameter called polarizability of the material. The Lorentz equation [27, 28, 29] connecting polarizability and refractive index is given by

$$\frac{4}{3} \pi N \alpha = \frac{(n^2 - 1)}{(n^2 + 2)} \quad (1.6)$$

Non-linear behavior can also be predicted using the linear optical properties by using Millers rule^[30]. The linear and non-linear response will be higher in glasses containing large number of polarizable loosely bound valence electrons. In the case of oxide glasses, NBOs generated by suitable modifiers are more polarizable than BOs in the network. The presence of lone pair of electrons in Te is also helpful in increasing the polarizability of the material.

Majority of glasses, mainly oxide glasses are transparent in a particular range of wavelengths due to the absence of grain boundaries or interfaces within them. The transparency range [figure 1.7] of tellurite glasses spans from near UV to near IR and is transparent in the visible region. Thus there exists a band gap in them due to the absence of free electrons^[9].

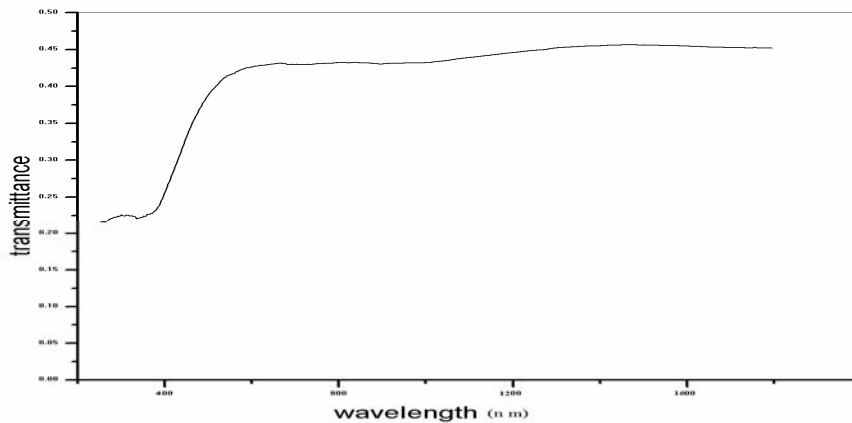


Figure 1.7: Transmittance spectra of tellurite glasses

Only UV photons have enough energy to excite the electrons which are forming the oxygen bonds in the network to higher energy levels. Therefore, the position of the UV absorption edge is determined by the electron binding energies which are related to the bonding energy of the atoms in the network^[24].

IR absorption and/transparency are determined by the type of vibration of the tellurite structural units. So as to have good and stable optical qualities in the prepared glass samples, we need to opt high purity raw materials for the glass preparation^[1, 10].

The nature of interaction between amorphous solids and electromagnetic wave depends on glass composition and structure. Interaction between an electromagnetic wave and bulk material is governed by the complex refractive index of the material and is given by^[1],

$$n^*(\omega) = n(\omega) + ik(\omega) \quad (1.7)$$

And

$$\varepsilon^*(\omega) = \varepsilon'(\omega) + i\varepsilon''(\omega), \quad (1.8)$$

where

$$\varepsilon'(\omega) = (n - k)$$

$$\varepsilon''(\omega) = 2nk$$

The first term in the complex refractive index is responsible for the reflection characteristics of the medium and given as,

$$R = \frac{(n-1)^2 + k^2}{(n+1)^2 + k^2} \quad (1.9)$$

but the second term is responsible for its absorption and is given by

$$k(\omega) = \alpha\lambda/4\pi, \quad (1.10)$$

where α = [Absorbance/ thickness], gives the absorption coefficient of the material of glass.

Equation (8), gives real and imaginary terms of complex permittivity of the medium.

It has been mentioned that the refractive index of a solid material varies with the wavelength. In crystalline solids, the refractive index values depend on the direction of the wave vector and differ in various directions. The transmission characteristics of the material change depending on the direction of the wave vector, and the material becomes birefringent and the light beam becomes polarized. In high electric fields, most materials exhibit optical nonlinearity.

The transparency of glass represents a major dilemma in theoretical physics because it is not known why a given glass absorbs radiation at some frequencies while transmitting others and why different frequencies travel at different speeds. The transparency of a crystalline insulator has been shown to be a consequence of the forbidden gap between the valence and conduction bands. Transparency of a crystalline insulator occurs when photon energies in the visible range are insufficient to excite an electron across the forbidden energy region. But glass too is transparent. It must therefore have a full valence band and an empty conduction band, and there must be a gap lying between them^[31]. The most common sources of color in glass are the electronic processes associated with transition elements. These have inner electrons which are not involved in covalent bonding and which are therefore available for absorbing and scattering light radiation.

Moreover, many of their transitions fall within the visible range of the spectrum. In the periodic table, the row of transition elements that starts with scandium contains the first elements encountered with electrons in the d orbital ^[1]. These are special in that their electron probability density (ρ) distributions have a multiplicity of lobes extending in various directions. This characteristic, which distinguishes these materials from those with the more symmetrical lower-energy states, leads to enhanced sensitivity to the local atomic environment. In an isolated atom of a transition element, the d -type energy levels are degenerate; they all have the same energy. In condensed matter, on the other hand, the relatively large spatial excursions made by the d electrons periodically bring them into close proximity with surrounding ions. It is generally recognized that the *refractive index* and *electron probability density* of many common glasses can be varied by changing the base glass composition, changing the sample temperature, subjecting the sample to pressure, and inducing a new transformation range history such as by reannealing.

Coloration of glass is caused by the presence of atoms of impurities. The most common sources of color in glass are the electronic processes associated with transition elements. One important way to deliberately color both glass and opaque ceramics is to produce in them small percentages of impurity atoms. Radiation energy is converted to kinetic energy of electron motion through the conduction band, and subsequent electron-atom collisions lead to a further conversion to heat energy. If the transfer is sufficiently large, the material is opaque to radiation at the frequency in question. In the absence of interband transitions, the material is transparent, with the atoms both absorbing and re-emitting light energy.

c) Nonlinear optical properties

Non-linear response is something very important for high index glasses like tellurite glasses. A material consists of nuclei surrounded by electrons. In dielectric materials these particles are bound, and the bonds have a degree of elasticity derived from the interaction between charged particles. When an electric field (E) is applied across the material, the positive charges (ions) are attracted, and the negative charges (electrons) are repelled slightly, which results in formation of a collection of induced dipole moments and hence polarization (P). The E can be in the form of voltage across the material, a light passing through the material, or a combination of both. A light wave comprises electric and magnetic fields, which vary sinusoidally at “optical” frequencies. The motion of charged particles in a dielectric medium when a light beam is passed through it is therefore oscillatory, and the particles form oscillating dipoles. Because the effect of the E is much greater than the effect of the magnetic field, the latter can, for all intents and purposes, be ignored. Also because the electrons have a lower mass than the ions, it is the motion of the former that is significant at high optical frequencies (UV and VISIBLE regions of the spectrum). The electric dipoles oscillate at the same frequency as the incident E and modify the way that the wave propagates through the medium. The electric displacement (D) is shown by the following equation^[32-38]:

$$D = \epsilon_0 E + P \quad (1.11)$$

where ϵ_0 is the free-space permittivity.

The field-dependent refractive index n_2 can be written as:

$$n_2 = 1 + \chi^{(1)} + \chi^{(2)} + \dots \quad (1.12)$$

Oscillation of the electromagnetic wave results in oscillation of the induced dipole moment which in turn results in the generation of light with different frequencies from that of the incoming light wave. It should be noted that the applied E used in the above equation is the total field and can be made up of a number of contributions (i.e., both optical and electric).

Hyperpolarizability can be pointed out as a measure of nonlinear response of materials. As we have pointed out high refractive index indicates high polarizability of materials and exhibiting high nonlinearity. Hyperpolarizability of tellurite glasses can be attributed to the empty 5 d orbital/ the lone pair of electrons present in the tellurium. Dense glass produced with particular modifiers increases the number of NBOs, which are highly polarizable and useful in nonlinear photonic device applications.

Simmons et al. [39] reported on nonlinear optical processes in glasses and glass-based composites. Applications of $\chi^{(1)}$ have been examined in lenses, optical fibers, and physical optics, whereas applications of $\chi^{(2)}$ have been accomplished by frequency doubling, in the second harmonic generation (SHG), and applications of $\chi^{(3)}$ are performed by frequency tripling in the third harmonic generation (THG).

1.4.5 Applications of tellurite glasses

Tellurite glasses are of interest for both scientific and technological viewpoints, due to their unique and promising physical properties. As stated

in the international glass database system^[1], applications of new glasses that are considered most promising and important include the following:

- 1) Optical glass fiber
- 2) Microlenses
- 3) Optical-wave guides
- 4) IC photo masking
- 5) Glass substrates for display uses
- 6) Glass hard disks
- 7) Zero-expansion glass and glass-ceramics
- 8) Press molding of spherical lenses
- 9) Light adjustment glasses
- 10) Glass-ceramic building materials
- 11) Glass substrates for solar cells
- 12) Artificial bones, dental implants, and crowns
- 13) Antibacterial glasses

1.5 Scope of the thesis

Tellurite glasses are finding widespread applications in the field of Photonics, due to some of its characteristic features like high refractive index, low phonon energy, low transition temperature and excellent infrared transmission^[17-22]. It has been reported that, these glasses are good candidates for hosting rare-earth ions because of their low phonon-energy environment, good chemical durability and optical properties^[17-22], which helps them find applications in pressure sensors or as a new laser host. The erbium-doped tellurite glasses also have shown optical and chemical properties suitable for photonic applications such as laser light modulators, optical limiters and are thermally stable for fiber drawing^[40-45]. Above description makes it clear that,

Tellurite glasses are known to be an important amorphous system that has many potential commercial applications.

Research on physical properties and structure of amorphous materials including glass is still to be understood. Today, research is being accelerated to overcome the considerable theoretical difficulties in understanding the properties and structures of amorphous solids. The benefits will include providing the fundamental bases of new optical glasses with many new applications, especially tellurite-glass-based optical fibers. New materials for optical switches; second-harmonic-generation, third-order-nonlinear optical materials; up-conversion glasses, and optical amplifiers need greater research attention, although there are many cases, in which researchers have studied and attempted to identify other uses. New tellurite glasses ^[1] are those that have novel functions and properties, such as a higher light regulation, extraordinary strength, or excellent heat and chemical durability, far beyond the characteristics of conventional glasses. These functions and properties are realized through high technologies, such as super high purification and ultra precise processing; controlled production processes, utilization of new materials as composites in glass, and full exploitation of various specific characteristics of conventional glasses.

The exhibited structural, thermal and optical properties of tellurite glasses prove them to be competing with fluorides and chalcogenides, two promising new glass systems designed by Yasui and Utsuno ^[46]. Structural measurements in tellurite glasses are very essential to interpret their physical and chemical properties. Tellurites are less toxic than chalcogenides, more chemically and thermally stable which makes them a highly suitable fiber material for nonlinear applications in the midinfrared and they are of

increased research interest in applications like laser, amplifier, sensor etc. Low melting point and glass transition temperature helps tellurite glass preparation easier than other glass families. The stability of tellurite glasses lends itself to the need for reliable structural measurements. In order to probe into the versatility of tellurite glasses in optoelectronic industry; we have synthesized and undertaken various optical studies on tellurite glasses.

1.6 Summary and conclusions

This chapter is an introduction to amorphous solids in general and the phenomena associated with them. The main focus in this chapter is on oxide glasses, where we confine our studies on tellurium oxide glasses. The importance of oxide glasses and its structural, thermal and optical properties are outlined. Zachariasen's continuous random network model which is applicable to covalently bonded glasses, such as tellurium oxide are explained in detail. The presence of defect states in tellurite glasses and the role of modifiers atoms in tuning the properties of these glasses have been discussed. Finally the scope of the thesis and applications of tellurite glasses in the field of photonics are discussed.

References

- [1] Raouf A. H. El-Mallawany, "Tellurite glasses Hand book-Physical properties and data", CRC press LLC, (2002).
- [2] Adler, D., "Amorphous Semiconductors", CRC Press, Boca Raton, FL, 5, (1971).
- [3] Vogel, W., "Chemistry of Glass", American Ceramics Society, Westerville, OH, (1985).
- [4] Masayuki Yamane, Yoshiyuki Asahara "Glasses for Photonics", Cambridge University Press, (2000).
- [5] Arun K Vashneya, "Fundamentals of inorganic glasses", Accademic press Inc, (1994).
- [6] W.H. Zachariasen, "The Atomic Arrangement in Glass". J. Amer. Chem. Soc. 54: 3841, (1932).
- [7] D.L.Wood, J. Tauc, "Weak absorption tails in amorphous semiconductors", Phy.Rev. B, 5, 8, (1972).
- [8] Mott, N. F. and Davis, E. A., "Electronic Processes in Non-Crystalline Materials", Oxford University Press, 1st ed. 1971, 2nd ed. (1978).
- [9] Nevill Mott, "Electrons in Glass", Nobel Lecture, Cavendish Laboratory, Cambridge, England, (1977).
- [10] David Munoz Martin, "TeO₂- based film glasses for photonic applications: structural and optical Properties", Laser Processing Group Universidad Investigaciones Cientcas Instituto de Optica Complutense de Madrid, (2009).
- [11] C. Wright, G. A. N. Conell, J. W. Allen, "Amorphography and the modeling of amorphous solid structures by geometric transformations", J. Non-Cryst. Solids 42, 69, (1980).
- [12] www.chemistryexplained.com
- [13] Barady, G. "X-Ray Study of Tellurium Oxide Glass", J. Chem. Phys., 24, 477, (1956).
- [14] Barady, G. "Structure of Tellurium Oxide Glass", J. Chem. Phys., 27, 300, (1957).
- [15] Winter, "Glass formation", J. Am. Ceram. Soc., 40, 54, (1957).
- [16] Wells, A. F., "Structure of Inorganic Chemistry", 4th ed., Oxford Univ. Press, Oxford, U.K., (1975).
- [17] A.A. Sidek, S. Rosmawati, Z.A. Talib, M.K. Halimah and W.M. Daud, "Synthesis and Optical Properties of ZnO-TeO₂ Glass System", Am. J. Applied Sci. 6 (8), 1489-1494, (2009).

- [18] D.L. Sidebottom, M.A. Hruschka, B.G. Potter, and R.K. Brow, “*Structure and Optical Properties of Rare Earth-Doped Zinc Oxyhalide Tellurite Glasses*,” J. Non-Cryst. Sol. 222, 282, (1997).
- [19] B Erariah, “*Optical properties of Lead-tellurite glasses doped with samarium trioxide*”, Bull. Mater Sci 33, 391–394, (2010).
- [20] R. El-Mallawany, M. Dirar Abdalla, I. Abbas Ahmed, “*New tellurite glass: Optical properties*”, Mater. Chem. and Phy., 109, 291–296, (2008).
- [21] M. R. Sahar, K. Sulhadi, M. S. Rohani, “*Spectroscopic studies of TeO₂–ZnO–Er₂O₃ glass system*”, Mater Sci 42:824–827, (2007).
- [22] Sun K, “*Preparation and characterization of rare earth glasses*”, Thesis, Brown University, (1988).
- [23] Richard K. Brow ,Web course, “*Physical properties of glass*”, Missouri University of Science & Technology Department of Materials Science & Engineering
- [24] Fernandez Navarro, J. M. El vidrio. CSIC, Madrid, (2003)
- [25] T. Komatsu, T. Noguchi, and R. Sato, “*Heat Capacity Changes at the Glass Transition in Mixed-Alkali Tellurite Glasses*”, J. Am. Ceram. Soc. 80, 1327 (1997).
- [26] T. Komatsu, T. Noguchi, and Y. Benino, “*Heat capacity changes and structural relaxation at glass transition in mixed-alkali tellurite glasses*” ,J. Non-Cryst. Solids 222, 206 (1997).
- [27] Charles Kittel, “*Introduction to Solid State Physics*”, - 7th ed. (ISBN 0-471-11181-3) Chapter 13, or 8th ed. (ISBN 0-471-41526-X)
- [28] D. E. Aspnes, “*Local -field effects and effective -medium theory: A microscopic perspective*”, Am. J. Phys. 50, 704, (1982).
- [29] Born, Max, and Wolf, Emil, “*Principles of Optics: Electromagnetic Theory of Propagation, Interference and Diffraction of Light*”, (7th Ed.) Cambridge University Press (1999).
- [30] MILLER R. C. “*Optical second harmonic generation in piezo-electric crystals*,” Appl. Phys. Lett., 5, 17, (1964).
- [31] Mott N F and Davis E A, “*Conduction in non-crystalline systems V. Conductivity, optical absorption and photoconductivity in amorphous semiconductors*”, Philos. Mag. 28, 903(1970).
- [32] Robert W. Boyd, “*Nonlinear Optics*”, Academic Press – Elsevier, Amsterdam, (2008).

- [33] P.N. Butcher and D. Cotter, “*The elements of Nonlinear Optics*”, Cambridge Univ.Press, Cambridge (1991).
- [34] M. Shubert and B. Wilhelmi, “*Nonlinear Optics and Quantum Electronics*”, Wiley, New Yorkk (1986).
- [35] F.A. Hopf and G.I. Stegeman, “*Applied Classical Electrodynamics, Vol. 1: LinearOptics and Vol.2: Nonlinear Optics*”, Wiley, New York (1986).
- [36] C. Flytzanis, “*Theory of nonlinear optical susceptibilities, in Nonlinear Optics*”, Part A, H. Rabin and C.L. Tang, eds., Academic Press, New York (1975).
- [37] R.L. Sutherland, “*Handbook of Nonlinear Optics*”, Marcel Dekker, New York (1996).
- [38] Y. R. Shen, “*The Principles of Nonlinear Optics*”, J. W. Wiley Interscience, New York, (1984).
- [39] Simmons, C., and El-Bayoumi, O., Ed., “*Experimental Techniques of Glass Science*”, The Am. Ceram. Soc., Westerville, OH, 129, (1993).
- [40] X. Feng et al. “*Single-mode tellurite glass holey fiber with extremely large mode area for infrared nonlinear applications*”, Opt. Express 16, 13651, (2008).
- [41] M. D. O’Donnell et al “*Tellurite and Fluorotellurite Glasses for Fiber optic Raman Amplifiers: Glass Characterization, Optical Properties, Raman Gain, Preliminary Fiberization, and Fiber Characterization`*”, J. Am. Ceram. Soc. 90, 1448, (2007).
- [42] J. S. Wang, E. M. Vogel, and E. Snitzer, “*Tellurite glass: a new candidate for fiber devices*”, Opt. Mater. Amsterdam, Neth.3, 187, (1994).
- [43] J. S. Wang, E. M. Vogel, E. Snitzer, J. L. Jackel, V. L. Da Silva, and Y.Silberberg “*1.3 μm emission of neodymium and praseodymium in tellurite-based glasses*”, J. Non-Cryst. Solids 178, 109, (1994).
- [44] J. S. Wang, D. P. Machewirth, F. Wu, E. Snitzer, and E. M. Vogel, “*Neodymium-doped tellurite single-mode fiber laser*”, Opt.Lett. 19, 1448, (1994).
- [45] P. Joshi, S. Shen, and A. Jha, “*Er³⁺-doped boro-tellurite glass for optical amplification in the 1530–1580nm*”, J. Appl. Phys. 103, 083543,(2008).
- [46] Yasui, F. Utsuno, “*Designing glass material systems using a database* “, Am. Ceram. Soc. Bull., 72, (1993).



ESSENCE OF CHARACTERIZATION TECHNIQUES

The present chapter deals with the description of various characterization techniques used in the present research work. First part of this chapter describes formation of glasses by melt quench method, emphasizing the fact that fast cooling is required from the glass melt in order to avoid crystallization. Structural characterization techniques such as X-ray Diffraction technique (XRD), Fourier Transform Infrared spectroscopy (FTIR); thermal characterizations such as Differential Scanning Calorimetry (DSC) and optical characterizations such as optical absorption spectroscopy, fluorescence spectroscopy etc. is described in detail. Experimental techniques such as thermal poling and Z-scan technique are discussed in this chapter. Thermal poling allow structural modifications in the glass network and the latter is a simple experimental set up to study the third order susceptibility of a material medium.

2.1 Introduction

Characterization techniques are important to researchers for they are the basic tools in identifying the structure and thereby properties of materials synthesized which help in determining whether the designed materials are suitable for particular applications. We present the preparation and the experimental techniques to find out the structural, thermal, linear and nonlinear optical properties of tellurite glasses.

2.2 Glass preparation

Most common glass preparation techniques in glass research are melt quench method, chemical vapor deposition and sol gel method. Bulk glasses in this research were prepared using melt quenching method. Melt quenching technique was the first glass preparation technique used in glass industry as well as in research field, before chemical vapour deposition and sol gel technique^[1, 2]. One of the important features of the melt quenching technique is the flexibility of preparing a large number of compositions of glass of silicate, borate, phosphate, oxide or non oxide systems. The doping or codoping of different types of active ions is quiet easy using this method. Compared to other glass preparation methods, the disadvantage is that the lack of purity of the prepared glass sample. In order to avoid contamination, the crucibles made of noble metals like Gold, Platinum etc can be used.

2.2.1 Melt quench method to prepare bulk tellurite glasses

The glass starting materials were weighed using electronic balance after batch calculation. The glass batch was melted in a platinum crucible at 800 °C and cast into a rectangular brass/Steel mold at room temperature. All the melting processes were done using an electric furnace manufactured by High heat furnace and refractories /Heat globe[figure 2.1]. Each glass sample was immediately transferred to an annealing furnace at 300°C and slowly cooled to room temperature^[3-5]. These samples were then polished using various grades of silicon carbide powder for obtaining parallel, smooth and clear surface for experiment. The thickness of the glass specimens was measured using a digital micrometer gauge.



Figure 2.1: Furnace used for melt quenching

2.3 Structural characterization techniques

X-RAY Diffraction and Fourier Transform Infrared spectroscopy are the structural investigation techniques used in this dissertation for tellurite glass samples.

2.3.1 X-ray diffraction spectroscopy

X-ray diffraction spectroscopy is the basic characterization technique that verifies whether the prepared sample is having Short Range Order (SRO), which is an indication of vitreous state. It is a rapid analytical technique primarily used for phase identification of a crystalline material and can provide information on unit cell dimensions. The material to be analyzed is finely ground, homogenized, and average bulk composition is determined. Hence it is also called the powder diffraction method. Max von Laue, in 1912, discovered that crystalline substances act as three-dimensional diffraction gratings for X-ray wavelengths similar to the spacing of planes in a crystal lattice. X-ray diffraction is now a common technique for the study of crystal structures and atomic spacing. X-ray diffraction is based on constructive interference of monochromatic X-rays and a crystalline sample. The interaction of the incident rays with the sample produces constructive

interference (and a diffracted ray) when conditions satisfy Bragg's Law ($n\lambda = 2d \sin\theta$) [6].

This law relates the wavelength of electromagnetic radiation to the diffraction angle and the lattice spacing in a crystalline sample. These diffracted X-rays are then detected, processed and counted. By scanning the sample through a range of 2θ angles, all possible diffraction directions of the lattice should be attained due to the random orientation of the powdered material. Conversion of the diffraction peaks to d-spacing allows identification of the mineral because each mineral has a set of unique d-spacing. If a material does not show this diffraction peaks it proves that the material is not a crystal and must be non crystalline. We have used the Bruker AXS D8 Advance diffractometer whose source of X rays is Cu, Wavelength 1.5406 Å.

2.3.2 Fourier Transform Infrared Spectroscopy (FTIR)

Fourier transform infrared spectroscopy is one of an effective tool for resolving the structure of local arrangements in glasses, along with Raman spectroscopy [7]. These non-destructive techniques provide extensive information about the structure and vibrational properties of glasses. The quantitative interpretation of the absorption bands of the IR spectra according to the value of the stretching force constant and reduced mass of the vibrating cation-anion has been discussed. Interpretation of the IR absorption curves show that, co-ordination number determines the nature of the spectra.

Infrared spectroscopy exploits the fact that molecules absorb specific frequencies that are characteristic of their structure. These absorptions are resonant frequencies, i.e. the frequency of the absorbed radiation matches

the frequency of the bond or group that vibrates. The energies are determined by the shape of the molecular potential energy surfaces, the masses of the atoms, and the associated vibronic coupling. In particular, in the Born–Oppenheimer and harmonic approximations, i.e. when the molecular Hamiltonian corresponding to the electronic ground state can be approximated by a harmonic oscillator in the neighborhood of the equilibrium molecular geometry, the resonant frequencies are determined by the normal modes corresponding to the molecular electronic ground state potential energy surface. Nevertheless, the resonant frequencies can be in a first approach related to the strength of the bond, and the mass of the atoms at either end of it. Thus, the frequency of the vibrations can be associated with a particular bond type.

Infrared spectroscopy exploits the fact that molecules have specific frequencies at which they rotate or vibrate. FTIR is used both to gather information about the structure of a compound and as an analytical tool to assess the purity of a compound. The IR region is divided into three regions: the near, mid, and far IR. The mid IR region is of greatest practical interest, which lies between wavelengths 3×10^{-4} and 3×10^{-3} cm. In IR spectroscopy, an organic molecule is exposed to infrared radiation. When the radiant energy matches the energy of a specific molecular vibration, absorption occurs. The wavenumber, plotted on the X-axis, is proportional to energy; therefore, the highest energy vibrations are on the left. The percent transmittance (%T) is plotted on the Y-axis. Absorption of radiant energy is therefore represented by a trough in the curve: zero transmittance corresponds to 100% absorption of light at that wavelength^[8].

IR source emits an IR beam which is split into two identical beams; one goes through the sample and the other through a reference cell.

Reference cell typically consists of the solvent that the sample is dissolved. IR spectroscopy is used to measure the amount of energy absorbed when the frequency of the infrared light is varied.

2.4 Thermal characterization

2.4.1 Thermal Annealing

Annealing is the process of reducing residual strain in glass by controlled heating and cooling. Annealing, in metallurgy and materials science, is a heat treatment wherein a material is altered, causing changes in its properties such as hardness and ductility. It is a process that produces conditions by heating to above the critical temperature, maintaining a suitable temperature, and then cooling. Annealing is used to induce ductility, soften material, relieve internal stresses, and refine the structure by making it homogeneous.

In the cases of copper, steel, silver, and brass, this process is performed by substantially heating the material (generally until glowing) for a while and allowing it to cool, so that it is softened and prepared for further work such as shaping, stamping, or forming.

Annealing occurs by the diffusion of atoms within a solid material, so that the material progresses towards its equilibrium state. Heat is needed to increase the rate of diffusion by providing the energy needed to break bonds. The movement of atoms has the effect of redistributing and destroying the dislocations in metals and (to a lesser extent) in ceramics. This alteration in dislocations allows metals to deform more easily, so increases their ductility

The amount of process-initiating Gibbs free energy in a deformed metal is also reduced by the annealing process. In practice and industry, this reduction of Gibbs free energy is termed stress relief. The relief of internal

stresses is a thermodynamically spontaneous process; however, at room temperatures, it is a very slow process. On annealing, mechanical properties, such as hardness and ductility, change as dislocations are eliminated and the metal's crystal lattice is altered. On heating at specific temperature and cooling, it is possible to bring the atom at the right lattice site and new grain growth can improve the mechanical properties.

2.4.2 Glass transition temperature measurement-DSC

Thermal characterization of the bulk tellurite glasses was done using Differential scanning Calorimetry (DSC). A Mettler-Toledo DSC model 822e is used to follow the thermal behavior of the samples. The apparatus is equipped with a ceramic sensor FRS5 (heat-flux sensor with 56 thermocouples Au-Au/Pd) [9]. The differential scanning calorimeter was previously calibrated using indium and zinc standards for temperature and power calibration. The autosampler available on the Mettler-Toledo DSC 822e is used to automate the experimental procedure. 10 mg of the samples were sealed in a pierced aluminum crucible and heated under nitrogen flow (200 mL/min outside the oven, 100 mL/min inside the oven). Sample was then heated at a rate of $10^0\text{C}/\text{min}$. This heating rate improves the calorimetric response (without a decrease of accuracy) and reduces the time of the analysis and, consequently, the risk of sample degradation.

The DSC curves are used to record the differential heat input to a sample, expressed as the heating rate (dH/dT) in meters per joule per second or meters per calorie per second on the ordinate against T or time (t) on the abscissa [8]. The idealized representation of the three major processes observed by DSC is as follows [11]:

- a) Exothermal upwards

- b) Endothermic downwards
- c) Displacement (d) for estimation of Cp

When the ΔH of a reaction is >0 , the sample heater in the DSC instrument is energized and a corresponding signal is obtained. For an exothermic change ($\Delta H < 0$), the reference heater is energized to equilibrate the sample and reference temperatures again and restore ΔT to zero, which gives a signal in the opposite direction. Because these energy inputs are proportional to the magnitude of the thermal energies involved in the transition, the records give calorimetric measurements directly. The peak areas in DSC are proportional to the thermal effects experienced by the sample. When the sample is subjected to a heating program in DSC, the rate of heat into the sample is proportional to its Cp. Virtually any chemical/physical process involves a change in the value of Cp for the sample. The technique of DSC is particularly sensitive to such change, which may be detected by the displacement of the base line from one nearly horizontal position to another. Such displacement occurs just to the right of the endothermic on the DSC record. So Tg can also be determined from the DSC curves.

2.5 Linear Optical characterization

2.5.1 Absorption spectroscopy

JASCO V-570 UV/VIS/NIR Spectrophotometer was used for the absorption, transmission and reflectance measurements of the samples. The spectrometer consist of Optical system: single monochromatic, UV/ VIS region 1200 lines/ mm plane grating, NIR region: 300 lines/ nm plane grating, Czerny –Turner mount double beam type Resolution: 0.1 nm (UV/ VIS region) 0.5 nm (NIR region). Light source: 30 mW deuterium

discharge tube in 190 nm to 350 nm region, 20 W tungsten iodine lamp in 330 to 2500 nm region, Wavelength range: 190 nm to 2500 nm^[11]. The beam from the light source is converged and enters the monochromator. It is dispersed by the grating in the monochromator and the light passes out through the exit slit. This light is split into two light paths by a sector mirror, one incident on the sample to be measured and the other on the reference sample such as solvent. The light that has passed through the sample or reference sample is incident on the photomultiplier tube and PbS photoconductive cell which are the detectors. In the reflectance measurement the set up has to be changed. The Model SLM-468 single reflection attachment^[12] is designed to measure the relative reflectance of sample using the forward reflected light from the aluminum-deposited plane mirror as reference. It permits the measurement of the reflectance of metal deposited film, metal plating etc. The wavelength range is 220 nm to 2200 nm with a beam port diameter of 7 mm and angle of incidence approximately 5°^[12].

For each wavelength of light passing through the spectrometer, the intensity of the light passing through the reference cell is measured (I_0). The intensity of the light passing through the sample cell is also measured for that wavelength (I). If I is less than I_0 , then obviously the sample has absorbed some of the light. For reasons to do with the form of the Beer-Lambert Law^[7], the relationship between A (the absorbance) and the two intensities are given by:

$$A = \log_{10} \frac{I_0}{I} \quad (2.1)$$

And the absorption coefficient, $\alpha=A/d$, d = thickness of the sample. Generally, the absorption edge of these glasses is determined by the oxygen

bond strength in the glass-forming network. Any change of oxygen bonding in the glass network, for instance, changes the formation of non bridging oxygen, thereby changing the characteristic absorption edge. For glasses and amorphous materials α is given by the Tauc^[14-19], s relation,

$$\alpha(\omega) = B(\hbar\omega - E_{\text{opt}})^n / \hbar\omega, \quad (2.2)$$

where, B is a constant and n is an index which takes values of 2, 1/2 for indirect and direct transitions.

Band gap of tellurite glasses are calculated for indirect transitions, using Tauc plot, with $(\alpha h\nu)^{1/2}$ along y-axis and E_{opt} along x-axis.

2.5.2 Refractive index (RI) measurement

Refractive index is a measure of the distortion of atomic electron clouds by the electromagnetic field of an external incident light beam. Refractive index for a particular transparent medium is the ratio of the speed of light in one media compared to another, mathematically expressed as $n_i = v_1 / v_2$, where refractive index = n_i at a specific wavelength i , and the speed of light in each media are v_1 and v_2 . For glass analysis, v_1 is the speed of light in a vacuum.

Refractive indices were determined from the band gap.^[20-23]

$$\left(\frac{n^2 - 1}{n^2 + 1} \right) = 1 - \sqrt{\frac{E_g}{20}} \quad (2.3)$$

Refractive index can be calculated from the measured Brewster angle, which is related to refractive index as^[13]

$$n = \tan \theta_B \quad (2.4)$$

Refractive indices were determined by measuring Brewster's angle using 633 nm He-Ne laser as light source.

2.5.3 Fluorescence spectroscopy

Optical fluorescence of glasses was carried out using Cary Eclipse Fluorescence spectrophotometer of VARIAN ^[24]. It has a single cell holder for liquid sample analysis and a solid sample holder accessory to perform fluorescence measurements on solid samples. The solid sample holder accessory provides both rotational and translational adjustment of the sample. The angle of incidence of the excitation may be varied from 20°- 35°C. This is the angle between the exciting light and a line perpendicular to the surface of the sample mounting slide. The source of excitation is xenon lamp.

2.5.4 Laser induced fluorescence spectroscopy

Laser induced photoluminescence is spontaneous emission from atoms or molecules that have been excited by laser radiation. Two radiative transitions are involved in the Laser induced photoluminescence process. First, absorption takes place, followed by a photon-emission. Laser induced photoluminescence is a dominant laser spectroscopic technique in probing of unimolecular and bimolecular chemical reactions. This technique serves as a sensitive monitor for the absorption of laser photons in fluorescence excitation spectroscopy. It is well suited to gain information on molecular states if the fluorescence spectrum excited by a laser on a selected absorption transition is dispersed by a monochromator. Experimental set up for Laser induced luminescence is shown in figure 2.2. The pump beam is taken from a Quanta Ray Q-switched Nd: YAG laser which emits pulses of 7 ns duration at 532 nm and 355 nm, at a repetition rate of 10 Hz ^[26]. A

cylindrical lens is used to focus the pump beam in the shape of a stripe on the sample. In the present case it is adjusted to a pump beam width of 7 mm. The output is collected from the edge of the front surface of the sample using an optical fiber in a direction normal to the pump beam. The emission spectra are recorded with Acton monochromator attached with a CCD camera. Princeton Instruments NTE/CCD air cooled detectors have three distinct sections. The front vacuum enclosure contains the CCD array seated on a cold finger. This finger is in turn seated on a four-stage Peltier thermoelectric cooler. The back enclosure contains the heat exchanger. An internal fan cools the heat exchanger and the heat exits the unit through openings in the housing ^[27].

The CCD array used is Roper Scientific NTE/CCD-1340/100-EM. The electronics enclosure contains the preamplifier and array driver board. This keeps all signal leads to the preamplifier as short as possible, and also provides RF shielding SPEC-10 controller of Princeton Instruments controls the CCD.

SpectraPro-500i is a 500 mm focal length monochromator/ spectrograph. It features an astigmatism-corrected optical system, triple indexable gratings and triple grating turret. The SpectraPro-500i includes a direct digital grating scan mechanism with full wavelength scanning capabilities, plus built-in RS232 and IEEE488 computer interfaces. The 1200 grooves/mm grating has an aperture ratio f/6.5. The scan range is 0 to 1400 nm (mechanical range) and an operating range of 185 nm to the far IR and a resolution of 0.05 nm at 435.8 nm. WinSpec, the spectroscopic software, of Princeton Instruments is used for collecting, storing and processing data from the Roper Scientific system. ^[28]

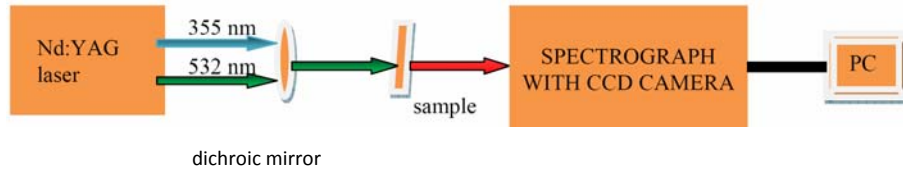


Figure 2.2: Laser induced luminescence experimental set up.

2.6 Nonlinear optical characterization

2.6.1 Non-linear optics

Nonlinear optics is the study of phenomena that occur as a consequence of the modification of the optical properties of a material system by the presence of light. Typically only laser light is sufficiently intense to modify the optical properties of a material system. In fact the beginning of the field of nonlinear optics is often taken to be the discovery of Second Harmonic Generation by Franken et.al in 1961, shortly after the demonstration of the first working laser by Maiman in 1960 [29]. Nonlinear optical phenomena are nonlinear in the sense that they occur when the response of a material system to an applied optical field depends in a nonlinear manner upon the strength of the optical field [29-35]. In the case of optical nonlinearity, the input variables are light waves and nonlinear phenomena is evidenced by changes in the optical properties as the intensity of the input light is increased. Non linear effects create new spectral components by shifting spectral energy to new frequencies.

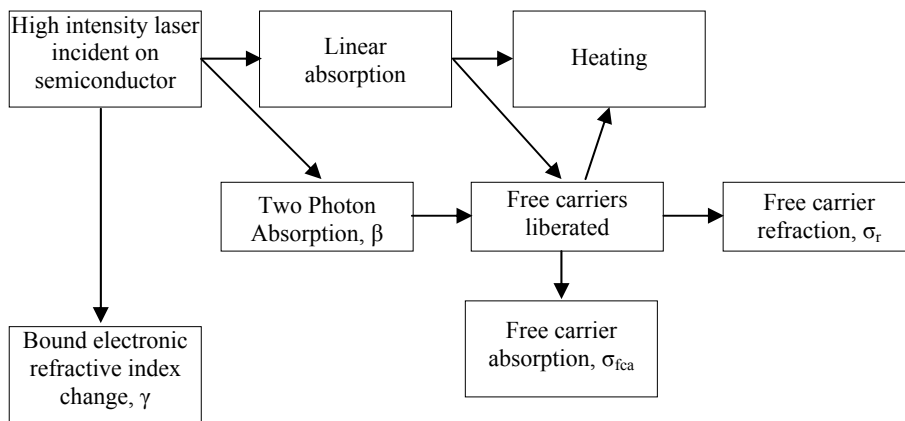
The polarization or the dipole moment per unit volume produced in the material medium, by the external electric field of an intense light beam is given by [29-35]:

$$P = \epsilon_0 \left[\chi^{(1)} E + \chi^{(2)} E^2 + \chi^{(3)} E^3 + \dots + \chi^{(n)} E^n \right] \quad (2.5)$$

where, $\chi^{(n)}$ is an (n+1)th rank tensor with 3^{n+1} terms.

Semiconductors exhibit a broad range of diverse nonlinearities such as two photon absorption, free carrier absorption, the electronic Kerr effect and nonlinear refraction associated with free carrier generation etc. Two photon absorption is being investigated for a material using a laser having photon energy sub-bandgap to it.

A summary of the various nonlinear processes is given below ^[36].



2.6.2 Open/closed aperture Z-scan

There are a number of techniques for measuring the optical nonlinearity exhibited by semiconductors such as degenerate four wave mixing, optical Kerr effect, ellipse rotation, interferometric methods etc. The z-scan technique was invented by Shiehe Bahae et.al ^[37]. It has many advantages over other nonlinear measurement techniques that it is simple, very sensitive and fast, giving the sign of optical nonlinearity immediately. There are closed and open aperture z-scan; the former is sensitive to both nonlinear absorption and refraction and the latter is sensitive to only nonlinear absorption. Figure 2.3 shows the experimental set up of z scan technique.

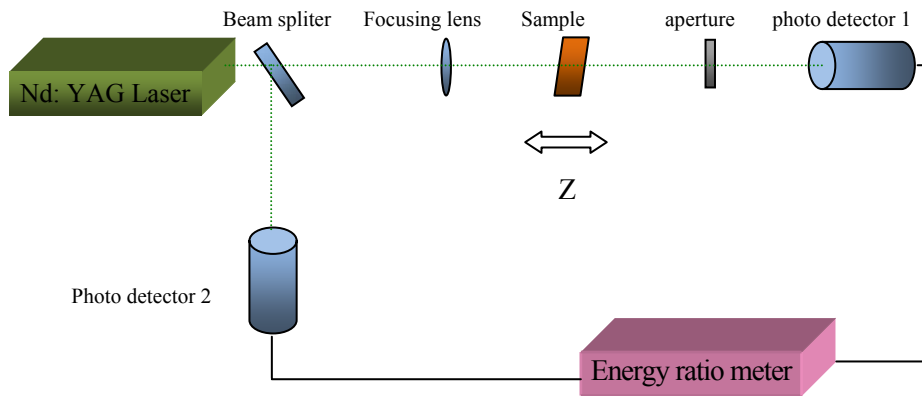


Figure 2.3: Experimental set up for z scan

In the present investigation, we have employed the single-beam z-scan technique with nanosecond laser pulses to measure the nonlinear optical absorption properties of zinc tellurite glasses. A Q-switched Nd: YAG laser (Spectra Physics LAB-1760, 532 nm, 7 ns, 10 Hz) is used as the light source. The sample is moved in the direction of the light incidence near the focal spot of the lens with a focal length of 20 cm radius of the beam waist ω_0 is calculated to be $42.56\mu\text{m}$. The Rayleigh length, $z_0 = \pi\omega_0^2 / \lambda$, is estimated to be 10.06 mm, much greater than the thickness of the sample, which is an essential prerequisite for z-scan experiments. The transmitted beam energy, reference beam energy, and their ratio are measured simultaneously by an energy ratio meter (Rj7620, Laser Probe Corp.) having two identical pyroelectric detector heads (Rjp735). The sample was moved along the z-axis by a motorized translational stage. At the focus the power output of the laser beam was measured in GW/cm^2 . The z-scan system is calibrated using carbon disulphide, which is taken as a standard nonlinear material. The effect of fluctuations of laser power is eliminated by dividing the transmitted power by the power obtained at the reference detector^[38]. Z-scan technique

is highly sensitive to the profile of the beam and also to the thickness of the sample. Any deviation from gaussian profile of the beam and also from thin sample approximation will give rise to erroneous results. For ensuring that the beam profile does not vary appreciably inside the sample, the sample thickness should always be kept less than the Rayleigh's range. The sensitivity of this z-scan method is used to monitor nonlinear refraction at low irradiance levels, where a third order nonlinearity attributed to n_2 caused by bound electrons can be observed. At higher irradiance levels the refraction caused by two photon absorption induced free charge carriers becomes significant.

Theory of Z-scan

The light irradiating the sample experiences an approximately homogeneous population distribution as it propagates through the medium. As the excitation intensity increases to levels where the photon density is comparable to the population density an induced regime transition may occur where the absorption coefficient is depleted or enhanced corresponding to increases or decreases in the transmission respectively. The resultant regime depends upon the absorption cross sections of the ground and excited state levels and the lifetimes of the various allowable transitions in the system.

A negative nonlinear refractive index giving rise to self-defocusing of a light beam can cause substantial amounts of the energy of the incident light to be absorbed by an exit aperture in the optical system. Materials with a positive nonlinear absorption coefficient exhibit Reverse Saturable Absorption (RSA) ^[39], and are characterized by a high transmission at normal light intensities and a decrease in transmission under high intensity or high fluence illumination. Conversely, the opposite situation, where the transmission increases with increasing incident intensity the process is

termed Saturable Absorption (SA) ^[40-42]. The materials with SA usually have a negative nonlinear absorption coefficient.

Non linear absorption of a sample is manifested in the open aperture z- Scan measurement. If the sample is having nonlinear absorption such as two photon absorption (TPA) ^[43], it is manifested in the measurement as a transmission minimum at the focal point. Otherwise, if the sample is a saturable absorber, the transmission increases with increase in incident intensity and results in transmission maximum at the focal region. In the absence of an aperture the transmitted light measured by the detector is sensitive only to intensity variations in the nonlinear absorption. The nonlinear absorption coefficient is obtained by fitting the experimental z-scan plot to Eq. (1)

$$T(Z, S = 1) = \sum_{m=0}^{\infty} \sum_{m=0}^{\infty} \frac{[-q_o(z)]^m}{[m+1]^{3/2}} |q_o(z)| < 1 \quad (2.6)$$

where:

$$q_o(z) = \frac{[I_0 \beta L_{eff}]}{1 + (Z^2 / Z_0^2)} \quad (2.7)$$

and $Z_0 = k \omega_0^2 / 2$, is the diffraction length of the beam

$k = 2\pi/\lambda$ is the wave factor, ω_0 = the beam waist radius at the focal point, $L_{eff} = (1 - \exp(-\alpha L)) / \alpha$, is the effective thickness of the sample.

The basis of closed aperture z-scan is the self refraction and self phase modulation effects. The technique relies on the transmittance measurement of a nonlinear medium through a finite aperture in the far field as a function of the sample position z with respect to the focal plane using a single gaussian beam in tight focus geometry. Consider, for instance, a material with a negative nonlinear refraction and thickness smaller than the

diffraction length of the focused beam being positioned at various points along the z -axis. This assumption implies that the sample acts as a thin lens of variable focal length due to the change in refractive index at each position ($n = n_0 + n_2 I$)^[38]. The irradiance is low and there is negligible nonlinear refraction. Hence the transmittance characteristics are linear. As the sample is moved close to the focus, the beam irradiance increases, leading to self lensing in the sample. A negative self lensing prior to focus will tend to collimate the beam, causing a beam narrowing at the aperture which results in an increase in the measured transmittance. As the scan in z direction continues and passes the focal plane, the sample which acts as a negative lens increases the defocusing effect thus increasing the beam divergence, leading to beam broadening at the aperture. Hence the transmittance decreases. Thus there is a null as the sample crosses the focal plane (z_0). The z -scan is completed as the sample is moved away from focus ($+z$) such that the transmittance become linear since the irradiance is again low. A prefocal transmittance maxima (peak) followed by a post focal transmittance minima (valley) is the z -scan signature of negative refraction nonlinearity^[38].

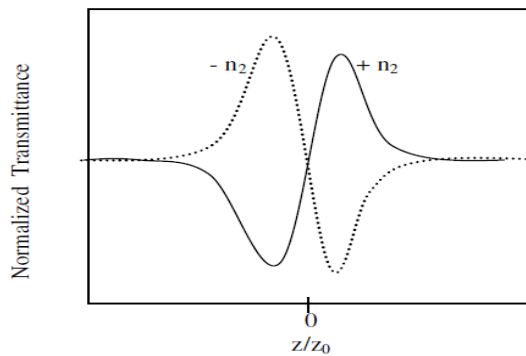


Figure 2.4: Typical closed aperture z -scan curves of samples having positive (solid line) and negative (dashed line) nonlinearity.

The curves for closed z-scan in the case of positive nonlinearity and negative nonlinearity shows opposite effects as depicted in figure 2.4. This is the case of purely refractive nonlinearity where nonlinear absorption is absent. In the presence of multiphoton absorption, there is a suppression of the peak and enhancement of the valley, whereas the opposite effect occurs if there is a saturation of absorption ^[43]. In a cubic nonlinear medium the index of refraction (n) is expressed in terms of nonlinear indices n_2 (m^2/W) through

$$n = n_0 + n_2 I \quad (2.8)$$

where n_0 is the linear index of refraction, n_2 the intensity dependent refractive index and I denotes the irradiance of the laser beam within the sample. For calculating the radial phase variations $\Delta\phi(r)$, the slowly varying envelope approximation (SVEA) ^[38] is used, by a pair of simple equations

$$\frac{d\Delta\phi}{dz} = \Delta n(I) k \quad (2.9)$$

$$\frac{dI}{dz} = -\alpha(I) I$$

where z is the propagation depth in the sample and $\alpha(I)$ in general includes linear and nonlinear absorption terms. In the case of cubic nonlinearity and negligible nonlinear absorption, the above equations can be solved to get the phase shift $\Delta\phi$ at the exit of the sample and is given by

$$\Delta\phi(z, r, t) = \Delta\phi(z, t) \exp\left(-\frac{2r^2}{\omega^2(z)}\right) \quad (2.10)$$

with

$$\Delta\phi(z, t) = \frac{\Delta\phi_0(t)}{\left[1 + \frac{z^2}{z_0^2}\right]} \quad (2.11)$$

where $\Delta\phi_0(t)$ is the on axis phase shift at the focus which is defined as

$$\Delta\phi_0(t) = kn_2 I_0(t) L_{eff} = \frac{\Delta T_{p-v}}{0.406(1-s)^{0.25}} \quad (2.12)$$

where $I_0(t)$ is the on axis irradiance at focus (i.e. at $z=0$). The far field condition $d \gg z_0$ can give a geometry-independent normalized transmittance for positive nonlinear refraction as

$$T(z) = 1 - \frac{4\gamma\Delta\phi_0(t)}{(\gamma^2 + 9)(\gamma^2 + 1)} \quad (2.13)$$

where $\gamma = z/z_0$

From the closed aperture z-scan fit, $\Delta\phi_0$ can be obtained. Then the nonlinear refractive index n_2 can be determined using equation

$$n_2 = \frac{\Delta\phi_0(t)}{kI_0(t)L_{eff}} \quad (2.14)$$

The n_2 is related to $\text{Re}(\chi^{(3)})$ by the relation,

$$\text{Re}(\chi^{(3)}) = \frac{n_o n_2}{3\pi} (esu) \quad (2.15)$$

From the real and imaginary part of $(\chi^{(3)})$, the modulus of third order nonlinear susceptibility can be found out.

$$|\chi^{(3)}| = \sqrt{[\text{Re}(\chi^{(3)})]^2 + [\text{Im}(\chi^{(3)})]^2} \quad (2.16)$$

The magnitude of $(\chi^{(3)})$ is significantly affected by the molecular orientation and it determines the strength of nonlinearity of the material.

2.6.3 Two Photon Absorption (TPA)

Two photon absorption is defined as the electronic excitation of a molecule induced by simultaneous absorption of pair of photons of same/different energy. This was first predicted by M.G. Mayer in 1931^[44] and calculated the transition probability for a two quantum absorption [figure 2.5] process. This occurs via a short lived virtual state. For a reasonable chance of it occurring, high intensity radiation is required, so that many photons are present in a small area.

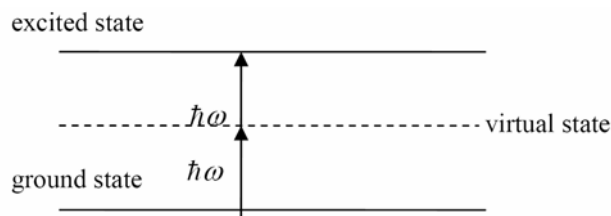


Figure 2.5: Schematic representation of TPA.

Two Photon Absorption is a third order non linear optical process and was first observed in a semiconductor in 1964^[45].

The energy absorbed through a two photon process is quadratically proportional to the intensity of the incident light. It is given by

$$\frac{dI}{dz} = -\alpha I - \beta I^2, \beta = \text{TwoPhotonAbsorptionCoefficient} \quad (2.17)$$

2.6.4 Free Carrier Absorption (FCA)

In addition to TPA, large refractive nonlinearities can occur due to free carriers generated in the material. These were first reported at band gap resonant wavelengths by Miller et al^[46]. If a photon of energy greater than

the bandgap of the material is absorbed, it will excite an electron to the conduction band, and so free carriers are generated. They will relax to the lower conduction band and at high intensities; they are again excited to the higher conduction band levels.

Free Carrier Absorption is given by:

$$\frac{dI}{dz} = -\alpha I - \sigma_c N_c(I)I \quad (2.18)$$

Where,

N_c = Intensity dependent carrier density

σ_c = FCA cross section.

Two photon induced free carrier absorption is

$$\frac{dI}{dz} = -\alpha I - \beta I^2 - \sigma_c N_c(I)I \quad (2.19)$$

2.6.5 Excited State Absorption (ESA)

When ground state absorption is bleached at high optical intensities, absorption of photo carriers in the excited state, to higher state takes place, and it is known as ESA.

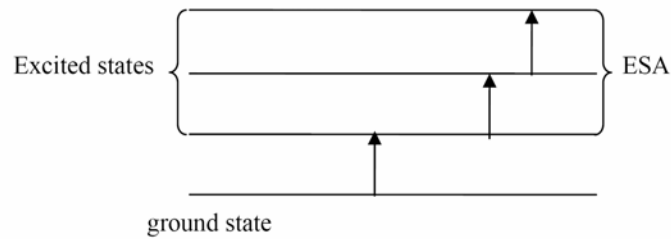


Figure 2.6: Schematic representation of ESA.

2.6.6 Saturable and Reverse Saturable Absorption (SA & RSA)

Saturable absorption refers to the case of excited state absorption (ESA), where the transmission increases with incident intensity, and indicates that the ground state absorption has bleached. The general expression for the absorption coefficient in terms of a parameter called the saturation intensity,

$$\alpha = \frac{\alpha_0}{\left(1 + \frac{I}{I_{sat}}\right)} \quad (2.20)$$

where I_{sat} is the intensity at which the absorption coefficient drops to half of its linear value. Investigations on the effect of excited-state absorption on the transmission of a saturable absorber, proves that it precluded the possibility of the absorption bleaching totally, and termed this effect as residual absorption. It can be noted that the intensity (I) and the pulse energy density (defined as $F = EPulse/(\pi\omega(z)^2)$, where $EPulse$ is the energy per pulse and $\pi\omega(z)^2$ is the surface area through which the pulse is propagating at any position denoted by z , are directly related to each other.

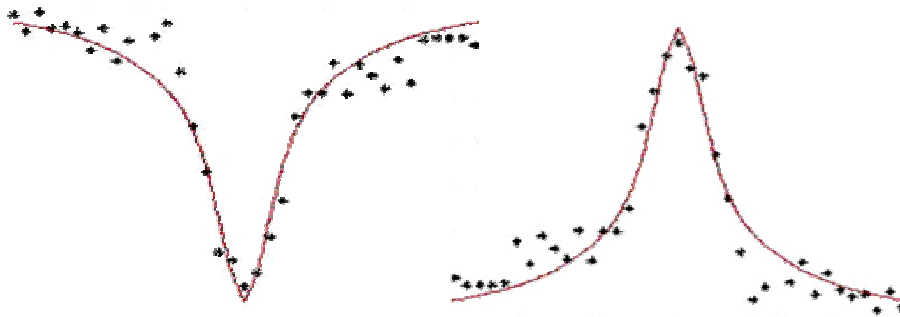


Figure 2.7: Schematic representation of RSA and SA.

Conversely, the opposite situation, where the transmission decreases with increasing incident intensity, is termed reverse saturable absorption (RSA). This occurs when the excited-state absorption cross-section is greater than that of the ground-state. Whenever the excited-state absorption cross section is greater than that of the ground state, RSA is observed as an increase in the normalized intensity-(or energy-density) dependent absorption coefficient with respect to increasing normalized pulse energy density. This shows the gross effects of RSA, and highlights the crucial role that the excited-state absorption plays in the overall absorption coefficient and approximates the limit of temporally long pulse widths (i.e., nanosecond irradiation) when all other lifetimes in the material are of the order of pico-seconds.

2.6.7 Optical Limiting [OL]

Optical limiting is an important application of nonlinear optics, useful for the protection of human eyes, optical elements and optical sensors from intense laser pulses. An important term in the optical limiting measurement is the limiting threshold. It is defined as the input fluence (or energy) at which the transmittance is reduced quickly [figure 2.8] from the linear transmittance^[47, 48]. It is obvious that the lower the optical limiting threshold, the better the optical limiting material.

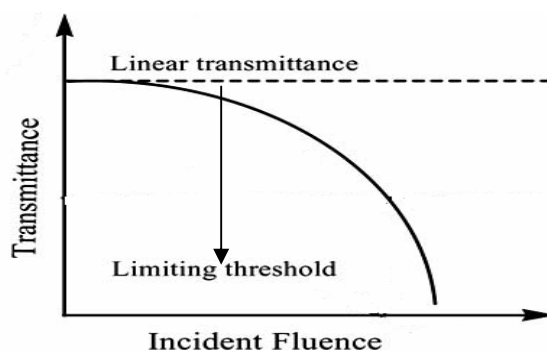


Figure 2.8: Schematic representation of Optical limiting.

RSA is the NLO property which leads to the concept of Optical Limiting: Strong attenuation of high intensity light and potentially damaging light such as focused laser beams, whilst allowing for the high transmission of ambient light. Usually, the most important mechanism for optical limiting is nonlinear absorption, nonlinear refraction and nonlinear scattering as well. In the case when the incident light is sufficiently intense so that a significant population accumulates in the excited state and if the material has an excited state absorption cross section that is larger than the ground state cross section, the effective absorption coefficient of the material increases. To achieve the largest nonlinear absorption, both a large excited state absorption cross section and a long excited state lifetime are required. When the lifetime of the excited state being pumped is longer than the pulse width of the incident light, the changes in the absorbance and the refractive index are fluence (J cm^{-2}), not intensity (W cm^{-2}) dependent. Therefore, in materials with long upper state lifetimes, it is the fluence rather than the intensity that is limited. Limiting the fluence is usually desirable, since damage to optical devices is also often fluence dependent. A practical optical limiter must operate over the wide range of incident intensities that might be encountered. The condition that excited state absorption cross section is greater than that of ground state is necessary, but it is not sufficient for a useful OL material. The nonlinear response should possess a low threshold and remain large over a large range of fluences before the nonlinearity saturates. High saturation fluence normally requires a high concentration of the nonlinear material in the optical beam.

2.6.8 Nonlinear refraction (NLR)

Nonlinear index of refraction is the change in refractive index or the spatial distribution of the refractive index of a medium due to the presence of optical waves, which has generated significant and technological interest. It

has been utilized for a variety of applications such as nonlinear spectroscopy, correcting optical distortions, optical switching, optical logic gates, optical data processing, optical communications, optical limiting, passive laser mode-locking, wave guide switches and modulators. The general dependence of the NLR on intensity is given by ^[38]:

$$n(r, t) = n_0(r, t) + \Delta n [I(r, t)] \quad (2.21)$$

This equation indicates that the change in the refractive index, Δn over its value at low intensities, n_0 , has a functional dependence on intensity, $I(r, t)$. Several physical mechanisms that contribute to the NLR include electronic polarization; Raman induced kerr effect, molecular orientational effects, electrostriction, population redistribution, thermal contributions, cascaded second order effects and photorefractive effect.

2.6.9 Merits and demerits of z-scan technique

This technique has several advantages, some of which are

- 1) Simplicity of the technique as well as simplicity of interpretation.
- 2) Simultaneous measurement of both sign and magnitude of nonlinearity.
- 3) Possibility of isolating the refractive and absorptive parts of nonlinearity.
- 4) High sensitivity, capable of resolving a phase distortion of $\lambda/300$.
- 5) Close similarity between z-scan and the optical limiting geometry.

Some of the disadvantages include,

- 1) Stringent requirement of high quality gaussian TEM₀₀ beam for absolute measurements.
- 2) Beam walk-off due to sample imperfections, tilt, or distortions.
- 3) Not suitable for measurements of off diagonal elements of the susceptibility tensor, except when a second non-degenerate frequency beam is employed.
- 4) The determination of the nonlinear coefficients depends on the temporal and spatial profiles, power or energy content and stability of the laser source.

2.7 Thermal poling

Second-order nonlinear (SON) optical properties are forbidden in glasses which exhibit inversion symmetry on a macroscopic scale. However, it is possible to induce a second-order nonlinear susceptibility in bulk glass using specific treatment like optically assisted poling or thermal poling^[49-59]. Among them, thermal poling that applies dc voltage at high temperature is most commonly used. Tellurium based glasses are one among the oxide/chalcogenide glasses which are finding a number of applications due to their properties such as high refractive index, low phonon energy, low transition temperature, excellent infrared transmission and very high optical nonlinearities. The purpose of thermal poling in this thesis is to investigate its effect on the optical properties of zinc tellurite glass samples.

Glass samples for the present work were synthesized by rapid melting quenching method. These samples were polished using various grades of

silicon carbide powder for obtaining parallel, smooth and clear surface for experiment. The thickness of the glass specimens was measured using a digital micrometer gauge. Thermal poling measurements were carried out by the setup shown in Figure 2.9. The poling was performed on 1.3 mm thick samples placed in between two flat electrodes made of stainless steel.

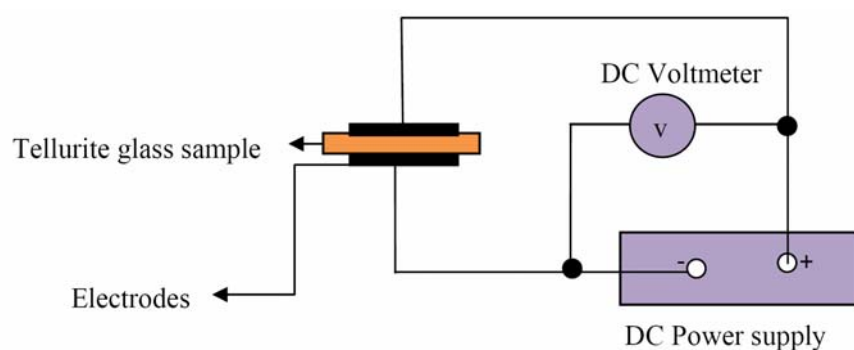


Figure 2.9: Experimental set up for thermal poling

The glass sample sandwiched between the electrodes were put into a furnace and heated to an aimed temperature from 100 - 300°C .After holding the samples at a temperature for 30 minutes, an electric field 1-2 kV was applied. The temperature was then decreased to room temperature while the voltage was held a constant. The applied dc field was removed after the sample reached the room temperature. References ^[60-63] describe the thermal poling experiment in detail. Maximum temperature range for thermal poling is limited to the glass transition temperature. Absorption spectra were taken before and after thermal poling. The optical absorption spectra of the glass samples were determined using JASCO V-570 double beam UV-visible spectrophotometer. The indirect band gap of the glass is estimated from the graph of $h\nu$ Vs $(\alpha h\nu)^{1/2}$.

To check the enhancement in the third order nonlinear optical absorption properties of $\text{TeO}_2 (1-x) - \text{ZnO } x$ glasses due to thermal poling, we have used the single-beam z-scan technique^[38] with nanosecond laser. A Q-switched Nd: YAG laser (Spectra Physics LAB-1760, 532 nm, 7 ns, 10 Hz) is used as the light source for the experiment.

2.8 Summary and conclusions

This chapter discusses the preparation and characterization techniques for melt quenched bulk tellurite glass used in the research work. The structural characterization techniques used such as X Ray Diffraction and Fourier Transform Infrared Spectroscopy, Differential Scanning Calorimetry used for thermal analysis and optical characterization techniques used for the absorption, transmission and reflectance measurements are discussed in detail. Photoluminescence studies of glasses carried out using Fluorescence spectrophotometer are also discussed.

The major experimental tools used for the study are Z scan technique for nonlinear characterization of the sample, thermal poling to tune the linear and non linear optical properties of zinc tellurite glasses and Laser Induced Fluorescence spectroscopy to probe into the defect states of these glasses.

References

- [1] Masayuki Yamane and Yoshiyuki, “*Glasses for Photonics*”, Cambridge University Press, Spain (2000).
- [2] Valentina Kokorina, “*Glasses for Infrared Optics*”, CRC Press, Boca Raton, Fla (1996).
- [3] M. R. Sahar, K. Sulhadi, M. S. Rohani, “*Spectroscopic studies of TeO_2 - ZnO - Er_2O_3 glass system*”, Mater Sci, 42:824–827, (2007).
- [4] Vogel E M, “*Glasses as Nonlinear Photonic Materials*”, J. Am. Ceram. Soc. 72, 719,(1989).
- [5] A.A. Sidek, S. Rosmawati, Z.A. Talib, M.K. Halimah and W.M. Daud, “*Synthesis and Optical Properties of ZnO - TeO_2 Glass System*”, Am. J. Applied Sci. 6 (8), 1489-1494, (2009).
- [6] A.L. Patterson, “*The Sherrer formula for X-Ray particle size determination*”, Phys.Rev. , 56(10), 978-982, (2002).
- [7] Online edition for students of organic chemistry lab courses at the University of Colorado, Boulder, Dept of Chem. and Biochem. (2002)
- [8] Arun K Vashneya, “*Fundamentals of inorganic glasses*”, Accademic press inc.,
- [9] A Mettler-Toledo DSC model 822e manual.
- [10] Raouf H. El-Mallawany, “*Tellurite glasses Hand book-Physical properties and data*”, CRC press LLC, (2002).
- [11] Model V-550/560/570 Spectrophotometer Hardware/Function manual (data station type).JASCO Corporation, Tokyo, Japan, (1996).
- [12] Model SLM-468 single reflection attachment instruction manual.JASCO Corporation, Tokyo, Japan, (1994).
- [13] H. E. Bennett and J. M. Bennett, “*Polarization, in Handbook of Optics*”, W. G. Driscoll and W .Vaughan , eds .McGraw-Hill , New York , 10-1 to 10-164, (1978) .
- [14] Mott N F and Davis E A, “*Conduction in non crystalline systems.5.conductivity, optical absorption and photoconductivity in amorphous semi conductors*”, Philos. Mag. 28, 903, (1970).
- [15] Burger H, Kneipp K, Hobert H, Vogel W, “*Glass formation, properties and structure of glasses in the TeO_2 - ZnO system*”, J Non-Cryst Solids 151,134-142, (1992).

- [16] Komatsu T, Tawarayama H, Mohro H and Mutusita K, “*Properties and crystallization behaviors of TeO₂LiNbO₃ glasses*”, J.Non-Cryst. Solids 135,105, (1991).
- [17] Sheenu Thomas, J.Philip, “*Optical band gap, infrared absorption and thermal diffusivity of Ge-Ga-Se glasses*”, *Phys.Stat. Sol.*, 200, 359-365, (1997).
- [18] Sidebottom DL, Hruschka MA, Potter BG, Brow RK, “*Structure and Optical Properties of Rare Earth-Doped Zinc Oxyhalide Tellurite Glasses*”, J Non-Cryst Solids 222,282(1997).
- [19] Sun K, “*In: Preparation and characterization of rare earth glasses*”, Thesis, Brown University (1988).
- [20] B Erariah, “*Optical properties of Lead-tellurite glasses doped with samarium trioxide*”, *Bull. Mater Sci* 33,391–394, (2010).
- [21] R. El-Mallawany, M. Dirar Abdalla, I. Abbas Ahmed, “*New tellurite glass: Optical properties*”, *Mater. Chem. and Phys.*, 109, 291–296, (2008).
- [22] V. Dimitrov, S. Sakka, “*Electronic oxide polarizability and optical basicity of simple oxides*”, *J. Appl. Phys.* 79 , 1736,(1996).
- [23] P. Gayathri Pavana, K. Sadhanab, V. Chandra Mouli, “*Optical, physical and structural studies of boro-zinc tellurite glasses*”, *Physica B*, 406, 1242–1247, (2011).
- [24] Cary Eclipse Hardware operation manual. VARIAN. Australia (2000).
- [25] Wolfgang Demtrder “*Laser spectroscopy: Basic concepts and instrumentation*”, (3rd edition) Springer, New Delhi, India (2004).
- [26] Quanta-Ray, Pulsed Nd: YAG lasers User’s manual GCR-100 series, Spectra-Physics, USA (1997).
- [27] Princeton Instruments NTE/CCD, Manual, Roper Scientific, Inc. USA, (2001).
- [28] Win Spec, “*spectroscopic software of Princeton Instruments*”, Roper Scientific, USA (2001).
- [29] Robert W. Boyd, “*Nonlinear Optics*”, Academic Press – Elsevier, Amsterdam, (2008).
- [30] P.N. Butcher and D. Cotter, “*The elements of Nonlinear Optics*”, Cambridge Univ. Press, Cambridge (1991).
- [31] M. Shubert and B. Wilhelmi, “*Nonlinear Optics and Quantum Electronics*”, Wiley, New York (1986).
- [32] F.A. Hopf and G.I. Stegeman, “*Applied Classical Electrodynamics, Vol. 1: Linear Optics and Vol.2: Nonlinear Optics*”, Wiley, New York (1986).

- [33] C. Flytzanis, “*Theory of nonlinear optical susceptibilities, in Nonlinear Optics*”, PartA, H. Rabin and C.L. Tang, eds., Academic Press, New York (1975).
- [34] R.L. Sutherland, “*Handbook of Nonlinear Optics*”, Marcel Dekker”, New York (1996).
- [35] Y. R. Shen, “*The Principles of Nonlinear Optics*”, J. W. Wiley Interscience, New York, (1984).
- [36] Trefor James Sloanes, “*Measurement and application of optical nonlinearities in indium phosphide, cadmium mercury telluride and photonic crystal fibers*”, University of St. Andrews, (2009).
- [37] Mansoor Sheike Bahae, Ali A. Said, Tai-Huei Wei, David J Hagan, E.W. Van Stryland, “*Sensitive measurement of optical non linearity’s using a single beam*”, IEE J. of quant. Electron., 26,760-769,(1990).
- [38] L. Irimpan, V. P. N. Nampoori, and P. Radhakrishnan, “*Spectral and nonlinear optical characteristics of nanocomposites of ZnO–CdS*” J. Appl. Phys. 103D, 094914, (2008).
- [39] N. K. M. Naga Srinivas, S. Venugopal Rao, and D. Narayana Rao, “*Saturable and reverse saturable absorption of Rhodamine B in methanol and water*”, J. Opt. Soc. Am. B, 20, 12, (2003).
- [40] A. Yariv. “*Quantum Electronics*”, 2nd ed., Wiley, New York, 165, (1975).
- [41] U. P. Wild, R. Renn, C. De Caro, S. Bernet, “*Spectral Hole Burning and Molecular Computing*”, Appl. Opt. 29, 4329, (1990).
- [42] R. M. Macfarlane, R. M. Shelby, “*Sub kilohertz optical line width of the 7F0-5D0 Transition in Y2O3:EU3+*”, Opt. Commun. 39, 169, (1981).
- [43] Richard L Sutherland; “*Handbook of nonlinear optics*”, CRC press (2003)
- [44] Goepfert-Mayer, “*Über Elementarakte mit zwei Quantensprüngen*”. M. Ann. Phys., 9, 273, (1931).
- [45] R. Braunstein, N. Ockman, “*Optical double-photon absorption in CdS*” Phys. Rev. 134, 499, (1964).
- [46] MILLER R. C., “*optical second harmonic generation in piezoelectric crystals*”, Appl. Phys. Lett., 5, 17, (1964).
- [47] J A Herman and J Staromlynska; “*Trends in optical switches, limiters and discriminators*”, Int. J. Nonlinear Opt. Phys. 2, 271, (1993).
- [48] L W Tutt and T F Boggess; “*A review of optical limiting mechanisms and devices using organics, fullerenes, semiconductors and other materials*” Prog. Quant. Electr. 17, 299, (1993).

- [49] R. A. Myers, N. Mukherjee, and S. R. J. Brueck, “Large second-order nonlinearity in poled fused silica”, *Opt. Lett.* 16, 1732, (1991).
- [50] N. Mukherjee, R. A. Myers, and S. R. J. Brueck, “Dynamics of second-harmonic generation in fused silica”, *J. Opt. Soc. Am. B* 11,665(1994).
- [51] P. G. Kazansky, V. Pruneri, and P. St. J. Russell, “Blue-light generation by quasi-phase-matched frequency doubling in thermally poled optical fibers”, *Opt. Lett.* 20, 8, 843, (1995).
- [52] L. J. Henry, A. D. DeVilbiss, and T. E. Tsai, “Effect of preannealing on the level of second-harmonic generation and defect sites achieved in poled low-water fused silica”, *J. Opt. Soc. Am. B* 12, 2037,(1995).
- [53] H. Nasu, H. Okamoto, K. Kurachi, J. Matsuoka, K. Kamiya, A. Mito, and H. Hosono, “Second-harmonic generation from electrically poled SiO₂ glasses: effects of OH concentration, defects, and poling conditions”, *J. Opt. Soc. Am. B* 12, 644 (1995).
- [54] T. Fujiwara, M. Takahashi, and A. Ikushima, “Second-harmonic generation in germanosilicate glass poled with ArF laser irradiation”, *Appl. Phys. Lett.* 71, 8, 1032, (1997).
- [55] P. G. Kazansky, A. Kamal, and P. St. J. Russell, “High second-order nonlinearities induced in lead silicate glass by electron-beam irradiation”, *Opt. Lett.* 18, 9, 693, (1993).
- [56] Kameyama, E. Muroi, A. Yokotani, K. Kurosawa, and P. Herman, “X-rayradiation effects on second-harmonic generation in thermally poled silica glass”, *J. Opt. Soc. Am. B* 14, 1088, (1997).
- [57] Kameyama, A. Yokotani, and K. Kurosawa, “Identification of defects associated with second-order optical nonlinearity in thermally poled high-purity silica glasses,” *J. Appl. Phys.* 89, 4707, (2001).
- [58] Kameyama, A. Yokotani, and K. Kurosawa, “Generation and erasure of second-order optical nonlinearities in thermally poled silica glasses by control of point defects”, *J. Opt. Soc. Am. B* 19, 2376 (2002).
- [59] Narazaki, K. Tanakai, K. Hirao, and N. Soga, “Effect of poling temperature on optical second harmonic intensity of sodium zinc tellurite glasses”, *J. Appl. Phys.* 83, 3986(1998).
- [60] Haitao Guo , Xiaolin Zheng , Xiujian Zhao ,Guojun Gao , Yueqiu Gong , Shaoxuan Gu, “Composition dependence of thermally induced second-harmonic generation in chalcogenide glasses”, *J Mater Sci* , 42:6549–6554 , (2007).

- [61] J. W. Dadge, S. K. Apte, S. D. Naik, B. B. Kale, R. C. Aiyer, “*Temperature dependent nonlinear coefficients and second harmonic generation in quaternary glass system doped with TiO₂*”, JOAM , 8, 1, 368 – 371,(2006).
- [62] Aiko Narazaki, Katsuhisa Tanaka, Kazuyuki Hirao, and Naohiro Soga, “*Effect of Poling Temperature on Optical Second-Harmonic Intensity of Lithium Sodium Tellurite Glass*”, J. Am. Ceram. Soc., 81 [10] 2735–37, (1998).
- [63] T. M. Proctor and P. M. Sutton, “*Space-Charge Development in Glass*”, J. Am. Ceram. Soc., 43 [4] 173–79 (1960).



STRUCTURAL, THERMAL, LINEAR AND NONLINEAR OPTICAL SPECTROSCOPY OF ZINC TELLURITE GLASSES

Third chapter focuses on the structural, thermal, linear and nonlinear optical studies of zinc tellurite glasses. Structural study using XRD reveals that the prepared material is amorphous in nature due to the absence of crystallization peaks. FTIR also contains information regarding the structural units TeO_4 and TeO_3 in the zinc tellurite glass network. From fluorescence studies we have observed a blue fluorescence emission, where the intensity was found to be proportional to the tellurium content. Tellurite glasses are in the category of highly nonlinear optical materials, due to their large refractive index. Our results also support this idea indicating the Two Photon Absorption behavior of zinc tellurite glasses. The reverse saturable absorption exhibited by these glasses proves them to be good optical limiters.

3.1 Introduction

Tellurite glasses are amorphous solids with special structural, physical and optical properties. The properties of tellurium oxides that give them their stability proves to be transferrable to their glass derivatives, allowing experimentation with a wider selection of elements in the composition of tellurite glasses and, thus, greater control over variations in performance characteristics ^[1]. According to Mallawany et al, glass formation occurs in materials of all chemical types, such as covalent, ionic, molecular, metallic and hydrogen bonded materials. A topic of great interest to glass researchers

and the optics industry, where we observe trends in industrial development, is preparation of glasses with high refractive index values, because such glasses possess special optical features.

Tellurium based glasses are of important today, because of their excellent optical and thermal properties^[1-9]. Among tellurite glasses, binary and ternary glasses containing zinc oxide are one of the stable systems which are under research, even though there are a number of research outcomes based on these systems. Our research outcomes prove that, at least a 40-60 % of tellurium dioxide (TeO_2) should be present in the in the zinc tellurite glass system in order to have the expected properties in them as shown in the phase diagram [figure 3.1].

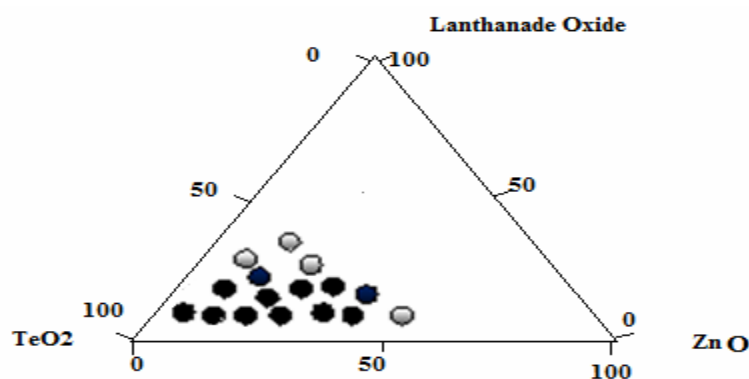


Figure 3.1: Phase diagram: Glass formation ranges of zinc tellurite glasses

The glass formation range of tellurite glass containing zinc oxide and lanthanide oxide are shown in the figure above. Considering the glass formation range we have selected three different basic combinations of glass

80 TeO_2 :20 ZnO , 75 TeO_2 :25 ZnO and 70 TeO_2 :30 ZnO respectively. The prepared glasses, appears pale /light or deep orange – brown and are transparent.

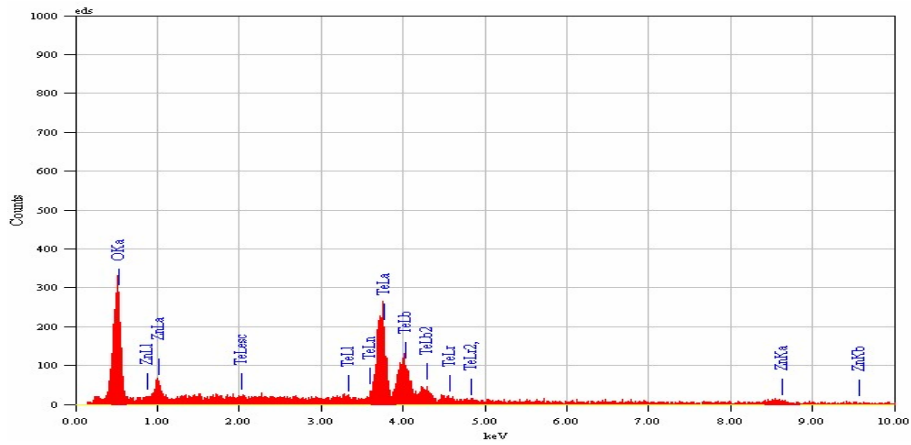
3.2 Structural properties of zinc tellurite glasses

Under normal conditions, tellurium dioxide itself is not a glass former, but forms glass with a modifier like alkali, alkaline earth and transition metal oxides or other glass formers^[10-12].

Several reasons can be listed out from the literature that^[13],

- a) Te – O bond is too strongly covalent to permit the requisite amount of distortion.
- b) The repulsive forces due to the lone pair of electrons resist the free movement of the basic structural unit of tellurite glass (trigonal bipyramid-TeO₄) in space during glass formation.

The structural modifications happening in the tellurite glass, with the modifier ions is such that the atomic arrangement lacks long range order and periodicity in its network. This type of short range/medium range order is similar to the atomic arrangement of liquids and is reflected in the X-ray Diffraction pattern of the glass. There is neither crystal lattice nor lattice point in the glass structure and therefore, instead of diffraction peaks a halo is seen in the X-ray Diffraction pattern^[2]. Figures given below [figure 3.2] shows X-ray Diffraction pattern of the three different glass samples prepared.



1

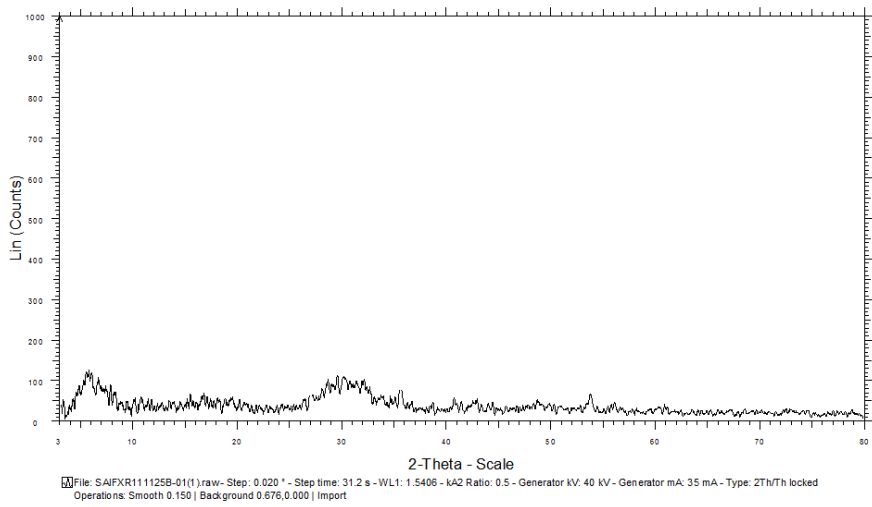


Figure 3.2: XRD and EDAX of 80 TeO₂:20 ZnO glass

Network modifiers play an important role in oxide glasses, because when a network modifier like ZnO enters into the tellurite glass network, Te - O - Te bridge breaks, producing Bridging Oxygen[(BO) ; Te - O - Te] and Non Bridging Oxygen[(NBO) ; Te - O - Zn, Zn - O - Zn]. Studies based on X-ray photoelectron spectroscopy reveal that the coordination states of tellurium atoms change from trigonal bipyramidal (tbp) TeO_4 to trigonal pyramidal (tp) TeO_{3+1} and TeO_3 with increasing ZnO contents^[14].

Based on the above said references, it is explained that the electron density of valence shell of BO atoms is equal to that of NBO atoms and cannot be distinguished from each other, because the electrons on the NBO atoms in TeO_n might be back donated to tellurium atoms and the electron might be delocalized through $p\pi - d\pi$ bonds between O 2p and empty Te 5d orbitals.

A Fourier transform Infrared spectrum is evidence to the structural modifications in the glass sample. Absorption peaks in the $400\text{-}500\text{ cm}^{-1}$ reported in the literature explain it has been due to symmetric stretching and bending vibration of Te-O-Te bridging bonds in TeO_4 sub units of the glass structure. The $550\text{-}750\text{ cm}^{-1}$ region in the spectra give idea about stretching vibrations of Te-O bonds in TeO_3 and TeO_{3+1} units^[1,15]. Intensity of IR absorption bands increases with increase in modifier ions. The absorption bands at $550\text{-}750\text{ cm}^{-1}$ range is reported^[15] to show a tendency to shift to higher wave number region as more TeO_3 and TeO_{3+1} units are produced in the glass network, though it is not clearly visible in the spectra recorded in our laboratory.

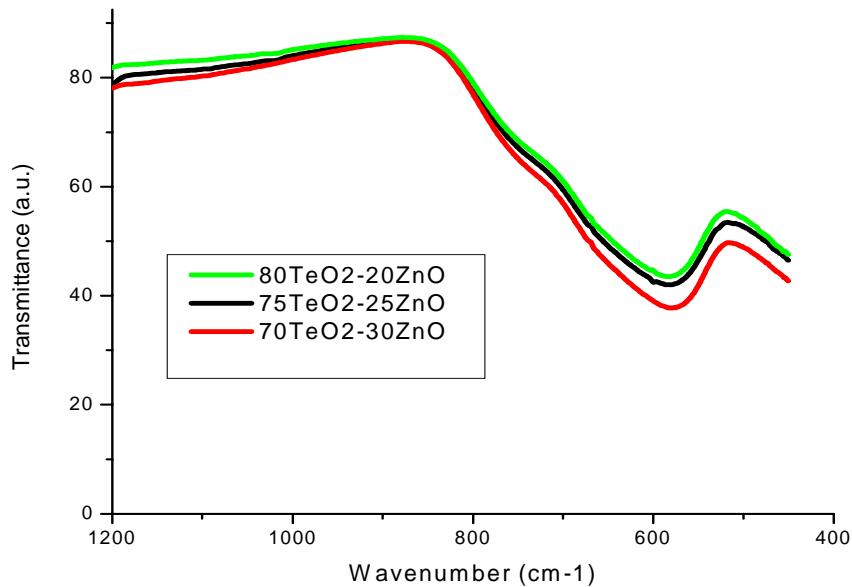


Figure 3.5: FTIR spectra of the zinc tellurite glasses

It is discussed above that the presence of network modifiers ,breaks some of the $\text{Te}-\text{O}_{\text{ax}}-\text{Te}$ bridges and the coordination state of tellurium is transformed from 4 to 3. The broken structural units include a $\text{Te}-\text{O}^-$ NBO bond and the other $\text{Te}-\text{O}$ bond elongates up to a distance higher than 2.2 \AA . This implies the formation of a structural unit of coordination 3 ,with one or two NBO [$\text{Te}-\text{O}^-$ or double bonded oxygen atoms $\text{Te}=\text{O}$] stabilized by the resonance between them. All these structural modifications studied using IR and Raman spectroscopy ^[5] reveal that each of the oxygen atom of the added modifier oxide ruptures a $\text{Te}-\text{O}-\text{Te}$ linkage forming two NBO and each of the two participating TeO_4 units transforms to TeO_3 with two NBOs. One of the terminal bonds of TeO_3 units is a double bond which delocalizes to both $\text{Te}-\text{O}^-$ NBO bonds and three $\text{Te}-\text{O}$ bonds are contributed by TeO_3 and TeO_{3+1} units and two bonds by TeO_4 units. From the structural investigation, we get an idea about the influence of

modifier ions to the stretching vibrations of Te-O bonds also, along with the transformation of structural units. The NB Te –O bonds created by the modifiers act as defects and destroy the three dimensional glass network and the cations with partial covalent bond with the oxygen stimulate the conversion of structural units ^[1]

Table 3.1: IR absorption bands in zinc tellurite glasses

IR absorption bands [Wave number (cm ⁻¹)]	Due to
400-500	Symmetric stretching and bending vibration of Te-O-Te bridging bonds in TeO ₄ sub units
550-750	Stretching vibrations of Te-O bonds in TeO ₃ and TeO ₃₊₁ units

3.3 Thermal characterization of zinc tellurite glasses

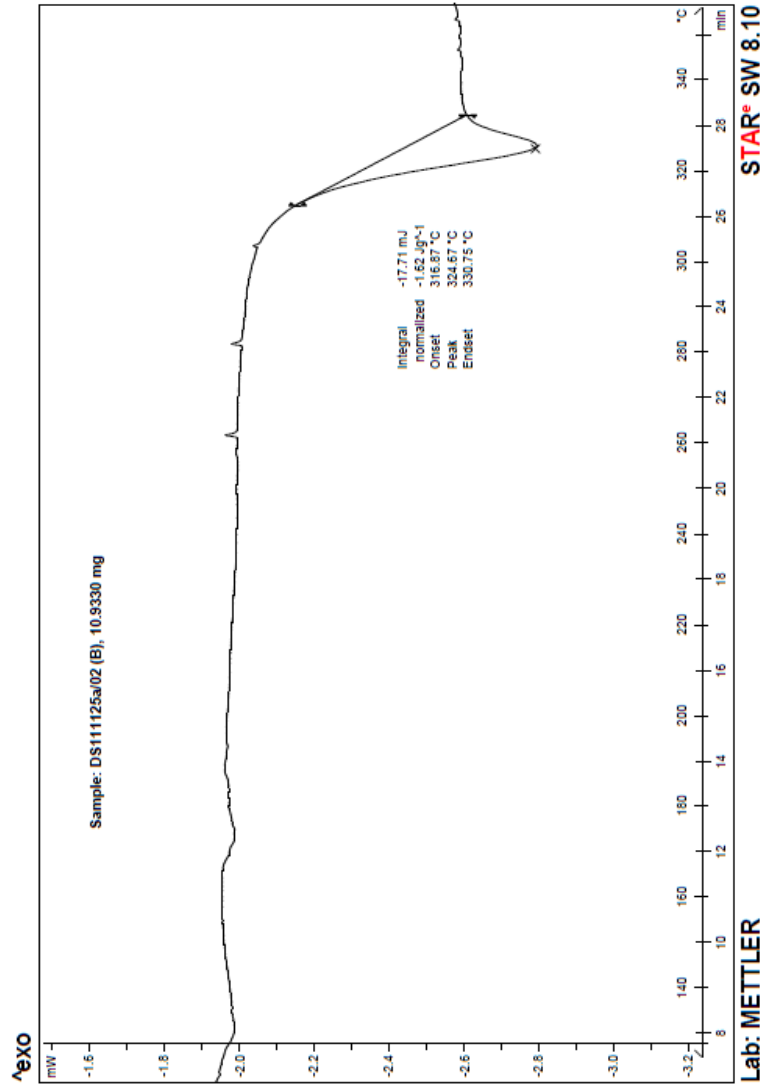


Figure 3.6: DSC Graph of 80 TeO₂:20 ZnO, glass sample.

One of the DSC graphs for tellurite glasses with varying ZnO concentration is shown above [figure 3.6]. The variation in glass transition temperature is such that, as the amount of modifier zinc oxide increases the glass transition temperature also increases. Changes in the molar volume can be attributed to changes in structure caused by decrease in interatomic spacing. The decrease in interatomic spacing results due to a corresponding increase in the stretching force constant of bonds in the glassy network.

Table 3.2: Glass transition temperatures of 80 TeO₂:20 ZnO, 75 TeO₂:25 ZnO and 70 TeO₂:30 ZnO glass samples.

sample	T _g (° c)
80 TeO ₂ :20 ZnO	325
75 TeO ₂ :25 ZnO	332
70 TeO ₂ :30 ZnO	336

The bond strength of modifier-oxygen are higher than that of tellurium–oxygen bonds which causes an increase in glass transition of the samples. Our results on structural and optical studies support the fact that there is a formation of Zn- O bonds, by rupture of bridging oxygen bonds, as the modifier enters in to the glass. This causes a dangling bond /localized state formation which is a characteristic feature of amorphous semi conductors. Hence the weak covalent bonds of Te-O-Te bridges gets replaced with strong O-Zn ionic bonds, in which the strong electrostatic field causes an increase in the glass transition temperature and melting point of the material of glass.

3.4 Linear Optical properties of zinc tellurite glasses

For transparent materials like glasses, optical properties are an important branch of study. Since tellurium dioxide itself is not a glass former its optical properties are compared with that of ionic tellurite crystal whose band gap is reported to be 3 eV. Optical constants are a measure of the optical properties exhibited by glasses. Optical absorption plot from which the band gap of glasses was determined is given in Figure 3.7. Band gap of the prepared samples were calculated from the expression [16]

$$\alpha(\omega) = B(\hbar\omega - E_{opt})^n / \hbar\omega \quad (1)$$

where, n is an index characterizing the transition,

$\alpha(\omega)$ = (Absorbance/thickness) of the sample,

$\ln(I_0/I)$ = absorbance

I_0 = incident intensity

I = intensity after traversing the thickness of the sample.

Extinction coefficient determined from $\alpha(\omega)$ is given by $k = \alpha(\omega)\lambda/4\pi$

It is observed that the band gap of the tellurite glasses decreases with increase in ZnO content. Refractive index calculated from Brewster angle measurements is given by

$$n = \tan \theta_B \quad (2)$$

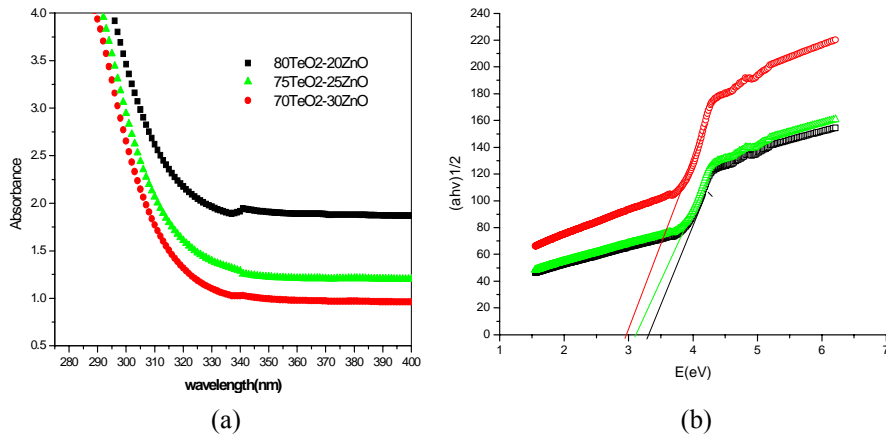


Figure 3.7: (a) Optical absorption spectra and (b) band gap of zinc tellurite glasses

It is understood from the data that the increase in density due to the addition of ZnO in the TeO₂ network results in an increase in the refractive index of the glass samples. Previous works on zinc tellurite glasses, reports that the addition of ZnO to tellurite glass structure creates a number of non-bridging ions in the network with the modifier ions (Zn²⁺) occupying the interstices of the network. Basic structural units TeO₄ is reduced in number with an increase in TeO₃ and TeO₃₊₁ polyhedra, where TeO₃₊₁ is the sub unit having a weak Te –O bond in the glass network [15, 17]. In other words defect states increases with the creation of dangling bonds in the Tellurite glass network [18]. The Urbach energy gives the width of localized states in to the gap at the band edge and is given by

$$\ln(\alpha) = B(\hbar\omega/\Delta E)$$

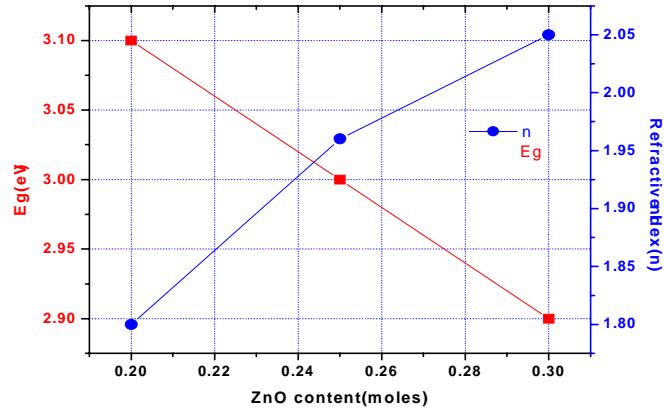


Figure 3.8: Variation of band gap and refractive index of zinc tellurite glasses

Addition of ZnO in tellurite glass network creates a more compact structure due to the production of nonbridging oxygen ions and an increase of defect states which in turn determines the band gap of the glass combinations.

The easier calculation for refractive index is that from the expression given by ^[19-25]

$$\left(\frac{n^2 - 1}{n^2 + 1} \right) = 1 - \sqrt{\frac{E_g}{20}} \quad (3)$$

Real and imaginary parts of dielectric constant can be determined from absorbance and refractive index values. The imaginary portion of the permittivity corresponds to a phase shift of the polarization \mathbf{P} relative to \mathbf{E} and leads to the attenuation of electromagnetic waves passing through the medium.

Linear susceptibility is related to dielectric constant by the relation $\epsilon(\omega) = 1 + \chi$. Simple empirical relation based on generalized Miller's rule ^[26] which can be used for the estimation of the nonlinear refractive index and

nonlinear susceptibility, predicts enhanced nonlinear effects with increase in ZnO in tellurite glasses.

Table 3.3: Optical constants of zinc tellurite glasses

Sample	E _g (eV)	n	ε	χ(esu)
80TeO ₂ -20ZnO	3.1	1.80	3.24	2.2
75TeO ₂ -25ZnO	3	1.96	3.84	2.8
70TeO ₂ -30ZnO	2.9	2.05	4.20	3.2

3.5 Fluorescence spectroscopy of zinc tellurite glasses

It is observed that TeO₂-ZnO glass shows fluorescence in two different wavelengths in the visible region when excited with 375 nm radiation. The major transition is located around violet region and the minor one at the green region. The intensity variation gives information that the major transition is due to the tellurium dioxide and the minor one sensitively depends on zinc oxide content. On considering 420 nm emission, the interesting observation is that there is a nonlinear enhancement of fluorescence intensity with TeO₂ content, which imply that there are two connected variations. Observations from the spectra are given below:

- The increase in intensity from 75TeO₂-25ZnO to 80TeO₂-20ZnO is tremendous than the variation from 70TeO₂-30ZnO to 75TeO₂-25ZnO.
- Green transition also increases with tellurium content, but for 75TeO₂-25ZnO there is another peak dominating, which is diminished in the 80TeO₂-20ZnO.

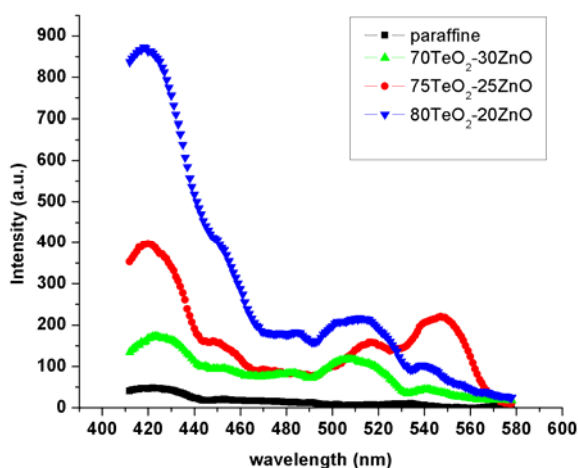


Figure 3.9: Fluorescence intensity variation in tellurite glasses with ZnO content

Variation of fluorescence spectral characteristics with ZnO is explained using Figure 3.9. The major transition which is located around 420 nm can be interpreted as due to the transitions involving the extended states of tellurium dioxide and the minor one at the green region as due to transitions involving defect states arising due to nonbridging oxygen ions. It is found that the fluorescence intensity of this major transition is proportional to the tellurium content. With increase in ZnO content, nonradiative relaxation originating by collision process gets enhanced which gives rise to a decrease in fluorescence intensity. A schematic energy level diagram and transitions involved are given in the Figure 3.10. The energy levels shown are vibronic levels of TeO₂ coupled with the lattice. The labels are based on the observed wavelengths of fluorescence emission by knowing the separation between various bands. The labels are based on the wavelengths of fluorescence emission obtained from our spectra.

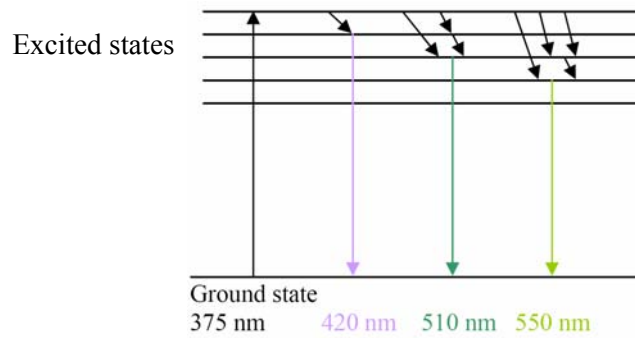


Figure 3.10: A schematic diagram of the energy transfer mechanism involved in the zinc tellurite glass system for one particular composition.

Due to the localized states within the bandgap, the optical transitions such as photoluminescence (PL) and the optical absorption process are difficult to be explained [27].

The radiative transition in amorphous semiconductors is the recombination of an electron in the conduction band tail and a trapped hole. The electron-phonon coupling is very strong and it distorts the lattice near the trapped hole, lowering its energy and broadening the luminescence band. The recombination centre is thought to be a charged dangling bond. Luminescence in amorphous silicon also originates from recombination between the band tails and deep centers [28, 29].

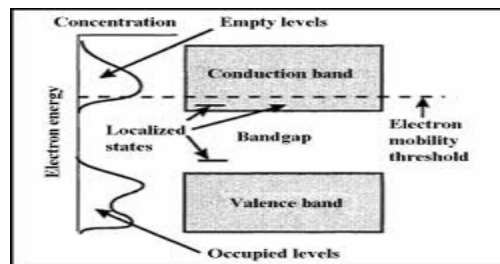


Figure 3.11: A schematic diagram of localized states in amorphous semiconductors

Amorphous semiconductors have localized states in band tails ^[27]. The localized states are randomly distributed and their electrostatic energies are also distributed. In a-Si: H electron-hole pairs are created by light irradiation. Holes are quickly trapped and electrons execute hopping-random walks among localized band tail states.

The lowest energy states for exciting electron-hole pairs in a-semiconductors are not the valence and conduction extended state edges (mobility edges). Due to the presence of tail and dangling bond states within the energy gap, the lowest possible energy states become the tail states, and therefore the photoluminescence of a-semiconductors has to be dominantly influenced by the tail states. Thus, all those optical and electronic properties that originate from the lowest energy states may be expected to be different in a-semiconductors in comparison with those in c-semiconductors.

The intensity variation gives information that the major and the minor transitions sensitively depends on zinc oxide content. Stokes shift for the prominent emission at 420 nm is calculated to be $2.22 \times 10^5 \text{ cm}^{-1}$. The concentration dependant deexcitation of excited molecules to various energy levels provide relative variations in the intensity of various peaks in the spectra. The excitation wavelength dependence of tellurite glasses with ZnO variation is shown below [figure 3.12].

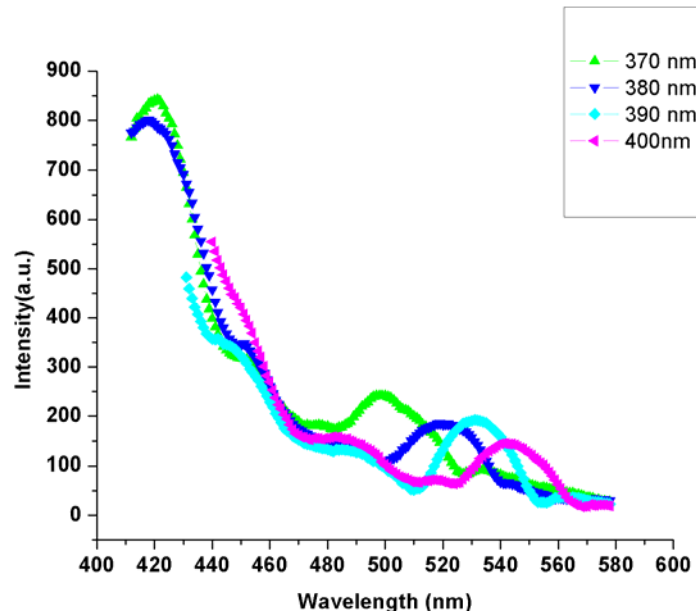


Figure 3.12 (a): Excitation wavelength dependence of Fluorescence intensity in 80 TeO₂:20 ZnO glass

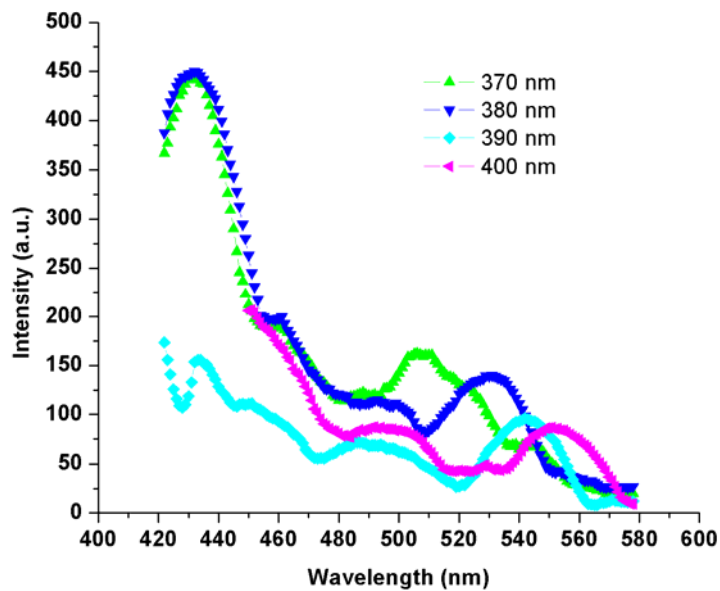


Figure 3.12 (b): Excitation wavelength dependence of Fluorescence intensity in 75 TeO₂:25 ZnO glass

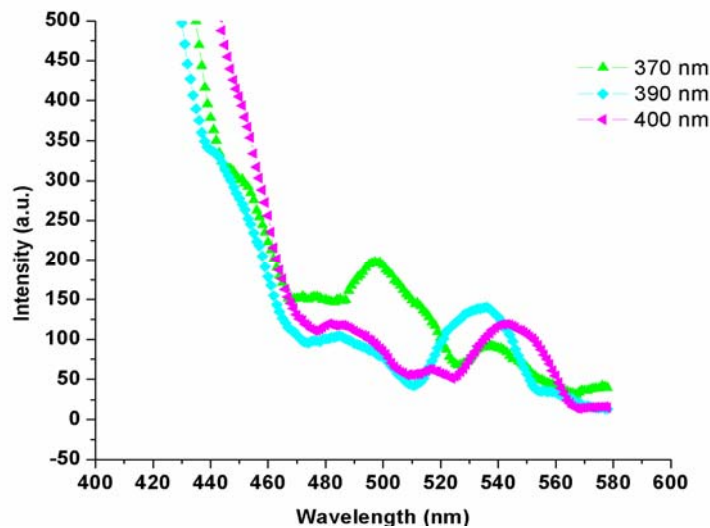


Figure 3.12 (c): Excitation wavelength dependence of Fluorescence intensity in 70 TeO₂:30 ZnO glass.

As explained above, the major transition is due to the transitions involving the extended states of tellurium dioxide and the minor one at the green region as due to transitions involving defect states arising due to nonbridging oxygen ions. With increase in ZnO content, nonradiative relaxation originating by collision process gets enhanced which gives rise to a decrease in fluorescence intensity.

When the wavelength of excitation is increased the only possible transitions are from the localized states to extended states or in between the localized states, which is followed by a shift in the emission peaks towards the lower energy region.

3.6 Nonlinear optical properties of zinc tellurite glasses

Tellurite glasses being high refractive index glasses are suitable materials for nonlinear device applications. Our attempt in the thesis is to study the nonlinear optical characteristics of zinc tellurite glasses, using a single beam z-scan technique^[30].

3.6.1 Nonlinear optical properties of 80 TeO₂:20 ZnO glass

In this section we analyse the nonlinear behavior of 80 TeO₂:20 ZnO glass at five different laser powers. The band gap of the glass sample is calculated to be 3.1 eV and correspondingly the refractive index is 1.8. The material transmits at lower laser intensities, but become opaque at higher intensities [Figure.3.13].

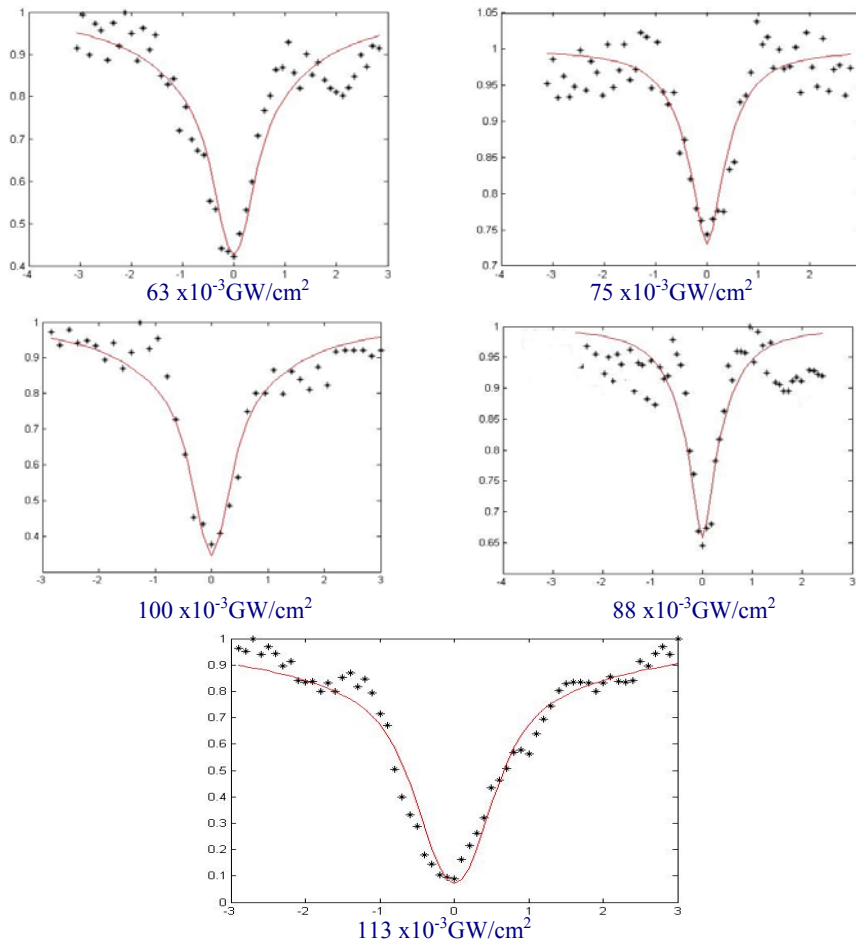


Figure 3.13: Open aperture z scan curves of 80 TeO₂:20 ZnO glass at various powers. Nonlinear transmittance along y-axis and z-translational position along x-axis.

3.6.2 Nonlinear optical properties of 75 TeO₂:25 ZnO glass

In the samples prepared, we have reduced the amount of tellurium dioxide, by increasing ZnO. This leads to an enhancement in the refractive index which is reflected in the nonlinear optical response. The Reverse Saturable Absorption observed in the glass sample is plotted below [Figure.3.14]

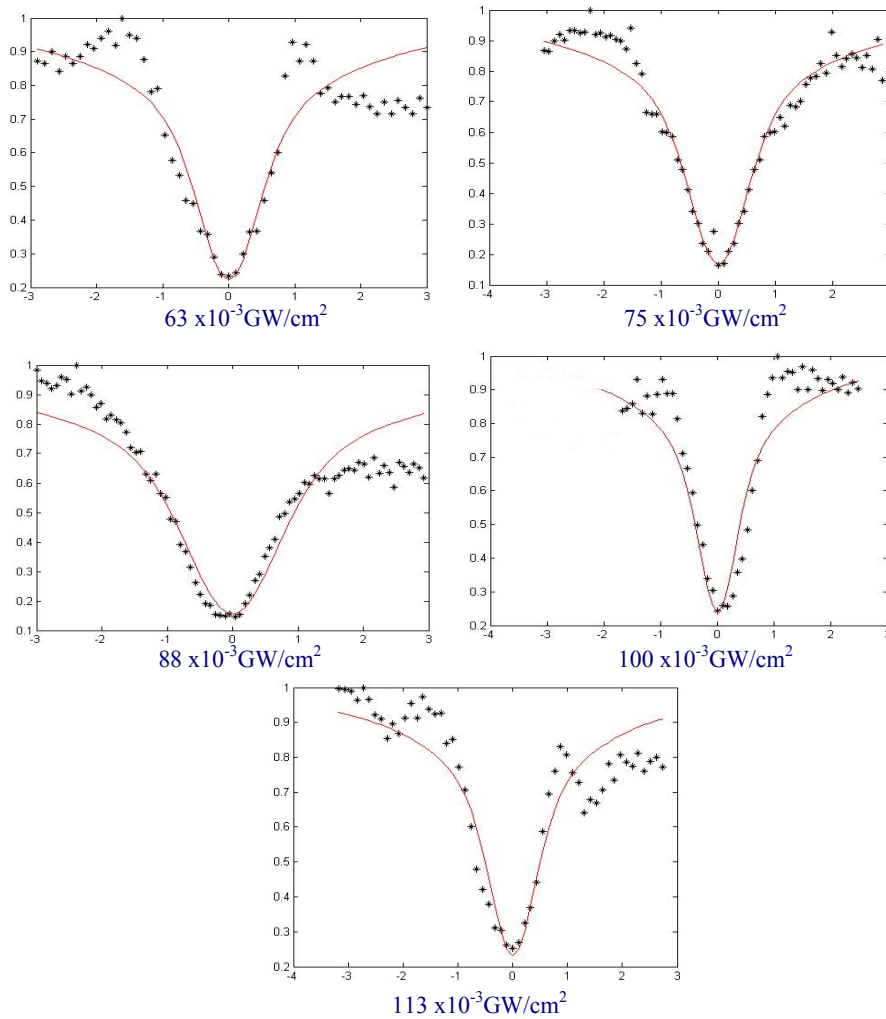


Figure 3.14.: Open aperture z scan curves of 75 TeO₂:25 ZnO glass at various powers. Nonlinear transmittance along y-axis and z-translational position along x-axis.

3.6.3 Nonlinear optical properties of 70 TeO₂:30 ZnO glass

It is clear from the calculated β values that the incorporation of 30 % of zinc oxide in the glass matrix makes it denser thereby enhancing the nonlinear absorption. The enhanced Two Photon Absorption of this sample is as shown in figure 3.15.

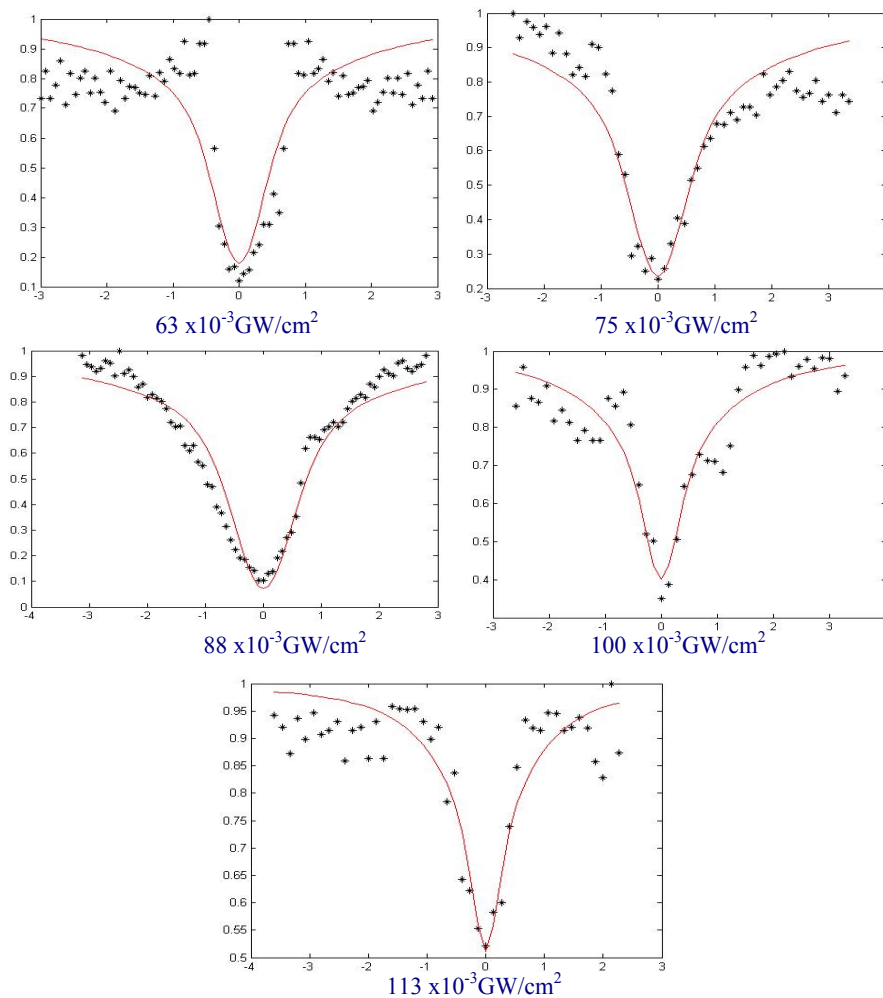


Figure 3.15: Open aperture z scan curves of 70 TeO₂:30 ZnO glass at various powers. Nonlinear transmittance along y-axis and z-translational position along x-axis.

In open aperture experiment, transmittance curve exhibited by the glass samples give an enhanced valley which is an indication of Reverse Saturable Absorption (RSA). It is clear from the data that the material is a two photon absorber. In figure 3.16, we have plotted the enhancement in nonlinear absorption of the sample, with the increase in modifier content in the tellurite glass network. The structural modifications in the glass, when ZnO is added in to the glass sample, modify the nonlinear optical properties. As more and more ZnO enters in the tellurite glass network more NBO s are being created, by rupture of Te-O-Te bonds, which are the major network forming bonds in tellurite glasses. As it is explained in the first section of this chapter, the density of the glass increases reducing its molar volume. Thus there is an enhancement in the refractive index of the samples and so is the nonlinear behavior as given in the curves [Figure 3.16] below.

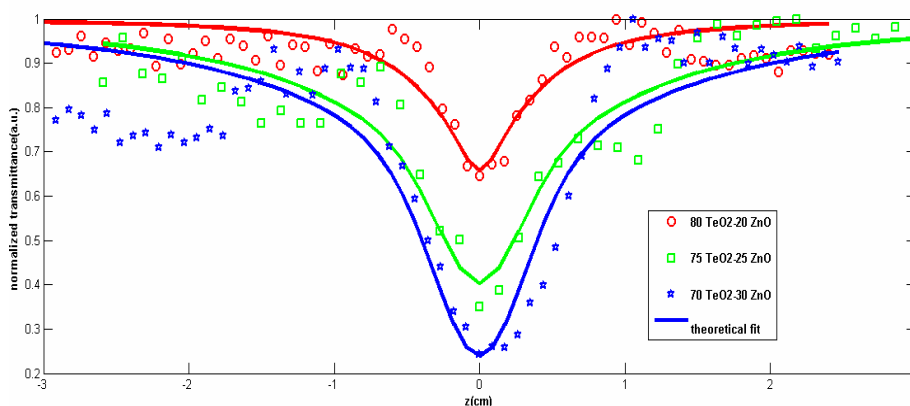


Figure3.16: Open aperture curve of $\text{TeO}_2 (1-x) - \text{ZnO}_x$ glass system at $.100 \text{ GW/cm}^2$ (The solid curves in figure are the theoretical fit to the experimental data)

It is observed that as ZnO content is increased, band gap is shifted to lower value. The band gap red shift enhances two photon absorption and results in an increase in nonlinear absorption. Non linear response will be

higher in glasses containing large number of polarizable loosely bound valence electrons. In zinc tellurite glasses, there are a number of NBOs created which are more polarizable than the BO's. The lone pair of electrons present in tellurium also helps in increasing the polarizability and so the nonlinearity of the sample. The non linear absorption coefficient is calculated from the fitted data. The open aperture curves of 75TeO₂-25ZnO at three different powers are plotted in Figure 3.17. Nonlinear absorption coefficient β is found to decrease with increase in laser power, as reported earlier ^[31, 32], which can be due to the removal of an appreciable fraction of photocarriers from ground state. Thus when incident intensity exceeds the saturation intensity, absorption coefficient of the medium decreases which is tabulated in Table.1.

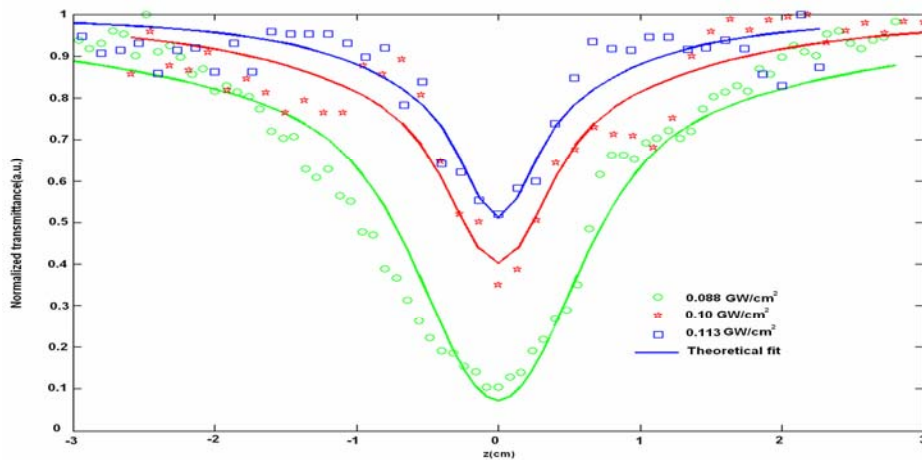


Figure 3.17: Open aperture curve of 80TeO₂-20ZnO at three different powers. (The solid curves in figure are the theoretical fit to the experimental data)

One of the applications of reverse saturable absorbing materials is for the fabrication of optical limiters ^[34, 35]. Optical limiters are materials that

allow light to pass through them at low input intensities, but become opaque at high inputs.

To study the performance of zinc tellurite glasses as efficient optical limiters, the nonlinear transmission of the glass is studied as a function of the input fluence. An important parameter in the optical limiting behavior is the limiting threshold. Lower limiting threshold, makes them potential candidates as optical limiters^[33].

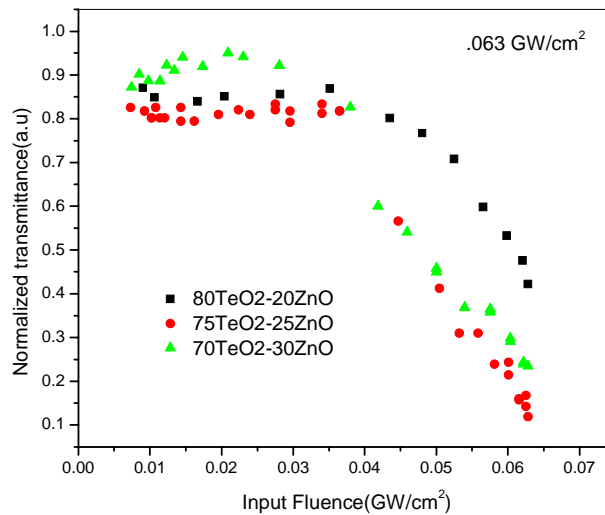


Figure 3.18: Optical limiting curves $\text{TeO}_2 (1-x) - \text{ZnO}_x$ glass system at $.063 \text{ GW/cm}^2$

Figure 3.18 gives the values of optical limiting thresholds for the three different samples at a laser power of 630 MW/cm^2 . There is an observed decrease in the optical limiting threshold as ZnO increases due to the increase in nonlinearity of the material. This observed increase in two photon absorption is contributed by the presence of increased number of polarizable NBO in the material of zinc tellurite glass. The observed values

of optical limiting threshold for various laser powers are tabulated below along with Two Photon Absorption coefficient.

Table 3.3: Nonlinear absorption coefficient and optical limiting threshold for various powers

sample	Eg(eV)	Refractive index n	Input laser power density $\times 10^{-3}$ (GW cm ⁻²)	β (cm/GW)	Optical limiting threshold $\times 10^{-3}$ (GW cm ⁻²)
80TeO2-20ZnO	3.1	1.80	63	396	35
			75	341	41
			88	296	49
			100	198	71
			113	255	80
75TeO2-25ZnO	3	1.96	63	574	36
			75	469	38
			88	424	56
			100	325	71
			113	269	72
70TeO2-30ZnO	2.9	2.05	63	1215	21
			75	1033	23
			88	888	42
			100	754	55
			113	673	67

3.6.4 Nonlinear refraction

Third order susceptibility of the material of zinc tellurite glasses is calculated by finding real and imaginary parts of third order susceptibility, from closed and open aperture z scan techniques. The nonlinear refraction data proves that the material has a positive nonlinear refractive index as shown in the closed aperture z scan plot below [Figure 3.19].

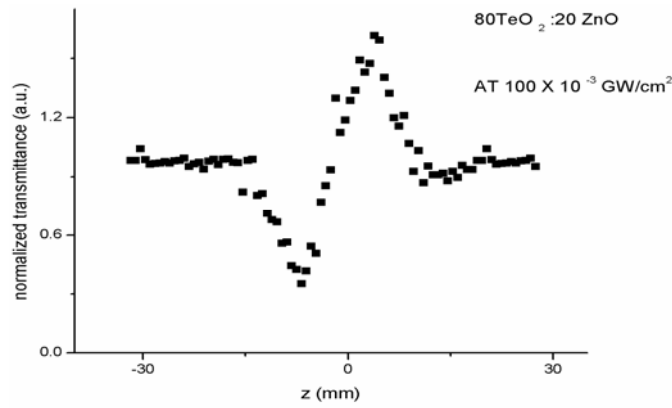


Figure 3.19: Closed aperture z scan curve for zinc tellurite glass

Table 3.4: Non linear refractive index and third order susceptibility for zinc tellurite glass

n_2 (m^2/W)	$\chi(3)$ (esu)
1.55×10^{-15}	2.302×10^{-9}

Non linear refractive index n_2 and third order susceptibility calculated are tabulated above. The value of n_2 is comparatively high, compared to references ^[36-38]. Zinc tellurite glasses are having positive nonlinear refractive index and they give a positive value for imaginary part of susceptibility, which is actually a measure of the induced absorption. The most important application of such a material is in optical limiting.

3.7 Summary and conclusions

The structural, thermal and optical properties of zinc tellurite glasses which we have undertaken are discussed in this chapter. The experiments were carried out on zinc tellurite glasses with varying ZnO concentration prepared using melt quench method.

- ❖ Structural investigations were based on XRD, EDAX and FTIR. Glass formation was confirmed by XRD and glass composition

by EDAX.FTIR spectra indicates the formation of new structural units. NBO ions are created with creation of dangling bonds, with the addition of modifiers.

- ❖ The Glass transition temperature is found to increase with ZnO content due to the formation of ionic bonds caused by modifiers.
- ❖ The optical band gap of tellurite glasses derived from the transmission and reflection spectra are found to be tunable with ZnO concentration. The band gap is found to decrease with increase in ZnO content due to the creation of localized states. The refractive index hike and band gap reduction with increase in ZnO concentration are attributed to the modifications in tellurite glass network produced by the increase in nonbridging oxygen ions. Another important property exhibited by these glasses is that it possesses strong fluorescence emission in the visible region with a nonlinear enhancement of fluorescence intensity with increase in optical band gap. Studies show that these materials are promising candidates for light-emitting and photonic devices.
- ❖ Non linear optical studies on zinc tellurite glasses determined using z scan technique shows that they are highly nonlinear exhibiting reverse saturable absorption. It is evident that the basic mechanism involved is the Two Photon Absorption. Non linear absorption is found to increase with ZnO content showing that the band gap red shift enhances Two Photon Absorption. Studies prove that Zinc tellurite glasses are potential candidates as optical limiters. Two Photon absorption coefficient is found to be fluence dependent. Positive nonlinear refraction is observed in the closed aperture z scan experiment.

References

- [1] Raouf H. El-Mallawany, “*Tellurite glasses Hand book-Physical properties and data*”, CRC press LLC, (2002).
- [2] Masayuki Yamane, Yoshiyuki Asahara “*Glasses for Photonics*”, Cambridge University Press, (2000).
- [3] B Erariah, “*Optical properties of Lead-tellurite glasses doped with samarium trioxide*”, *Bull. of Mater. Sc.* 33, 391–394, (2010).
- [4] R. El-Mallawany, M. Dirar Abdalla, I. Abbas Ahmed, “*New tellurite glass: Optical properties*”, *Mater. Chem. and Phys*”, 109, 291–296, (2008).
- [5] M. R. Sahar K. Sulhadi , M. S. Rohani, “*Spectroscopic studies of TeO₂–ZnO–Er₂O₃ glass system*,” *J. of Mater. Sc.*, 42, 824–827, (2007).
- [6] Rose Leena Thomas¹, Vasuja¹, Misha Hari¹, V P N Nampoori¹, P Radhakrishnan^{1,2}, Sheenu Thomas² “*Optical non-linearity in ZnO doped TeO₂ glasses*”, *JOAM* , 13, , 5, 523(2010).
- [7] Burger H, Kneipp K, Hobert H, VogelW, “*Glass formation, properties and structure of glasses in the TeO₂-ZnO system*”, *J Non-Cryst Solids* 151,134-142, (1992).
- [8] Vogel E M , “*Glasses as Nonlinear Photonic Materials*”,*J. Am. Ceram. Soc.* 72, 719,(1989).
- [9] Keiji Tanaka, “*Optical nonlinearity in photonic glasses*”,*J of mater.sc : mater in electron* ,16,633-643(2005).
- [10] S. Neov, V. Kozhukharov, I. Gerasimova, K. Krezhov, B.Sidzhimov, “*A model for structural recombination in tellurite glasses*”, *J. Phys. C: Solid State Phys.* 12 , 2475,(1979).
- [11] S. Neov, I. Gerassimova, K. Krezhov, B. Sydzhimov, V. Kozhukharov, “*Atomic arrangement in tellurite glasses studied by neutron diffraction*”; *phys. stat. sol. (A)* 47, 743(1978).
- [12] E.F. Lambson, G.A. Saunders, B. Bridge, R.A. El-Mallawany” *The elastic behavior of TeO₂ glass under uniaxial and hydrostatic pressure*”, *J. Non-Cryst. Solids* 69 , 117(1984).
- [13] Y. Dimitriev, V. Dimitrov, M. Arnaudov, “*IR spectra and structures of tellurite glasses*” *J. Mater. Sci.* 18, 1353,(1983).
- [14] Y. Shimizugawa, T. Maeseto, S. Inoue, A. Nukui, “*Structure of Teo₂.Zno Glasses By Rdf And Te, Zn K Exafs*”, *Phys. and Chem.of Glasses*, 38(4), 201-205,(1997).

- [15] A.A. Sidek, S. Rosmawati, Z.A. Talib, M.K. Halimah and W.M. Daud, “*Synthesis and Optical Properties of ZnO-TeO₂ Glass System*”, Am. J. of Appl. Sc. 6 (8), 1489-1494(2009).
- [16] Mott N F and Davis E A, “*Conduction in non crystalline systems.5.conductivity, optical absorption and photoconductivity in amorphous semi conductors*”, Philos. Mag. 28,903,(1970).
- [17] D. Maniu, I. Ardelean, T. Iliescu, S. Astilean, N. Muresan, “*Influence of preparation technique and Pr³⁺ doping on the absorption edge, photoluminescence, and Raman spectra of 70TeO₂·30PbCl₂ glasses*”, JOAM, 9, 3, 737 – 740, (2007).
- [18] D.L.Wood and J Tauc, “*Weak absorption tail in amorphous semiconductors*”, Phys. Rev. B,5(8),3144-3151,(1972).
- [19] B Erariah, “*Optical properties of Lead-tellurite glasses doped with samarium trioxide*”, Bull. of Mater.Sc. 33 ,391–394, (2010).
- [20] R. El-Mallawany, M. Dirar Abdalla, I. Abbas Ahmed, “*New tellurite glass: Optical properties*”, Materials Chemistry and Physics 109,291–296, (2008).
- [21] V. Dimitrov, S. Sakka, “*Electronic oxide polarizability and optical basicity of simple oxides.*”, J of Appl. Phys. 79 , 1736, (1996).
- [22] P. Gayathri Pavana, K. Sadhanab, V. Chandra Mouli “*Optical, physical and structural studies of boro-zinc tellurite glasses*” Phys. B :Conden. Mat.,406 , 1242–1247, (2011).
- [23] Gupta V P& Ravindra N M, “*Comments on the Moss Formula*”, Phys. Stat. Sol. B,100,715,(1980).
- [24] Reddy PR,Nazeer Ahammed Y.Rama Gopalk. et al, “*Optical electro negativity and refractive index of materials*”, Opt. Mater., 10,95,(1998).
- [25] V Kumar ,J K Singh, “*Model for calculating refractive index of different materials*”, Ind. J. of Pure & Appl. Phys, 48,(2010).
- [26] Miller R. C., “*optical second harmonic generation in piezoelectric crystals*”, Appl. Phys. Lett., 5 ,17,(1964).
- [27] R. A. Street, “*Luminescence in amorphous semiconductors*”, Advan. In Phys., 25, 397-454 (1976).
- [28] Munetoshi Seki, Kan Hachiya, Katsukuni Yoshida, “*Photoluminescence excitation process and optical absorption in Ge-S chalcogenide glasses*”, J.of Non-Cry. Solids., 324, 127–132 (2003).

- [29] S.G. Bishop and D.L. Mitchell, "Photoluminescence excitation spectra in chalcogenide glass", *Phys. Rev. B.*, 8, 5696-5701 (1973).
- [30] Mansoor Sheike Bahae, Ali A. Said, Tai-Huei Wei, David J Hagan, E.W. Van Stryland, "Sensitive measurement of optical nonlinearities using a single beam", *IEEE J. of Quantum Electron.*, 26, 4(1990).
- [31] L. Irimpan, V. P. N. Nampoory, and P. Radhakrishnan, "Spectral and nonlinear optical characteristics of nanocomposites of ZnO–CdS", *J. Appl. Phys.* 103, 094914 (2008).
- [32] K. Ogusu, J. Yamasaki, S. Maeda, M. Kitao, and M. Minakata, "Linear and nonlinear optical properties of Ag-As-Se chalcogenide glasses for all-optical switching", *Opt. Lett.* 29, 265(2004).
- [33] Yu Chena, Lili Gaoa, Miao Fenga, d, Lingling Gua, Nan Hea, Jun Wang, Yasuyuki Arakic, Werner J. Blaub and Osamu Itoc, "Photophysical and Optical Limiting Properties of Axially Modified Phthalocyanines", *Mini-Rev. in Organ. Chem.*, 6, 55-65 (2009).
- [34] J A Herman and J Staromlynska; "Trends in optical switches, limiters and discriminators", *Int. J. Nonlinear Opt. Phys.* 2, 271 (1993)
- [35] L W Tutt and T F Boggess; "A review of optical limiting mechanisms and devices using organics, fullerenes, semiconductors and other materials" *Prog. Quant. Electr.* 17, 299 (1993)
- [36] Sean Manning, Heike Ebendorff-Heidepriem, and Tanya M. Monro, "Ternary tellurite glasses for the fabrication of nonlinear optical fibers" 2, 2 / *Opt. Mater. Exp.* 140, (2012).
- [37] T. M. Monro and H. Ebendorff-Heidepriem, "Progress in micro structured optical fibers," *Ann. Rev. Mater. Res.* 36, 467–495 (2006).
- [38] C. C. Wang, "Empirical relation between the linear and the third-order nonlinear optical susceptibilities," *Phys. Rev. B* 2, 2045–2048 (1970).



BAND GAP TUNING AND ENHANCEMENT OF TWO PHOTON ABSORPTION COEFFICIENT IN ZINC TELLURITE GLASSES VIA THERMAL POLING

This chapter discusses the thermal poling technique, which is an effective method in modifying the structure of the material of glass and tuning its linear and nonlinear optical properties. Thermal poling is done by heating the sample and applying a potential across it. The voltage is removed only after the sample has been cooled down to room temperature in order to create a change in the dipole arrangement in the glass. The modification of dipoles allows the glass to increase the density and allows tuning of its optical properties. The interesting results are that thermal poling leads to the tuning of optical properties such as band gap, refractive index and enhancement of Two Photon Absorption in the glass.

4.1 Introduction

Glasses are amorphous materials possessing inversion symmetry on a macroscopic scale and hence second order nonlinearity (SON) is absent in them. This makes it impossible to use glasses for efficient second-order nonlinear processes. There are reports on second order processes generated by photoinduced processes from centrosymmetric materials during 1980s^[1-5].

Coherent photo-galvanic effect was identified as the cause of the photoinduced second order phenomena, through which a spatially modulated static electric field along the material medium is established^[6-10]. The

electric field couples with third order nonlinearity (TON), of the glass and results in an effective value of second order nonlinearity. The period of the self-organized electric field in the material medium alternates spatially to provide constructive interference through quasi-phase matching (QPM). Considerable research has been carried out in order to understand the fundamental physics behind the observed phenomenon and assess the compatibility of the new method with nonlinear crystals. The figure of efficiencies reported on second order process ^[11-17], did not make the photoinduced second order processes attractive for real applications. An important point in the search for an efficient glass-based second-order nonlinear material was the work of Myers et. al. in 1991 ^[18]. The optical second harmonic generation (SHG) in poled oxide glasses was originally discovered by Myers et al ^[1].

Second order nonlinear processes indicate a long-range order in the orientation of electric dipole moments realized in a disordered lattice. Attempts are in progress to achieve more devices for second order processes using a glass material. Poled tellurite glasses are known to show second-order non-linear optical effects as well. Many basic functions in optical information processing like switching or modulation require nonlinear optical effects. For applications in optical switching, modulation and second-harmonic generation (SHG), a sufficiently large $\chi^{(2)}$ is indispensable. An interesting way to induce an effective second order nonlinear process in glass is by thermal poling of the material. Myers et al. reported such experiments for the first time ^[18], and further investigations have been successful ^[19,20]. The mechanism that leads to the establishment of the SON in the glass has not yet been fully understood. The origin of the electro-static field E_{dc} responsible for χ^2 , has been a subject of debate since 1990s, although poling had been studied before in the context of polymers ^[21-23].

We have studied optical properties of thermally poled zinc tellurite glasses in the present chapter, so as to investigate the structural changes that lead to the tuning of optical constants.

4.2 Experiment

Glass samples for the present work were synthesized by rapid melt quenching method. The samples consists of $\text{TeO}_2(1-x)\text{-ZnO}_x$ with $x = 0.2, 0.25, 0.30$. The experimental details of melt quench technique for glass preparation is explained in detail in chapter 2 of the thesis. Thermal poling measurements were carried out by the setup shown in Figure 2.8. References^[30-32] describe the thermal poling experiment in detail. Absorption spectra were taken before and after thermal poling. The optical absorption spectra of the glass samples were determined using JASCO V-570 double beam UV-visible spectrophotometer. The indirect band gap of the glass is estimated from the graph of $h\nu V_s (\alpha h\nu)^{1/2}$ ^[41]

To check whether there is an enhancement in the third order nonlinear optical absorption properties of $\text{TeO}_2(1-x)\text{-ZnO}_x$ glasses due to thermal poling, we have used the single-beam z-scan technique with nanosecond laser. A Q-switched Nd: YAG laser (Spectra Physics LAB-1760, 532 nm, 7 ns, 10 Hz) is used as the light source for the experiment. Details of the single beam z scan technique are given in chapter 2 along with other experimental techniques. The data were analyzed using the procedure described by Sheik Bahae *et al*^[42] and the Two Photon Absorption coefficients were obtained by fitting the experimental z-scan plot with the theoretical plots. Reference^[43,44] give details about z scan experiment on zinc tellurite glasses before thermal poling. Optical limiting behavior was also studied using the open aperture z scan plots after thermal poling experiment.

4.3 Theory

Structural information on tellurite glasses given in chapter 3 is to be reloaded here in order to understand the structural modifications taking place in the sample after poling process. When some modifier ions enter in the tellurite glass network, the major bridging network Te-O-Te breaks forming non bridging oxygen ions in the network. The modifier ions bonded ionically to the non bridging oxygen sites may drift under the action of electric fields. The raman and/infrared spectroscopy proves that there is a conversion of basic structural units TeO_4 to TeO_3 , with a change in the coordination of tellurium. Thus there exist polarizable non bridging oxygen ions in the zinc tellurite glass matrix.

It was known, from the work of Myers' and co-workers^[18], that the nonlinearity is located in a thin layer, beneath the surface of the glass plate that had been in contact with the anode electrode and there exists a connection between second and third order susceptibility via

$$\chi^{(2)} = 3 \chi^{(3)} E_{dc} \quad (4.1)$$

Kameyama et al reports that there is a possible generation of third order nonlinearity in a poled sample by the dc field E_{dc} that results from NBOs, as given in the above equation. The nonlinearity is generated by the space charge field E_{dc} and an increase in the third order susceptibility is observed resulting from the increased near surface nonlinearity. This is observed with an increase in the refractive index, which is generated by the non bridging oxygen ions and defect states created in the glass network via thermal poling process^[10,13,14,24].

It is proposed that the nonlinearity was caused by orientation of bonds or by the creation of a space charge field, both leading to a DC electronic

polarization ^[25, 26]. The high temperature involved in the poling process increases the mobility of the impurities present in the glass. Therefore, upon the application of an electric field, the positively charged ions drift towards the cathode, leaving a negatively charged depleted region behind at a few microns beneath the anodic surface. Due to the lack of mobile charges the depleted region has a much larger resistivity than the rest of the glass. Like in a voltage divider, the applied voltage tends to mainly drop across the more resistive depleted region. As a consequence, a large static electric field is established between the depleted layer and the anode. Kazansky et. al. distinguished between two possibilities that could arise at this stage ^[26].

- 1) Orientation of NBO bonds or
- 2) Glass ionization under the action of the high electrostatic field.

The first hypothesis says that the high temperature increases the mobility of the NBO dipoles, whereas the applied electric field forces them all to orient in the same direction. Thus dipoles would be frozen in one direction, breaking the symmetry of the glass after cooling.

The second one says, the static field is responsible for the ionization of the glass in the anodic region, leading to the creation of a positive charge layer that screens the external field and stops the process. When the sample is cooled down the ions are trapped in their positions. A high static electric field, between the positive layer and the negatively charged region, is then frozen in the glass once again breaking the centro - symmetric structure.

Even though there are strong arguments against a significant contribution to the effective nonlinearity due to the orientation of dipoles ^[27-32] the existing theoretical models suggested for the poling process can be classified into two main groups, namely single carrier and multiple carrier models.

Single carrier model was developed by researchers in 1953^[33] and can be easily adapted to the case of positive charge carriers. As we have discussed above Zn^{2+} are the only mobile charge carriers, which are assumed to be bonded to negatively charged immobile non bridging oxygen sites. The anode is assumed to act as a blocking electrode, and under these circumstances electrical neutrality requires an equal amount of fixed negative charges to be present in the glass, for instance negatively charged NBO.

As we discussed above, the high temperature environment of poling process increases the mobility of the impurities present in the glass. Therefore, upon the application of an electric field, the positively charged ions drift towards the cathode where they are neutralized by injected electrons, leaving a negatively charged depleted region behind them at anode.

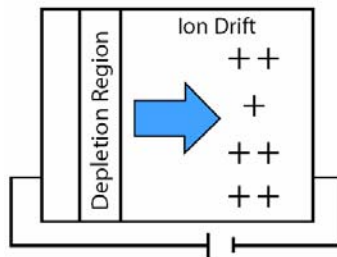


Figure 4.1: Space charge formation in zinc tellurite glasses.

The thickness of the depletion region generated is given by this single carrier model as

$$d_{dep} = \sqrt{\left(\frac{2\varepsilon V}{q_e N}\right)} \quad (4.2)$$

where q_e is the elementary charge, N is the fixed charge density associated with the NBO-hole centers and ε is the dielectric permittivity of glass. The motion of the charge front can be measured by the current that flows through the

glass, taking into account that d_{dep} is much smaller than the thickness of the glass and E_{dc} depends on the charge carrier concentration. From this simple model it is possible to infer that a glass sample having lower charge concentration will exhibit lower nonlinearity and a wider depletion region^[33-36].

Although the single carrier model describes the general features of the poling process reasonably well, it did not account for some of the experimental evidence. Researchers doubt the existence of more charge carriers in the sample during poling. Indiffusion of H^+ from the atmosphere, driven by the high electrostatic field, was thought to be taking place during the poling. Indeed the presence of a positive charge layer between the negatively charged depleted region and the anodic surface was revealed using a technique called laser-induced pulse pressure (LIPP)^[29]. Some researchers pointed out the relevance of the poling atmosphere by performing poling in air or under vacuum (10^{-8} atm.)^[37]. Samples poled in vacuum exhibit wider depletion regions and consequently lower nonlinearity compared to samples poled in air for the same time. It was speculated that $\text{H}^+/\text{H}_3\text{O}^+$ may in-diffuse from the atmosphere, while poling in air^[34]. LIPP measurements also showed a different charge distribution for poling in vacuum and air. A positive charge layer was revealed to be present also in the samples poled in vacuum. It was therefore thought that, in vacuum, glass ionization with liberation of electron must take place. The same phenomenon is probably occurring in air as well, but in that case in-diffusion of positive species from the atmosphere is believed to be the dominant mechanism.

Recent studies on dependence of thickness of the sample and poling time shows that there exists an optimum poling time, depending on the sample thickness, for which the achieved SON was maximized^[38]. The

decrease in SON for longer poling times cannot be explained by a single carrier model. It is also to be considered whether there is some effect on higher poling temperature on thermal poling process. The existing study say that the second order nonlinearity increases with increase in poling temperature, reaches a maximum near the glass transition temperature and then decreases with further increase in poling temperature. One possible mechanism for the decrease in second harmonic intensity with increasing poling temperature, near glass transition, is due to the migration of oxide ions to the anode side and reduction of space charge layer^[39,40]. In order to account for the new experimental findings new models have to be developed.

Towards the conclusion of the analysis of the theoretical aspects of thermal poling technique the following points are to be highlighted:

The initial stage of poling is the migration of mobile cations, leaving negative charges due to nonbridging oxygen ions in the glass surface region.

- A space charge layer is formed in the vicinity of anode side glass surface and is composed of cations and oxide ions, which are separated from each other in the direction of the external electric field and such a situation leads to a very large electric field near the anode-side glass surface.
- Poling increases the number of TeO_3 trigonal pyramid and/or non-bridging oxygen increases in the glass network structure.
- The electric dipole moments whose long-range orientation gives rise to second order nonlinearity are probably ascribed to asymmetrical structural units such as TeO_4 trigonal bipyramids

and TeO_3 trigonal pyramids, and the orientation of these structural units in the direction of the external dc electric field can occur more readily in a more flexible glass network structure like that of tellurite glasses.

- It is reported that some electrochemical reaction under the large dc field may convert the tellurite glass structural unit from the TeO_4 to the deformed TeO_3 resulting in possible precipitation of metallic tellurium of small particles.
- When glass is under the dc bias at elevated temperature (below T_g), dipoles are formed in the medium due to the induced polarization of the dopant. As the dc bias is removed after reaching the room temperature, the orientation of dipoles will be frozen and thereby breaking inversion symmetry of the medium.
- The optical second harmonic generation in poled tellurite glasses indicates that the SHG is suppressed in tellurite glasses containing cations with large electron polarizability.

4.4 Results

4.4.1 Thermal poling on 80 TeO_2 :20 ZnO glass

Results of thermal poling on 80 TeO_2 :20 ZnO sample are given below.

When thermal poling was done at 1 kV, there was no much results obtained. So we raised the poling voltage to 2kV. The poling temperatures were 100°C , 200°C and 300°C . The temperature was limited just below glass transition temperature, since reports show that the second order nonlinearity gets diminished with poling temperatures greater than glass transition temperature.

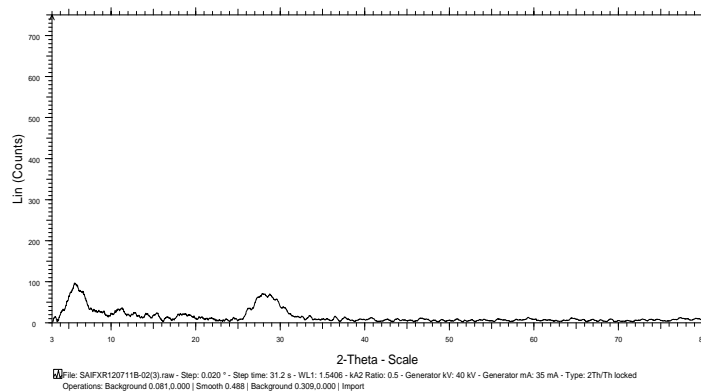


Figure 4.(a): XRD of Thermally poled 80 TeO_2 : 20 ZnO glass.

4.4.1.1 Linear optical properties

Linear optical bandgap variation is studied after poling with 100^o C, 200^o C and 300^o C. A slight decrease in the bandgap of 80 TeO₂:20 ZnO glass sample is observed as shown in the figure 4.2.

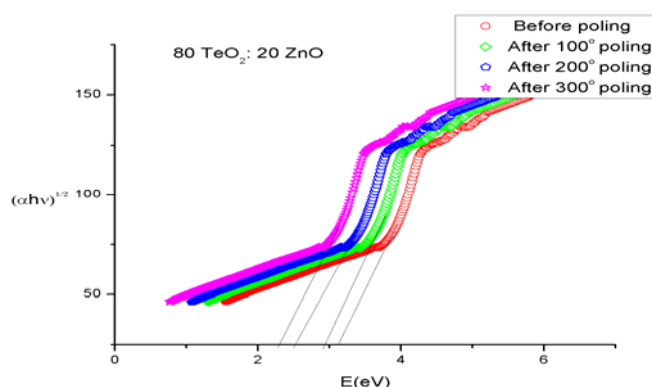


Figure 4.2: Band gap tuning of 80 TeO₂ : 20 ZnO glass.

From the literature overview it is found that amorphous semiconductors are characterized by localized states found in the band gap. Another important thing to be mentioned along with localized states, is the tailing effect of band edges, which play an important role in determining the band gap of vitreous materials. Our results on thermal poling of zinc tellurite glasses prove that there is a possibility of new localized states created by the process. As shown above, the band gap of poled samples decreases with increase in poling temperature, which can be attributed to the creation of non bridging oxygen ions in the glass matrix. Based on the explanations given in chapter 3, the localized states increases as a result of modifiers entering in to the glass. Thus there is a possibility of conversion of TeO₄ structural units into TeO₃ and so the band gap gets tuned according to the change in poling temperature.

4.4.1.2 Nonlinear optical properties

After poling the nonlinear optical properties of 80 TeO₂:20 ZnO samples were studied using a single beam z scan technique. Reverse Saturable Absorption is observed for the sample for all the powers used. One of the RSA plot for the sample poled at 300^o c is given below[figure 4.3] compared to the open aperture curve before poling. It was recorded for a laser power of 0.0063 GW/cm².

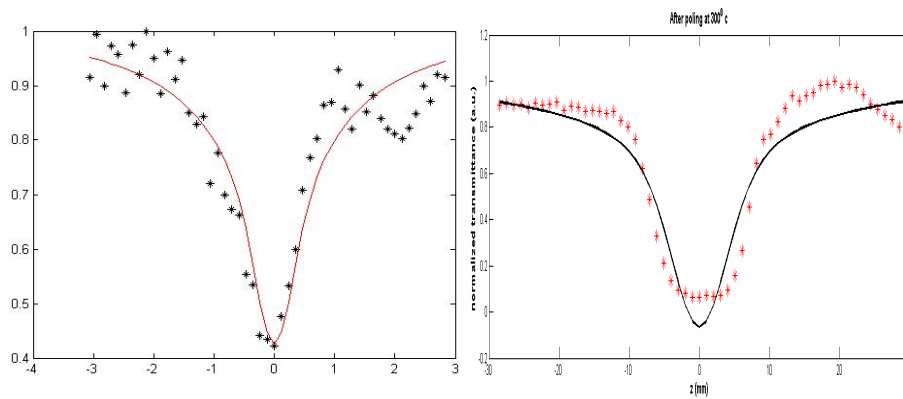


Figure 4.3: RSA curves before and after thermal poling of 80 TeO₂: 20 ZnO glass. Normalized transmittance along y-axis and z in cm/mm along x-axis

The previous discussion on band gap tuning specifies that there is a possibility of creation of localized states, which allow an increase in the refractive index of the sample, along with the band gap reduction. As expected we were able to measure an enhancement in the optical nonlinearity also. The observed enhancement in the two photon absorption of the sample is attributed to the increased number of polarizable non bridging oxygen ions. Thus the band gap decrease enhances the two photon absorption of the material of glass.

Comparing the depth of valley of the z scan plots before and after poling, it gives a rough idea on the enhancement of nonlinear absorption shown by the sample. Eg, n and Two Photon Absorption coefficient before and after poling is listed in the table below.

Table 4.1: Band gap reduction and enhancement of TPA in 80 TeO₂ : 20 ZnO glass

Sample	Eg(eV)	n	$\beta(\text{cm/GW})$ at 0.0063 GW/cm ²
80TeO ₂ -20ZnO	3.13	1.80	396
after 100 ^o poling	2.93	1.84	400
after 200 ^o poling	2.60	1.91	475
after 300 ^o poling	2.35	1.98	480

As the poling temperature increases there is a reduction in the bandgap and also an increase in the refractive index of the sample. A small enhancement of Two Photon Absorption coefficient is also observed for the sample with poling temperature.

4.4.2 Thermal poling on 75 TeO₂:25 ZnO glass

Results of thermal poling on linear and nonlinear optical properties of 75 TeO₂:25 ZnO glass ,after poling at 2 kV and by varying the poling temperature are given below.

4.4.2.1 Linear optical properties

Optical bandgap variation is analysed using Tauc plots from absorbance spectra taken after poling at each temperature. The optical absorption edge shifts to lower energy side as shown in the Tauc plots[figure 4.4] below. The optical band gap is found to vary from 3 eV to 2.2 eV as the poling temperature increases.

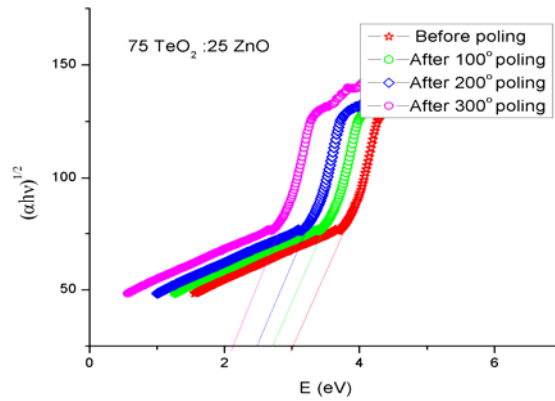


Figure 4.4: Band gap tuning of 75 TeO₂:25 ZnO glass

4.4.2.2. Nonlinear optical properties

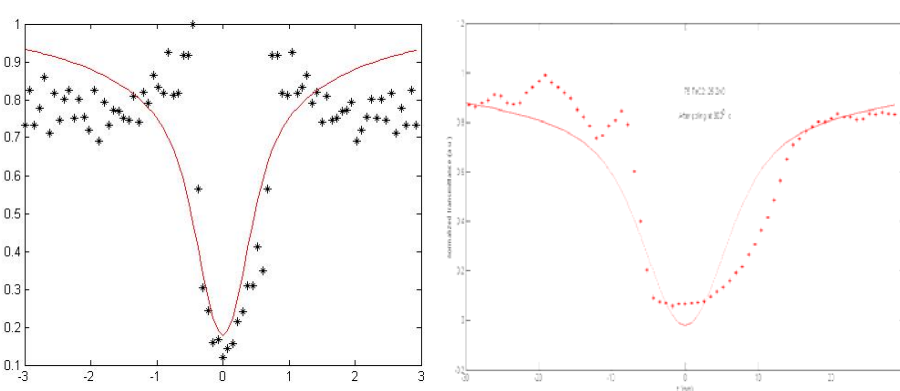


Figure 4.5: RSA curves before and after thermal poling of 75 TeO₂:25 ZnO glass. Normalized transmittance along y-axis and z in cm/mm along x-axis.

The results of nonlinear absorption studies using z scan technique on 75 TeO₂:25 ZnO glass also show that there is an enhancement of optical nonlinearity of the sample after poling. This is dominant at the highest poling temperature 300⁰ C. Two Photon Absorption observed for the sample are plotted in figure 4.5. An increase in the density of the sample is observed when compared to that obtained for the previous sample containing more

tellurium dioxide content. The enhancement of β value is more pronounced as for the optical bandgap.

Table 4.2: Band gap reduction and enhancement of TPA in 75 TeO₂:25 ZnO glass

Sample	E _g (eV)	n	β (cm/GW)at 0.0063 GW/cm ²
75TeO₂-25ZnO	3.03	1.96	574
after 100 ⁰ poling	2.80	2.00	588
after 200 ⁰ poling	2.52	2.07	612
after 300 ⁰ poling	2.22	2.15	625

4.4.3 Thermal poling on 70 TeO₂:30 ZnO glass

Thermal poling at 2 kV was done on 70 TeO₂:30 ZnO glass samples, by varying the poling temperature from 100⁰ C to 300⁰ C. It is found that thermal poling is an effective tool for modifying the structure of zinc tellurite glasses.

4.4.3.1 Linear optical properties

The measurement of linear optical properties of 70 TeO₂:30 ZnO glass after thermal poling reveal that the structural modification via thermal poling enables the sample to tune its band gap from 2.97-2.02 eV as shown in the plot 4.6.

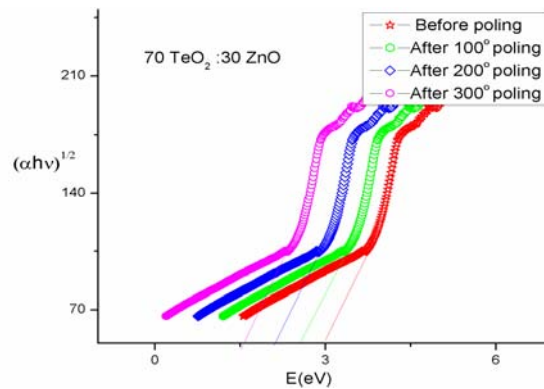


Figure 4.6 : Band gap tuning of 70 TeO₂:30 ZnO glass

The creation of dangling bonds in the zinc tellurite glass network causes some densification of localized states contributing to the reduction of band gap of the material.

4.4.3.2 Nonlinear optical properties

Reverse Saturable Absorption observed in the 70 TeO₂:30 ZnO glass before and after thermal poling is shown below [figure 4.7].

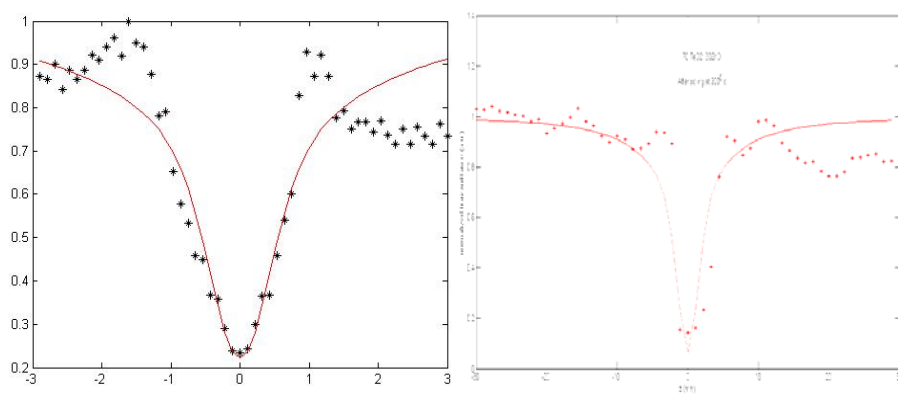


Figure 4.7 : RSA curves before and after thermal poling of 70 TeO₂:30 ZnO glass. Normalized transmittance along y-axis and z in cm/mm along x-axis.

Electrochemical reaction via thermal poling ,creates more Non Bridging oxygen ions in the zinc tellurite glass increasing the polarizability of the material. The electrostatic field created in the sample by thermal poling process also contributes to the polarizability of the material. The observed enhancement in the Two Photon Absorption coefficient can be attributed to this increase in polarizability of the material of glass. The table below shows reduction in the band gap and enhancement of Two Photon Absorption coefficient for various poling temperatures.

Table 4.3: Band gap reduction and enhancement of TPA in 70 TeO₂:30 ZnO glass

Sample	E _g (eV)	n	β(cm/GW)at 0.0063 GW/cm ²
70TeO ₂ -30ZnO	2.97	2.05	1215
after 100 ^o poling	2.70	2.09	1225
after 200 ^o poling	2.41	2.17	1240
after 300 ^o poling	2.02	2.28	1265

4.5 Discussion

The optical absorption spectra of TeO₂ - ZnO glass samples before and after poling are shown in the above results. The position of the fundamental absorption edge is seen to shift to higher wavelength region with increasing poling temperature for all the three samples. The nonlinearity of oxide glasses increases as the number of TeO₃ trigonal pyramid and/or non-bridging oxygen increases in the glass network structure, because of the creation of polarizable non bridging oxygen ions. The electric dipole moments for which long-range orientation gives rise to the second harmonic generation are probably ascribed to asymmetrical structural units such as TeO₄ trigonal bipyramids and TeO₃ trigonal pyramids. The orientation of these structural units in the direction of the external dc electric field can occur more readily in a more flexible glass network structure. During the thermal poling process, an increase in the quantity of dipoles per volume means that more dipoles can be aligned in the direction of electrical field. In other words, network structure will increase the defect states giving rise to a decrease in the band gap. The structural rearrangement reduces the molar volume and thereby increases the density of the zinc tellurite glass network. The density increase is indicated by an enhancement of refractive index of the glass sample, which in turn reduces the band gap as shown in the results above.

The variation of Two Photon Absorption coefficient with ZnO concentration in tellurite glasses was discussed in one of our research papers [44]. Comparing the results of open aperture z scan experiments on zinc tellurite glasses before and after the process of thermal poling, we could find that there is an enhancement in the Two Photon Absorption coefficient. This again can be correlated with the reorientation of the structural units in the tellurite glass structure and nonbridging oxygen atoms that possess permanent electric dipoles resulting in an increased refractive index of the material medium. Refractive index is a measure of the distortion of atomic electron clouds by the electromagnetic field of an external incident light. It is reflected in a parameter called polarizability. Therefore refractive index of a material is an indication of the range of third order optical nonlinearity. We have found that there is an enhancement in the nonlinear optical coefficient β which is calculated from the open aperture z scan curves for all the three samples before and after thermal poling. The enhancement is assumed to be due to the formation of higher energy levels contributing TPA. The enhancement of two photon absorption coefficient for the three samples is shown in Figure.4.8.

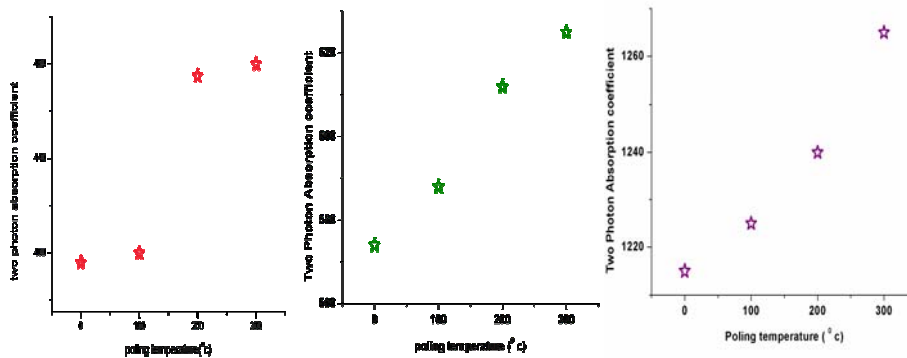


Figure 4.8: Enhancement of Two Photon Absorption coefficient in zinc tellurite glasses

To analyze the optical limiting of the samples after thermal poling, the nonlinear transmission of the glass is studied as a function of the input fluence using the open aperture z scan data. Optical limiters are materials that allow light to pass through them at low input intensities, but become opaque at high inputs. Limiting threshold is determined from the optical limiting curves given below.

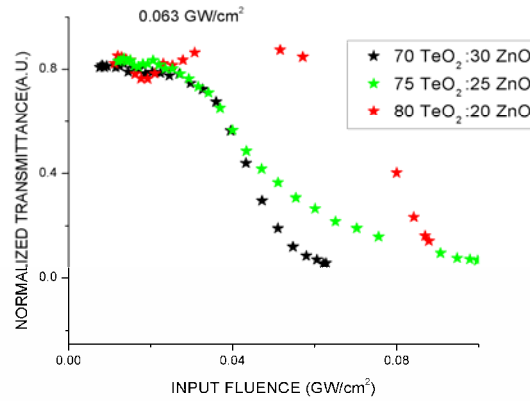


Figure 4.9: Optical limiting of zinc tellurite glasses at 0.0063 GW/cm^2

Table 4.4 : Optical limiting threshold of zinc tellurite glasses at 0.0063 GW/cm^2

sample	Before poling ($\times 10^{-3}$ GW/cm^2)	After 100°C poling ($\times 10^{-3}$ GW/cm^2)	After 200°C poling ($\times 10^{-3}$ GW/cm^2)	After 300°C poling ($\times 10^{-3}$ GW/cm^2)
80TeO ₂ -20ZnO	35	32	30	29
75TeO ₂ -25ZnO	36	35	32	30
70TeO ₂ -30ZnO	21	20	19	19

There is also an observed decrease in the optical limiting threshold of the material, due to the enhanced two photon absorption of the sample. The bandgap reduction due to thermal poling helps to decrease the transmittance of the material at high intensities and the material improves its ability of optical limiting.

4.6 Summary and Conclusions

This chapter focuses on thermal poling studies of zinc tellurite glasses with varying ZnO content. Thermal poling was done by heating and applying a potential across the sample.

- ❖ Heating increases the mobility of the ions present in the glass. It is observed that very large electric field causes orientation of tellurite structural units with nonbridging oxygen atoms that possess permanent electric dipoles. The breakdown of the macroscopic inversion symmetry is caused by the creation of a space-charge layer and the orientation of tellurite structural units. Dipoles are formed in the medium due to induced polarization of the dopant
- ❖ Network structure is found to increase the defect states with thermal poling giving rise to a decrease in the band gap. This can be attributed to electrochemical reactions under the large dc field which convert the tellurite glass structural units from the TeO_4 to the deformed TeO_3 . Structural rearrangement reduces the molar volume and thereby increases the density of the zinc tellurite glass network.
- ❖ Non linear optical studies on zinc tellurite glasses exhibits reverse saturable absorption after thermal poling. Two photon absorption is found to increase with ZnO content and an enhancement of two photon absorption is also observed with thermal poling. Materials induced of second order polarization using such a technique find applications as difference frequency generation, sum frequency generation, second harmonic generation etc.

References

- [1] Y. Fujii, B. Kawasaky, K. O. Hill, and D. C. Johnson, "Sum-frequency light generation in optical fibers", *Opt. Lett.*, 5, 48 (1980).
- [2] Y. Sasaki and Y. Ohmori, "Characteristics of phase matched sum-frequency light in optical fibers", *Appl. Phys. Lett.*, 39, 466 (1982).
- [3] U. Osterberg and W. Margulis, "Dye laser pumped by Nd:YAG laser pulses frequency doubled in glass optical fibre", *Opt. Lett.*, 11, 517 (1986).
- [4] R. H. Stolen and H. W. K. Tom, "Self-organized phase-matched harmonic generation in optical fibers", *Opt. Lett.*, 13, 585 (1987).
- [5] M. C. Farries, P. St. J. Russell, M. E. Fermann, and D. N. Payne, "grating", *Electron. Lett.*, 23, 322 (1987).
- [6] E. M. Dianov, P. G. Kazansky, and D. Y. Stepanov, "Problem of photoinduced second harmonic generation", *Sov. J. of Quant. Electron.*, 19, 575 (1989).
- [7] E. M. Dianov, P. G. Kazansky, and D. Y. Stepanov, "Photovoltaic model of second harmonic generation in optical fibers", *Sov. Lightwave Comm.*, 1, 247 (1991).
- [8] E. M. Dianov, P. G. Kazansky, D. S. Starodubov, and D. Y. Stepanov, "Observation of phase mis matching during the preparation of second order susceptibility gratings in glass optical fibers", *Sov. Light wave Comm.*, 1, 385 (1991).
- [9] E. M. Dianov, P. G. Kazansky, and D. Y. Stepanov, "Photoinduced second harmonic generation: observation of charge separation due to the photovoltaic effect", *Sov. Light wave Comm.*, 3, 83 (1992).
- [10] V. Dominic and J. Feinberg, "Appendix A: Thermal poling of glass: a brief introduction", *Phys. Rev. Lett.*, 73, 3446 (1993).
- [11] R. W. Terhune and D. A. Weinberger, "Second-harmonic generation in fibers" *J. Opt. Soc. Am. B*, 4, 661 (1987).
- [12] V. Mizrahi and U. Osterberg and C. Krautchik and G. E. Stegeman and J. E. Sipe and T. P. Morse, "Direct test of a model of efficient second harmonic generation in optical fibres", *Appl. Phys. Lett.*, 53, 557 (1988).
- [13] M. V. Bergot, M. C. Farries, M. E. Fermann, L. Li, L. J. Poyntz-Wright, P. St.J. Russell, and A. Smithson, "Generation of optically induced second order nonlinearities in optical fibres by poling", *Opt. Lett.*, 13, 592 (1988).
- [14] V. Mizrahi, Y. Hlbino, and G. Stegeman, "Polarization study of photoinduced second harmonic generation in glass optical fibres", *Opt. Comm.*, 78, 283 (1990).

- [15] A. Kamal, D. A. Weinberger, and W. H. Weber, "Spatially resolved raman study of self organized $\chi^{(2)}$ gratings in optical fibres" *Opt. Lett.*, 15, 613,(1990).
- [16] D. Anderson, V. Mizrahi, and J. E. Sipe, "model for second harmonic generation in glass optical fibres based on asymmetric photoelectron emission from defect sites" *Opt. Lett.*, 16, 796, (1991).
- [17] D. M. Krol, D. J. DiGiovanni, W. Pleibel, and R. H. Stolen, "Observation of resonant enhancement of photoinduced second harmonic generation in Tm -doped alumino silicate glass fibres" *Opt. Lett.*, 18, 1220, (1993).
- [18] R. A. Myers, N. Mukherjee, and S. R. J. Brueck, "Large second order nonlinearities in poled fused silica" *Opt. Lett.*, 16, 1732 (1991).
- [19] C.J.S.Matos et al., "Charge emission in thermal poling of glasses with carbon film anode", *J. of NonCry. Solids*,273, 25-29 (2000)
- [20] V.Pruneri et al., "Greater than 20%-efficient frequency doubling of 1532-nm nanosecond pulses in quasi-phase-matched germanosilicate optical fibers", *Opt. Lett.*,24, 4, 208-210, 1999
- [21] K. D. Singer, J. E. Sohn, and S. J. Lalama, , "Second harmonic generation in poled polymer films", *Appl. Phys. Lett.*, 49, 248, (1986).
- [22] J. Zyss, ed., "Molecular Nonlinear Optics. Material Physics and Devices. Quantum Electronics - Principles and Applications", Academic Press Inc., 1994.
- [23] D. E. Carlson, "Ion Depletion of Glass at a Blocking Anode: II, Properties of Ion-Depleted Glasses", *J. of the Am. Ceramic Society*, 57, 7, 291 (1974).
- [24] Akihiro kameyama,Atsushi yokotani,Kou kurosawa,"Second order optical non linearity and change in refractive index in silica glasses by a combination of thermal poling and x-ray irradiation", *JAP*, 95(8),2004.
- [25] N. Mukherjee, R. A. Myers, and S. R. J. Brueck, "Dynamics of second harmonic generation in fused silica" *J. Opt. Soc. Am. B*, 11, 4, 665 (1994).
- [26] P. G. Kazansky and P. St. J. Russell, "Thermally poled glass: frozen in electric field or oriented dipoles", *Opt. Comm.*, 110, 611 (1994).
- [27] R. Kashyap, G. J. Veldhuis, D. C. Rogers, and P. F. Mckee, "Phase matched second harmonic generation by periodic poling of fused silica", *Appl. Phys. Lett.*, 64, 11, 1332 (1994).
- [28] T. G. Alley, S. R. J. Brueck, and M. Wiedenbeck, "Secondary ion mass spectrometry study of space-charge formation in thermally poled fused silica", *J. of Applied Physics*, 86, 12, 6634 (1999).

- [29] P. G. Kazansky, A. R. Smith, and P. St. J. Russell, “*Thermally poled glass: Laser induced pressure pulse probe of charge distribution*” *Appl. Phys. Lett.*, 68, 2, 269 (1996).
- [30] F. C. Garcia, I. C. S. Carvalho, W. Margulis, and B. Lesche, “*Inducing a large second-order optical nonlinearity in soft glasses by poling*”, *Appl. Phys. Lett.*, 72, 25, 3252 (1998).
- [31] B. Lesche, F. C. Garcia, E. N. Hering, W. Margulis, I. C. S. Carvalho, and F. Laurell, “*Eching of Silica Glass under Electric Fields*”, *Phys. Rev. Lett.*, 78, 11, 2172 (1997).
- [32] Von Hippel, E. P. Gross, J. G. Jelatis, and M. Geller, “*Photocurrent, Space-Charge Buildup, and Field Emission in Alkali Halide Crystals*”, *Phys. Rev.*, 91, 3, 568 (1953).
- [33] T. G. Alley, S. R. J. Brueck, and R. A. Myers, “*Space charge dynamics in thermally poled fused silica*”, *Journal of Non-Crystalline Solids*, 242, 165 (1998).
- [34] Y. Quiquempois, G. Martinelli, P. Duthelage, P. Bernage, P. Niay, and M. Douay, “*Localisation of the induced second-order non-linearity within Infrasil and Suprasil thermally poled glasses*”, *Opt. Comm.*, 176, 479 (2000).
- [35] Kameyama, A. Yokotani, and K. Kurosawa, “*Identification of defects associated with second-order optical nonlinearity in thermally poled high-purity silica glasses*”, *J. of Appl. Phys.*, 89, 9, 4707 (2001).
- [36] T. M. Proctor and P. M. Sutton, “*Static Space Charge Distributions with a Single Mobile Charge Carrier*”, *J. of Chem. Phys.*, 30, 1, 212 (1959).
- [37] Y. Quiquempois, N. Godbout, and S. Lacroix, “*Model of charge migration during thermal poling in silica glasses: Evidence of a voltage threshold for the onset of a second-order nonlinearity*”, *Phys. Rev. A*, 65, 043816 (2002).
- [38] V. Pruneri, F. Samoggia, G. Bonfrate, P. G. Kazansky, and G. M. Yang, “*Thermal poling of silica in air and under vacuum: The influence of charge transport on second harmonic generation*”, *Appl. Phys. Lett.*, 74, 17, 2423 (1999).
- [39] Aiko Narazaki, Katsuhisa Tanaka, Kazuyuki Hirao, and Naohiro Soga, “*Effect of Poling Temperature on Optical Second-Harmonic Intensity of Lithium Sodium Tellurite Glass*”, *J. Am. Ceram. Soc.*, 81 [10] 2735–37 (1998).
- [40] T. M. Proctor and P. M. Sutton, “*Space-Charge Development in Glass*,” *J. Am. Ceram. Soc.*, 43 [4] 173–79 (1960).
- [41] Davis E A and Mott N F, “*Conduction in non-crystalline systems V. Conductivity, optical absorption and photoconductivity in amorphous semiconductors*”, *Philos. Mag.* 22 903, (1970).

- [42] Mansoor Sheike Bahe, Ali A. Said, Tai-Huei Wei, David J Hagan, E.W. Van Stryland, "Sensitive measurement of optical non linearities using a single beam", IEE J. of Quantum Electron., 26, 4(1990).
- [43] L. Irimpan, V. P. N. Nampoore, and P. Radhakrishnan, "Spectral and nonlinear optical characteristics of nanocomposites of ZnO-CdS", J. Appl. Phys. 103 (2008)094914.
- [44] Rose Leena Thomas, Vasuja, Misha Hari, V P N Nampoore, P Radhakrishnan, Sheenu Thomas, "Optical non-linearity in ZnO doped TeO₂ glasses", JOAM, 13, 5, 523(2010).



INFLUENCE OF LANTHANIDES ON STRUCTURAL, THERMAL, LINEAR AND NONLINEAR OPTICAL PROPERTIES OF ZINC TELLURITE GLASSES

The focus of this chapter is on the influence of lanthanide ions in the zinc tellurite glass matrix. We have incorporated oxides of lanthanum, samarium, europium and holmium in the study because of their capability in modifying the linear and nonlinear optical properties in the tellurite vitreous network. All of the lanthanide ions doped in the zinc tellurite glasses, exhibit their characteristic absorption bands in the absorption spectra. The major result we report in this chapter is the observed switching of optical nonlinearities from Reverse Saturable Absorption to Saturable Absorption in zinc tellurite glasses without and with rare earth content. Our studies reveal that the Two Photon Absorption gets enhanced in the rare earth doped zinc tellurite glasses in the decreasing order of atomic number.

5.1 Introduction

Lanthanides and lanthanide doped glasses have received much attention as they offer a handful of application possibilities in the area of optical communication. A variety of materials showing nonlinear optical properties, applicable for devices in the field of photonics have been investigated during the last decades. Tellurite glasses appear to be promising candidates for many applications, due to their high polarizability and non linear optical properties. In the low phonon energy tellurite glasses, the rare earth ion replaces the network modifiers in it and thus they are capable of dissolving higher concentration of rare earth ions enabling the fabrication of highly compact devices.

Research on tellurite glasses has gone a long way, during the last decades. Research outcomes in the photonic field like photo luminescent devices, laser applications, memory devices, communication applications etc. are clear evidence to the upcoming glass based optoelectronic era. Materials exhibiting non linear optical properties are of great interest in the present world. In the literature we find a number of amorphous non linear optical materials which are useful in nonlinear photonic applications^[1-4]. Tellurites are less toxic than chalcogenides, more chemically and thermally stable and hence a highly suitable fiber material for nonlinear applications in the mid infrared and they are of increasing research interest in applications like laser, amplifier, sensor etc ^[5-10].

Optical limiting is an important mechanism which is a useful subject of study these days. Reverse Saturable Absorbers (RSA) are the candidates exhibiting optical limiting and the basic mechanism under study is Two Photon Absorption (TPA). Optical limiters are transparent at lower laser intensities and become opaque at higher intensities ^[11-13]. Saturable absorbers (SA) are another class of materials which become transparent as the incident laser intensity is increased. The materials exhibiting SA usually have a negative nonlinear absorption coefficient ^[14-17]. This chapter is intended to study some of the structural, thermal linear and nonlinear optical properties of lanthanide doped zinc tellurite glasses. The major result we report is the switch over of nonlinear refractive index from positive to negative, when rare earth ions are incorporated in the zinc tellurite glass network. Switching of optical non linearity between RSA and SA, is an important research area as it is exhibited by few materials.

5.2 Influence of rare earth ions on structure of zinc tellurite glasses

Rare earth ions are well suited in low phonon energy glass matrices like tellurite glasses. To analyse the influence of lanthanide series on zinc tellurite glasses, we have selected a number of rare earth ions from different positions of the periodic table, as the atomic number increases from left to right.

57	58	59	60	61	62	63	64	65	66	67	68	69	70
La	Ce	Pr	Nd	Pm	Sm	Eu	Gd	Tb	Dy	Ho	Er	Tm	Yb
138.91	140.12	140.91	144.24	145	150.36	151.96	157.25	158.93	162.50	164.93	167.26	168.93	173.04

Figure 5.1: Lanthanide series

The first element chosen is lanthanum, which is the first element of the lanthanide series having atomic number 57. Samarium (62), europium (63), which are in the middle of the series and holmium (67), which is almost at the end of the series are also chosen. For to study the changes in the structural, thermal and optical properties of zinc tellurite glasses, especially in the nonlinear optical properties we have selected one of the combinations of zinc tellurite glasses having higher Two Photon Absorption coefficient before rare earth doping. The prepared samples are listed out in the table below.

Table 5.1: Prepared sample compositions of Lanthanide doped zinc tellurite glasses.

Sample name	TeO ₂ (Wt %)	ZnO (Wt %)	La ₂ O ₃ (Wt %)	Sm ₂ O ₃ (Wt %)	Eu ₂ O ₃ (Wt %)	Ho ₂ O ₃ (Wt %)
TZL	70	25	5	-	-	-
TZS	70	25	-	5	-	-
TZE	70	25	-	-	5	-
TZH	70	25	-	-	-	5

All the samples were prepared using melt quench technique. The weighed chemicals were taken in a platinum crucible and kept in a furnace, which is set to a temperature of 900 °C for one hour. It is then quenched to a stainless steel mould at room temperature and moved to an annealing furnace set for a temperature 300 °C and gradually cooled to room temperature. Powdered sample is used to obtain the XRD, EDAX and FTIR of the samples prepared. X ray diffraction spectra prove that all the selected compositions are glass forming.

The following are the XRD and EDAX spectra [figure 5.2], which show the compositions of the prepared samples.

6

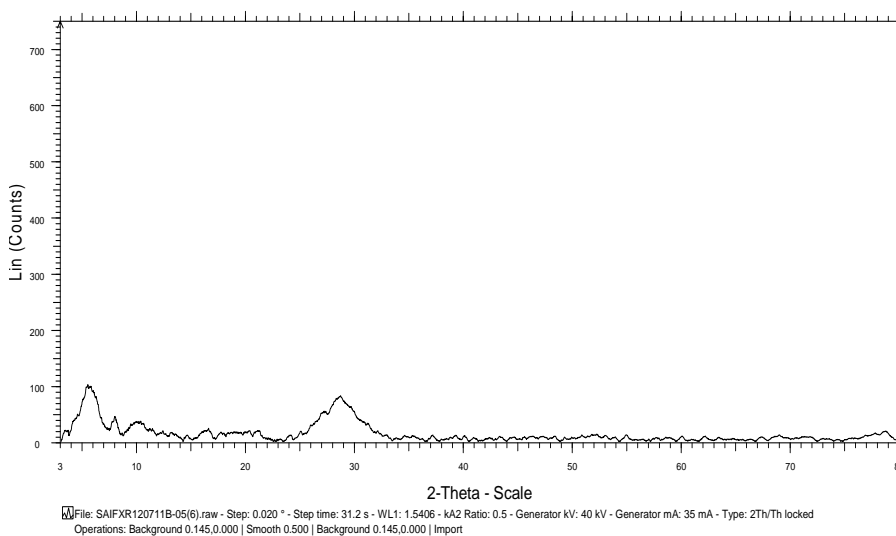


Figure 5.2(a): XRD of Europium doped zinc tellurite glasses

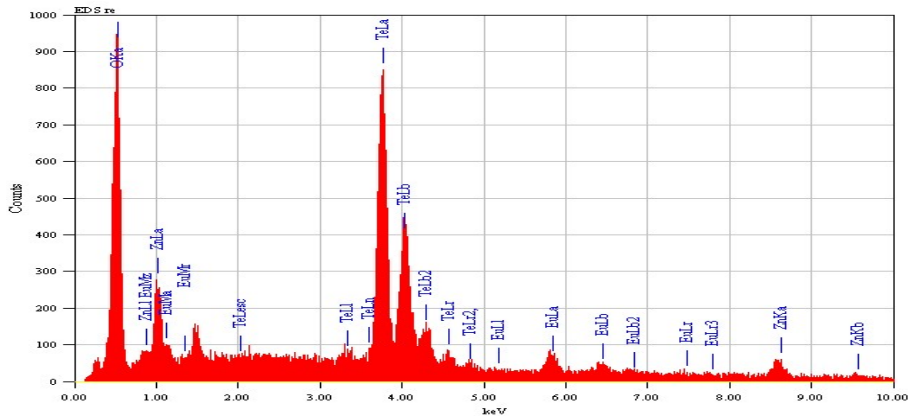


Figure 5.2(b): EDAX of Europium doped zinc tellurite glasses

To have a clear idea on the structural changes taken place in zinc tellurite glasses when rare earth ions are incorporated in them, we have analysed the fourier transform infrared spectra. FTIR give indication about the structural changes taking place in zinc tellurite glasses as the rare earth ions enter in the network. There is a formation of new structural units and so bonds of different vibrational modes appear in the spectra of the glass samples. We have analysed the effect of rare earth ion with the variation of tellurium dioxide content. It is observed that when more tellurium dioxide is present in the glass network there is lesser modifications in the glass. With an increase in modifier ions the glass structure densifies due to the fact that the modifier gives rise to an increase in dangling bonds in the structure. These dangling bonds correspond to the formation of defect states or localized states within the energy gap between the conduction and valence bands.

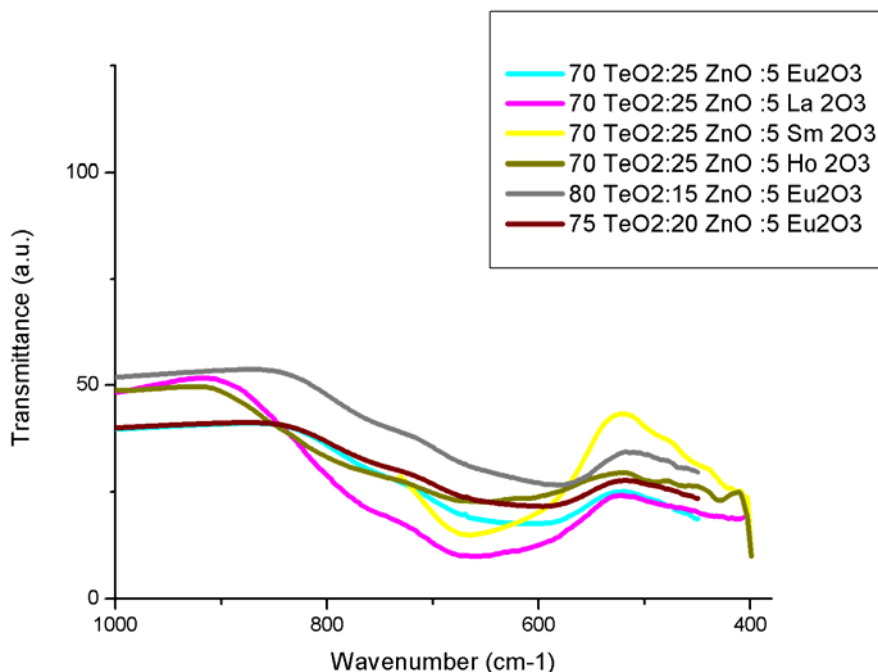


Figure 5.3: FTIR of Lanthanide doped zinc tellurite glasses

From the FTIR spectra we can explain the various vibrational modes of basic structural units of zinc tellurite glasses. Absorption peaks in the $400\text{-}500\text{ cm}^{-1}$ is due to the symmetric stretching and bending vibrational modes of Te-O-Te bonds in TeO_4 subunits^[18,19]. The $550\text{-}750\text{ cm}^{-1}$ infrared absorption bands corresponds to stretching vibrations of Te-O bonds in TeO_3 and TeO_{3+1} subunits. Also there is a possibility of increasing the intensity of absorption bands as the modifier ion increases in the glass sample. The presence of large amount of ZnO helps breaking Te-O-Te linkages, producing a number of non bridging oxygen ions in the network along with the rare earth ions. All these are indications of conversion of TeO_4 structural units in to new TeO_3 trigonal pyramids.

Concentration effect of europium

Detailed analysis of europium doped 70 TeO₂ :30 ZnO glass is done by varying the amount of europium oxide doped. The concentration of europium oxide is varied from 1-5 %. On increasing the concentration of rare earth ions from 0 % to 5 %, the modification of the network also increases.

XRD of the samples, indicates no identities of crystallization of the prepared samples. Analysis of FTIR spectra helps to have deeper understanding over the changes in the structure. The structural evaluation is always important to predict the properties and so the application of the prepared sample. The fourier transform infrared spectra of the three samples are given below [Figure 5.5]. The IR absorption bands are observed in the 550- 750 cm⁻¹ region indicating the conversion of basic structural units TeO₄ into TeO₃. The shift of these bands to higher wave number side also supports the idea of formation of Non Bridging Oxygen ions, which increases the polarizability of the glass samples.

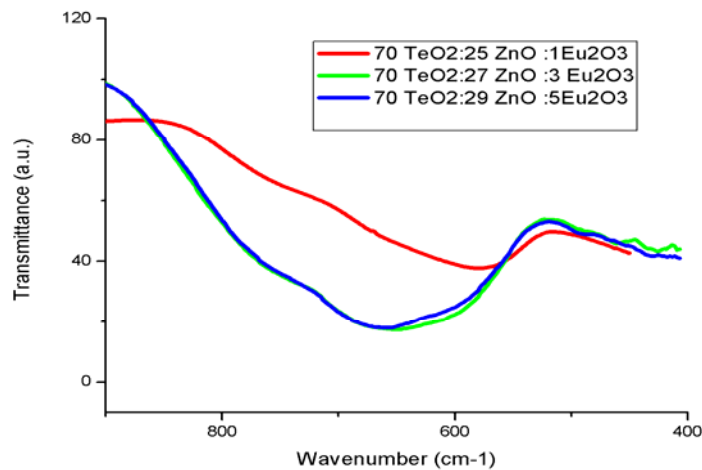


Figure 5.5: FTIR spectra of zinc tellurite glasses by varying europium content

The major bands in the spectra in the 550-750 cm^{-1} region are ascribed to the stretching vibration of equatorial and axial Te-O bonds in TeO_3 units. The more the modifiers accommodate the zinc tellurite glass network the intensity of IR absorption bands increases indicating the network breaking. Possible occupation of modifier ions in the interstitials also creates defect states in the energy gap.

5.3 Influence of rare earth ions on thermal properties of Zinc Tellurite glasses

The structural and optical studies reveal that rare earth ions enter in to zinc tellurite glass finding trap states or say localized states. This is an indication of formation of strong bonds like zinc-oxygen, rare earth ion – oxygen etc. Glass transition is found to increase with the added modifiers and rare earth ions due to the formation of these strong bonds in the zinc tellurite glass network.

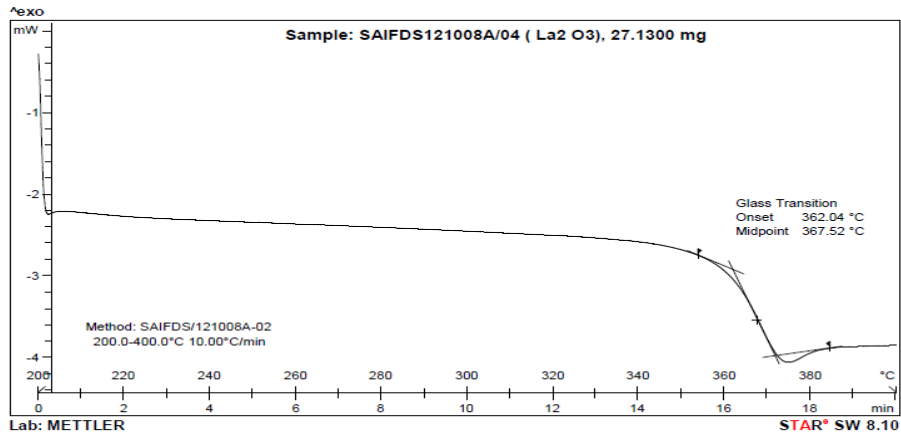


Figure 5.6(a): DSC of lanthanum doped zinc tellurite glasses

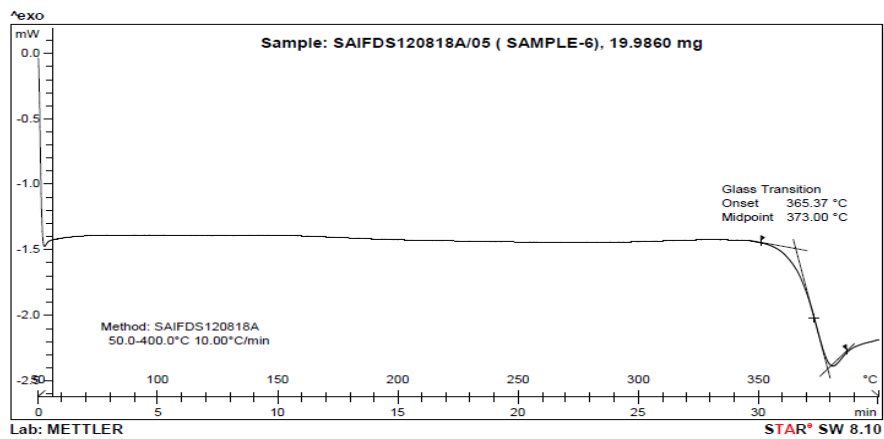


Figure 5.6(b): DSC of Europium doped zinc tellurite glasses

The table below gives the range of glass transition temperatures

Table 5.2: Glass transition temperature of lanthanide doped zinc tellurite glasses

sample	Tg (⁰ c)
70 TeO ₂ :25 ZnO:5La ₂ O ₃	368
70 TeO ₂ :25 ZnO:5Sm ₂ O ₃	375
70 TeO ₂ :25 ZnO:5Eu ₂ O ₃	373
70 TeO ₂ :25 ZnO:5Ho ₂ O ₃	385

Structural study explains the conversion of structural units, which causes formation of IR bands at 550-750 cm⁻¹ region, indicating formation of new bonds. The major building blocks of tellurite glasses are covalently bonded TeO₄ structural units. On formation of new TeO₃ structural units, the covalent bonds get replaced with ionic bonds. Ionic bonds are based on strong electrostatic force of attraction and so stronger than the covalent bonds present in the less modified structures. Thus the density increase implies that there is a possibility of increase of glass transition temperature in rare earth doped zinc tellurite glasses.

Concentration effect of europium

The explanation given in the above paragraph list out reasons for an increase in glass transition temperature of zinc tellurite glasses. As the europium content increases formation of non bridging oxygen ions increases, by rupturing Te- O-Te bridges. Tellurium is replaced by europium ions along with zinc ions, increasing glass transition temperature.

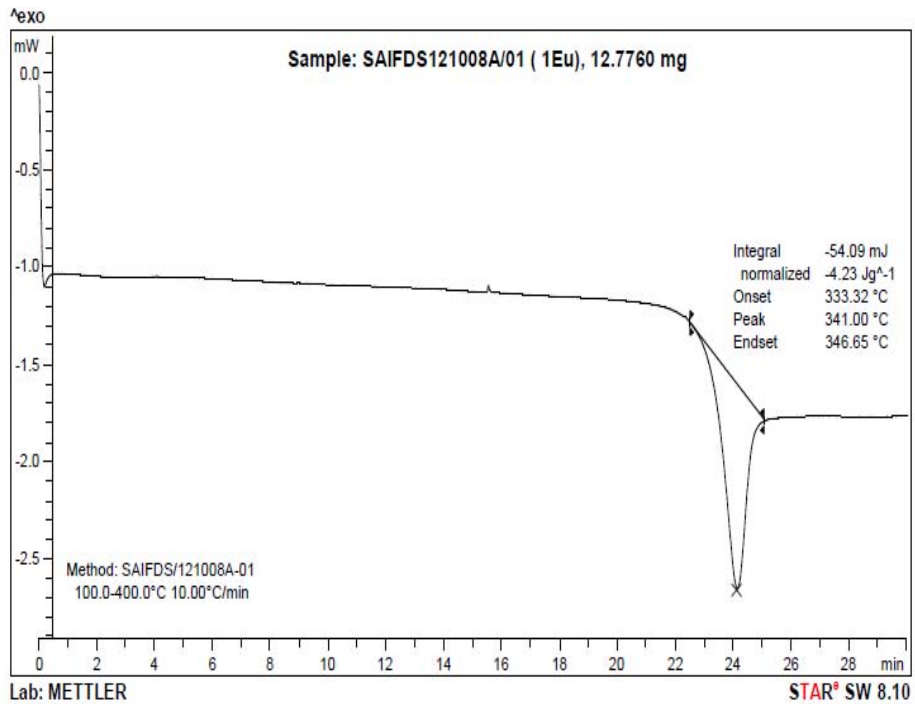


Figure 5.7(a): DSC of zinc tellurite glasses with 3Eu₂O₃ europium content

The table (Table 5.3) below gives the range of glass transition temperatures. As rare earth concentration increases from 0% to 5% the glass transition temperature gets varied from 336 °C to 373 °C. This gives a clear idea of the amount of new ionic bonds created in the network by replacing the covalent bonds.

Table 5.3: Glass transition temperature of zinc tellurite glasses by varying europium content

sample	T _g (°C)
70 TeO ₂ :30 ZnO	336
70 TeO ₂ :29 ZnO:1Eu ₂ O ₃	341
70 TeO ₂ :27 ZnO:3Eu ₂ O ₃	361
70 TeO ₂ :25 ZnO:5Eu ₂ O ₃	373

5.4 Influence of rare earth ions on linear optical properties of Zinc Tellurite glasses

Tellurite glasses are well known for their excellent optical properties like high refractive index and broad infrared transparency. Rare earths are in the sixth row of the periodic table and are characterized by a partially filled 4f shell that is shielded from external fields by 5s² and 5p⁶ electrons^[20]. It

means that rare earth radiative transitions in solid hosts resemble those of the free ions and their electron–phonon coupling is very weak. The positions of rare earth electronic levels are much more influenced by spin-orbit interactions than by the applied crystal field, due to this shielding effect. Rare earths exist as divalent /trivalent ions in the host matrix. It is also to be noted that rare earths in semiconductors occupy isoelectronic substitutional sites like trap centres^[21] in which there is a strong interaction between free carriers and the partially filled 4f shell of rare earth ion. Optical absorption spectra of rare earth doped zinc tellurite glasses are shown below[Figure 5.8].

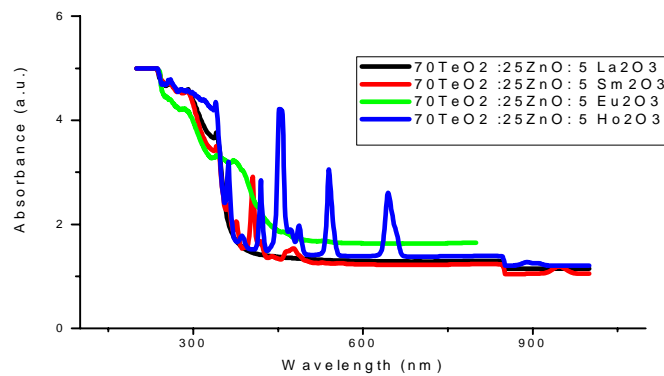


Figure 5.8: Absorbance spectra of Lanthanide doped zinc tellurite glasses

Absorption spectra contain absorption peaks which are signatures of rare earth ions, which can be seen in the absorbance spectra of samarium, europium and holmium. Lanthanum does not show much absorption bands as shown in the absorption spectra. Samarium shows absorption bands from its ground level that is $^6H_{5/2}$ to the higher levels like $^4G_{5/2}$, $^4G_{7/2}$ etc. The absorption bands of Europium originate from the ground 7F_0 level and end up at the excited states 7F_1 , 5D_0 and 5D_1 ^[21]. The ground state of Holmium is

5I_8 . There are a number of characteristic absorption bands of holmium as shown above. These bands correspond to transition from ground to 5I_7 , 5I_6 , 5I_4 , 5F_5 , 5F_4 and 5F_3 .

Mallawany et al^[20] reports that there is a possibility of band gap increase when rare earth ions are doped in pure tellurium dioxide glasses. It is verified by measuring the optical band gap by varying the glass former and modifier content.

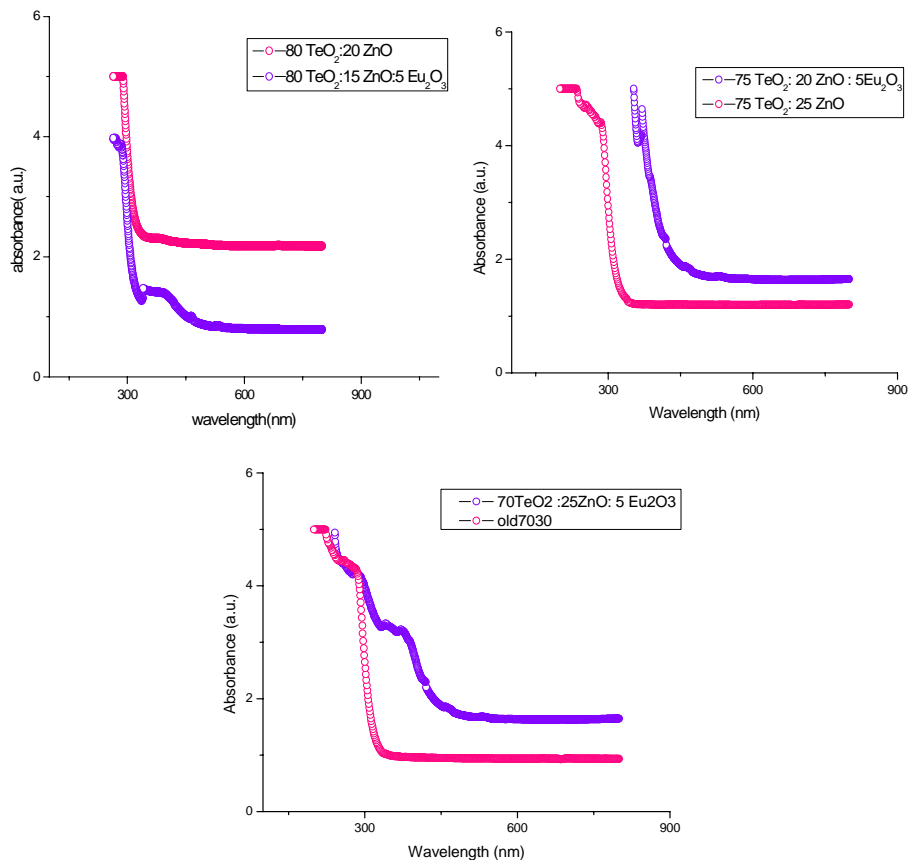


Figure 5.9: Absorbance spectra of Lanthanide doped zinc tellurite glasses: comparison with the undoped zinc tellurite glasses.

The above figures[Figure 5.9] show that when modifier content is least, the optical band gap is high. As the modifier is increased, band gap shifts to lower value as shown in the figure above. The variation of band gap depends on the amount of modification in the zinc tellurite glass network. The band gap increase and then decrease, when the rare earth ions are incorporated, with varying glass former/modifier content is shown in the figure[Figure 5.10] and the band gap so obtained are tabulated below.

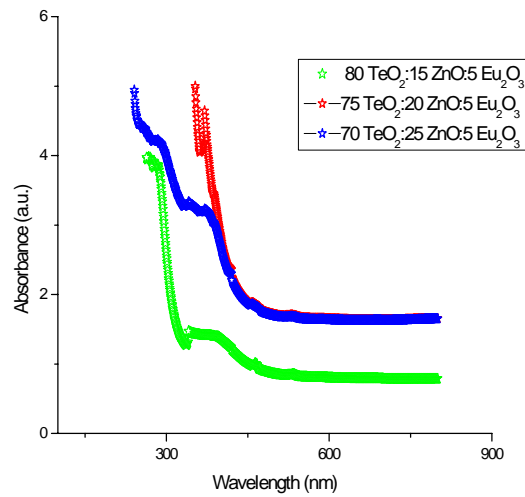


Figure 5.10: Absorbance spectra of Lanthanide doped zinc tellurite glasses

Table 5.4: Band gap of Lanthanide doped zinc tellurite glasses

Sample	Eg(eV)
80 TeO ₂ :20 ZnO	3.13
75 TeO ₂ :25 ZnO	3.05
70 TeO ₂ :30 ZnO	2.97
80 TeO ₂ :15 ZnO:5Eu ₂ O ₃	3.40
75 TeO ₂ :20 ZnO:5Eu ₂ O ₃	2.71
70 TeO ₂ :25 ZnO:5Eu ₂ O ₃	2.53

The influence of rare earth ions in tellurite glasses depends on its composition. Increase in band gap of rare earth doped tellurite glasses is attributed to the larger size of rare earth ions. In 1992, Burger et al^[22] reported that in zinc tellurite glasses, band gap increases/decreases with TeO₂/ZnO contents and a major influence is with the tellurium content, which is due to the decrease in nonbridging oxygen ions. The absorption edge of rare earth doped glasses becomes sharper in the UV region, due to the UV absorption of rare earth ions.

These sharp bands are caused by forbidden transitions involving the 4*f* levels, and these 4*f* orbits are very effectively shielded from interaction with external fields of the hosts by 5*s*² and 5*p*⁶ shells. Hence, the states arising from the various 4*f*^{*n*} configurations are only slightly affected by the surrounding ions and remain practically invariant for a given ion in various compounds. The rare-earth ions in tellurite glasses occupy the center of a distorted cube, which is made of a four tetrahedral of phosphate, silicate, borate, and germinate glasses. Each tetrahedron contributes two oxygen atoms to the coordination of the rare-earth ions. The overall coordination number is 8, the most common coordination number of the rare-earth oxides^[20].

But a decrease in TeO₂ content and/or an increase in ZnO content help rare earth doped zinc tellurite glasses to increase its nonbridging oxygen ions and increase its density, since the europium content is kept constant. This can be attributed to the formation of dangling bonds due to the modifier ions ZnO added to the glass network. In semiconducting amorphous hosts rare earths occupy isoelectronic substitutional sites such as trap centres in which there is a strong interaction between free carriers and the partially filled 4*f* shell of rare earth ion. Rare earth traps have relatively large carrier

capture cross-sections, and readily form bound excitons through coulombic interaction between trapped and free carriers. The resultant band gap variation is tabulated below along with other optical constants.

Table 5.5: Optical constants of Lanthanide doped zinc tellurite glasses

sample	Eg(eV)	n(at 633 nm)	ϵ	$\chi^{(1)}$ (esu)
70 TeO ₂ :30 ZnO	2.97	2.05	4.20	3.20
70TeO ₂ :25ZnO:5La ₂ O ₃	2.83	2.14	4.58	3.58
70TeO ₂ :25ZnO:5Sm ₂ O ₃	2.79	2.18	4.75	3.75
70TeO ₂ :25ZnO:5Eu ₂ O ₃	2.53	2.25	5.06	4.06
70TeO ₂ :25ZnO:5Ho ₂ O ₃	2.77	2.16	4.67	3.67

The increased density of localized states decreases the effective gap between the tailed extended states. Band gap reduction in turn causes refractive index hike and enhancement of other optical constants.

Concentration effect of europium

To analyse the concentration effect of rare earth ions on optical properties of zinc tellurite glasses, we have varied europium content as 1%,3% and 5%.The results can be summarized in the optical absorption spectra given below[Figure 5.11].

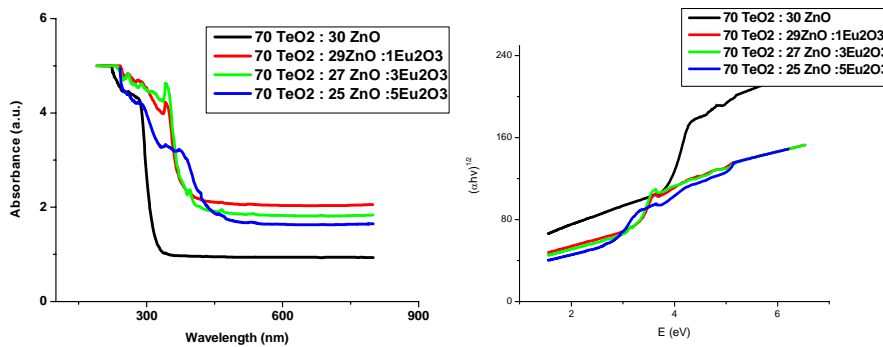


Figure 5.11: Absorbance spectra and band gap of zinc tellurite glasses by varying europium content

Table 5.6: Band gap of zinc tellurite glasses by varying europium content

sample	Eg (eV)
70 TeO ₂ :30 ZnO	2.97
70 TeO ₂ :29 ZnO:1Eu ₂ O ₃	2.87
70 TeO ₂ :27 ZnO:3Eu ₂ O ₃	2.80
70 TeO ₂ :25 ZnO:5Eu ₂ O ₃	2.53

As the modifier increases, the band edge is getting redshifted in the case of rare earth doped zinc tellurite glasses. The absorption band edges are also sharpened due to the high UV absorption of rare earth ions. The density of localized states determines the effective band gap of amorphous semiconductors. The band gap is seen to reduce in the samples as europium ions modify zinc tellurite glass matrix. It can be connected with increased density of localized states within the band gap.

5.5 Influence of rare earth ions on linear fluorescence of Zinc Tellurite glasses

Amorphous semiconductors have localized states in band tails. The localized states are randomly distributed and their electrostatic energies are also distributed. In amorphous solids electron-hole pairs are created by light irradiation, where holes are quickly trapped and electrons execute hopping-random walks among localized band tail states. Thus at low temperatures PL occurs dominantly from the radiative recombinations in the tail states. In the tail states excited charge carriers, usually localized on different sites, must move to the same site for recombination. The photoluminescence in amorphous semiconductors may consist of a major band and weaker bands of longer wavelength attributed to dangling bonds. The main photoluminescence band arises from the radiative recombination of electrons and holes both trapped in band tail states ^[23].

The linear fluorescence studied using spectro fluorometer reveals that it has a prominent emission between 530-610 nm region, when excited from 370 nm- 450 nm. In our previous work, we have studied luminescence spectra of zinc oxide doped tellurite glasses by varying ZnO concentration. Blue emission was the major one and a weak band of emission is also observed at the green region. The luminescence intensity was found to be proportional to the TeO₂ content. In the present work we have incorporated europium ions in the zinc tellurite glass network to study the effect of the ions in the fluorescence intensity of the glass. The fluorescence intensity was found to be a constant, unlike from our study with undoped zinc tellurite glasses.

This is due to the compensating action of europium ions in the tellurite glass. There is also a shift in the emission peak with the excitation wavelength, from green to red. All these are some of the evidences for the high influence of europium ions on the tellurite glass structure. The radiative transition in amorphous semiconductors is due to the recombination of an electron in the conduction band tail and a trapped hole. A strong electron-phonon coupling distorts the lattice near the trapped hole, lowering its energy. This interaction is responsible for the broadness of the luminescence band and its position at about half the band gap energy. The recombination centre is thought to be a charged dangling bond. The same centre is observed in the hole drift mobility, and thermally stimulated conductivity. Luminescence in amorphous solids also originates from recombination between the band tails and deep centres, with three separate transitions identified^[23]: (a) both excited electron and hole are in their extended states, that is, electron in the conduction and hole in the valence extended states, (b) electron is in conduction extended and hole in valence tail states, (c) electron is in conduction tail and hole in valence extended states, and (d) both are in

tail states, that is, electron in conduction and hole in valence tail states. Let us consider the first possibility that an exciton is created by exciting an electron in the conduction and hole in valence extended states.

Other than the electron-phonon coupling, the shape and intensity of the spectra are very sensitive to sample preparation and treatment, and correlate with other electrical and optical properties.

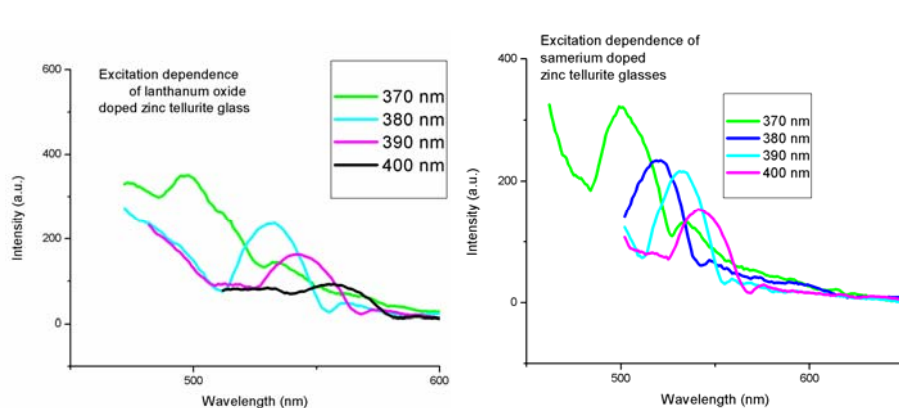


Figure 5.12(a): Fluorescence spectra of lanthanum and samerium doped zinc tellurite glasses

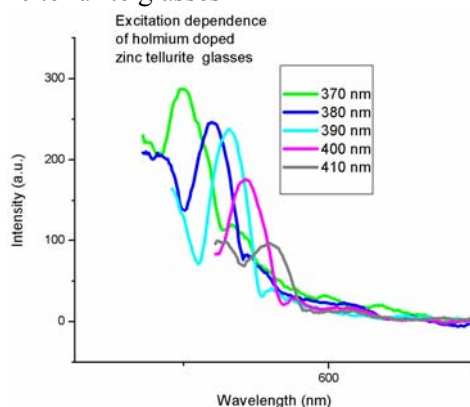


Figure 5.12(b): Fluorescence spectra of holmium doped zinc tellurite glasses

An electron phonon coupling possibly distorts the lattice near the trapped hole and causes broadening of the luminescence band ^[23-25]. The charged

defects, which have energy levels in the bandgap with a spectral bandwidth ΔE , are responsible for the photoluminescence and related properties in tellurite glasses. It is to be noted that, as the excitation wavelength (λ_{ex}) increases the PL peak intensity decreases. As the concentration increases, the non radiative relaxation of the excited state to the defect centres is seen to overcome radiative relaxation. The non radiative relaxation originating via collision process, results to a quenching of fluorescence intensity and so the possible transitions are that of lower energy including localized states. In bulk samples the decrease in such quantum efficiency at higher excitation energy has been explained due to strong non radiative surface recombination.

5.6 Influence of rare earth ions on TPA of Zinc Tellurite glasses

Reports show that crystal field parameters are sensitive to the electrostatic interactions^[26-28] in the tellurite glass site. This means that the ligands in zinc tellurite glasses are closer to rare earth ions than other glass types, indicating an increased charge density in the present glass combination.

To analyse the nonlinear optical properties of rare earth doped zinc tellurite glasses, we have studied the open aperture z scan^[29-31] data. The results of the single beam z scan technique shows a switch over from RSA [Reverse Saturable Absorption] to SA [Saturable Absorption], when rare earth ions are present in the glass matrix. Our study without rare earth ions in zinc tellurite glasses exhibit RSA, due to the Two Photon Absorption taking place in the sample. Rare earth doped zinc tellurite glasses show an increased transmittance at higher intensities, due to saturation of absorption. This means that the absorption process in rare earth doped glass is essentially in respect of the rare earth ion, which show Soft this change from RSA to SA, also show that

the presence of rare earth ion changes the nonlinear component of refractive index to negative.

Reverse Saturable Absorption occurs via TPA when the excited state cross section is greater than the ground state cross section. Possible existence of Free Carrier Absorption along with TPA causes the enhancement of TPA and that makes the cross section of the excited state greater than that of the ground state and so, as the intensity at the focus is increased it exhibits significant increase in absorption. Saturation absorption is due to the accumulation of molecules in the singlet excited state leading to depletion of the ground state and the intensity at the focus is highly reduced and exhibit high transmittance. L. C. Olivier et al^[32] reports that the behavior is due to the occurrence of a photon-assisted off-resonance energy transfer. Naga Srinivas et al^[35] attributed the switch over from SA to RSA behavior with increasing the sample concentration to localization of energy which leads to resonant TPA, and the change over from RSA to SA is attributed to the aggregation and fast decay times in molecules which get populated through energy transfer^[32-34]. The figure below[Figure 5.13] shows RSA in zinc tellurite glasses and SA in rare earth doped zinc tellurite glasses.

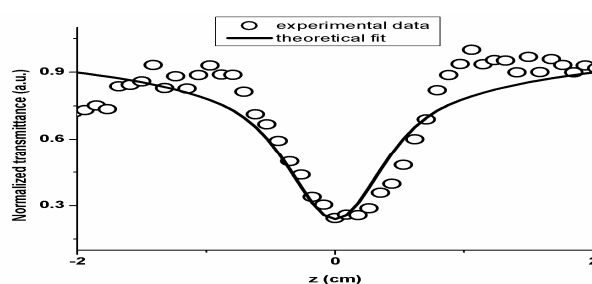


Figure 5.13(a): Open aperture z scan curve of zinc tellurite glasses before doping rare earth ion.

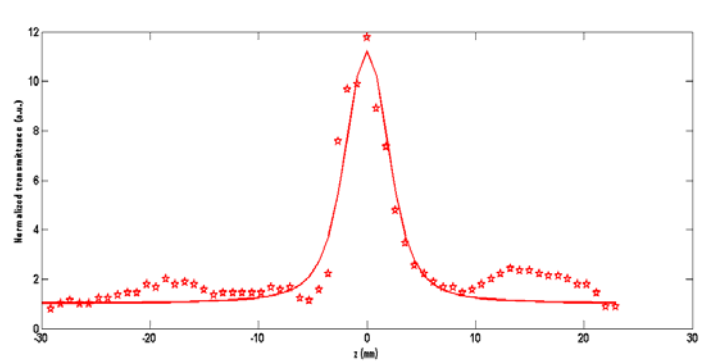


Figure 5.13 (b): Open aperture z scan curves of lanthanum doped zinc tellurite glasses.

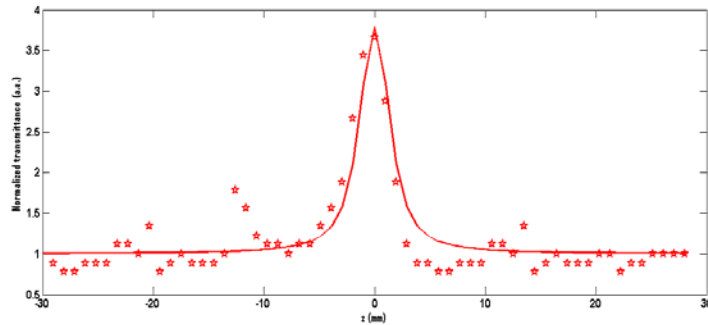


Figure 5.13 (c): Open aperture z scan curves of samerium doped zinc tellurite glasses.

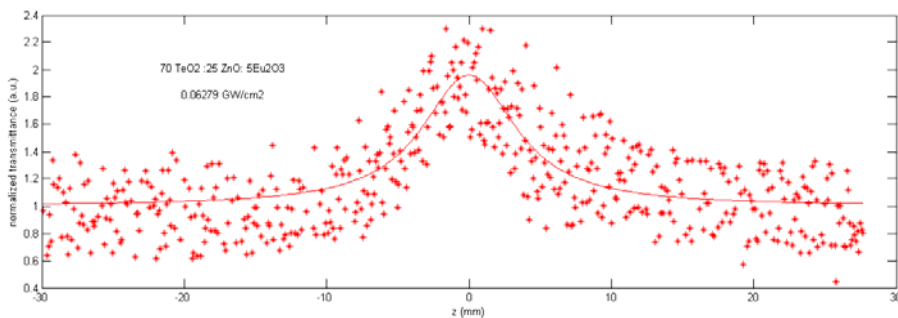


Figure 5.13(d): Open aperture z scan curves of europium doped zinc tellurite glasses.

According to Venugopal Rao et al ^[34], this kind of behavior is intriguing and has not been reported earlier and several factors account for this kind of

performance. Solvent effect and intensity effect are some of the reasons for the observed switch over from RSA to SA, found in the literature. 2PA, 3PA, and ESA [excited state absorption] are all intensity dependent processes and it is also well established that there could be other complicated nonlinear absorption processes. Another factor which is of importance is that, at different concentrations there is a possibility of aggregation thereby modifying the lifetimes of the excited states influencing the nonlinear absorption behavior. The absorption properties of a molecule are itself altered at higher concentrations, as evident from the absorption spectra, again affecting the nonlinear absorption. Continuum generation and sample damage are the other possibilities which can be omitted, at very high intensities thereby affecting the nonlinear transmission, because the results obtained in this work are reproducible [33].

Reasons for this switch over from RSA to SA, is attributed to the sign reversal of χ^3 caused by the modification of the local field factor by Naga Srinivas et al. [35] observed a similar transition in a charge-transfer salt with increasing intensity and is due to fifth-order nonlinearity, as the excitation wavelength was 1064 nm and absorption peaked near 532 nm for their sample.

There are also reports of crossover from RSA to SA due to the saturation of ESA in the ground level to excited state transition by P. Prem Kiran et al [36]. It is found that the irradiance at which the turnover from RSA to SA occurs, strictly depends on the magnitude of the relaxation time from second to first excited state. As the lifetime of the second excited state increases, the intensity at which the switch from RSA to absorption reduction takes place remains approximately constants. Moreover for small values of excited state lifetime, the RSA is not so effective because the transmittance decreases by

approximately 5% with respect to the linear regime before SA is activated. In the case of the largest excited state lifetime considered, on the contrary, a decrease of greater than 55% with respect to the linear case is obtained due to RSA. This can be explained by considering that when the decay time of the second excited state is long, there are many molecules in that level which can undergo transitions. In addition, with this method, it has been possible to estimate high-lying excited-state lifetimes. These parameters are relevant for characterization of the nonlinear response of these materials and for evaluating their possible use in all-optical switching devices^[36,37].

Saturable absorbers are of great interest among optoelectronic researchers, since they are having applications in Q-switching and mode-locking. Lasers with solid state saturable absorbers are in demand, because of their applications in medical field and in scientific areas like nonlinear optics and laser spectroscopy. In rare earth doped zinc tellurite glasses, saturable absorption is due to intra f-f configuration or interconfiguration transitions of rare earth ions. So the nonlinear transmission of rare earth doped zinc tellurite glasses give information regarding the solutions for the emerging requirements in laser spectroscopy. The table below shows the nonlinear optical constant at three different laser powers.

Table 5.7: TPA coefficient of rare earth doped zinc tellurite glasses.

sample	β (cm/GW)		
	at laser power density 63×10^{-3} (GW cm ⁻²)	At laser power density 88×10^{-3} (GW cm ⁻²)	At laser power density 113×10^{-3} (GW cm ⁻²)
70 TeO ₂ :30 ZnO	1215	888	673
70TeO ₂ :25ZnO:5La ₂ O ₃	466	458	436
70TeO ₂ :25ZnO:5Sm ₂ O ₃	317	222	177
70TeO ₂ :25ZnO:5Eu ₂ O ₃	278	251	206

Concentration effect of europium

To study the effect of concentration of rare earth ions on nonlinear optical properties of zinc tellurite glasses, we have varied europium oxide concentration from 0% to 5%. The switching effect was observed when the concentration of europium oxide changed from 0% to 1%. The plots obtained are given below [Figure 5.14].

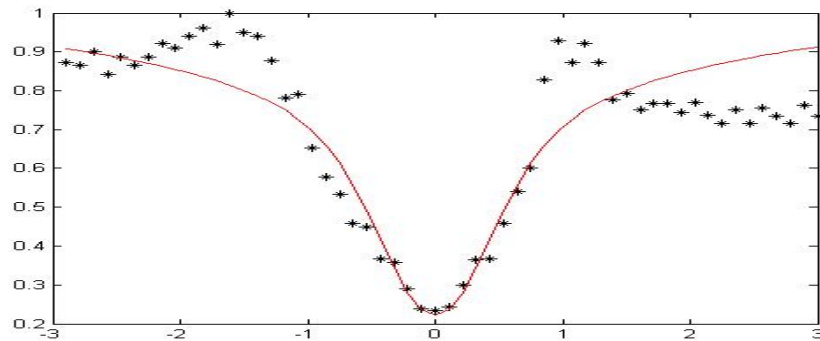


Figure 5.14(a) : Open aperture z scan curves of 0Eu₂O₃ doped zinc tellurite glasses: normalized transmittance across y-axis and z along x-axis.

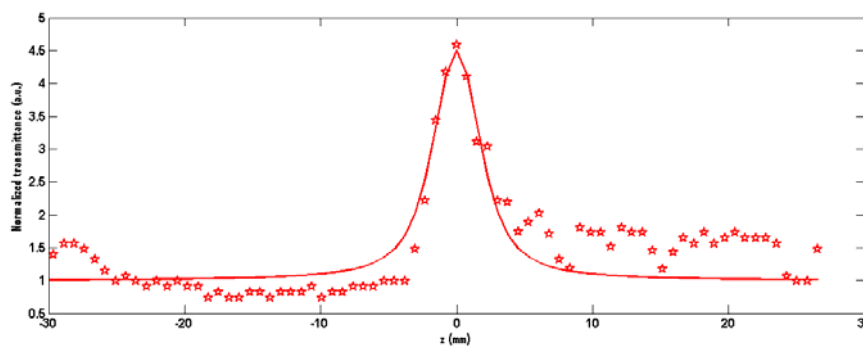


Figure 5.14(b) : Open aperture z scan curves of 1Eu₂O₃ doped zinc tellurite glasses.

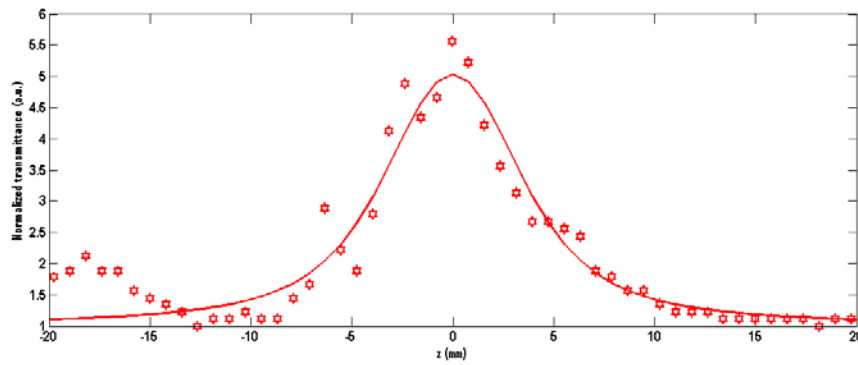


Figure 5.14(c): Open aperture z scan curves of 3Eu₂O₃ doped zinc tellurite glasses.

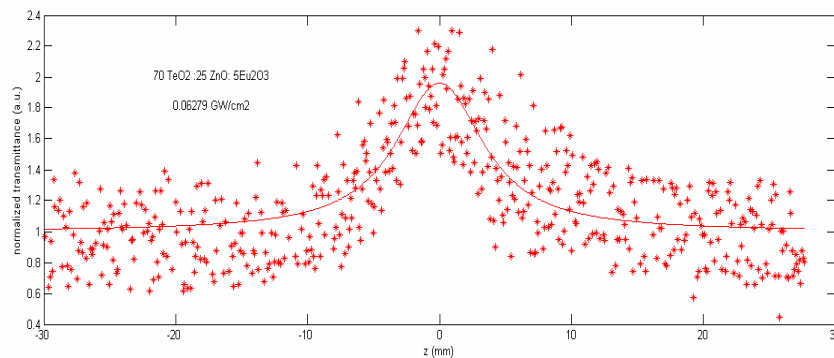


Figure 5.14(d): Open aperture z scan curves of 5Eu₂O₃ doped zinc tellurite glasses.

The observed switching can be attributed to the sign reversal of third order susceptibility due to change in local field factor of zinc tellurite glass matrix. The modification of excited state life time with concentration variation is also another reason for the observed transition from RSA to SA. Saturation of absorption is due to the accumulation of molecules in the excited state leading to the depletion of ground state and thereby reducing the intensity at the focus. Thus an increased nonlinear transmittance is observed in the case of rare earth doped zinc tellurite

glasses. The table below shows the nonlinear optical constant at three different laser powers.

Table 5.8: TPA coefficient of rare earth doped zinc tellurite glasses by varying europium concentration.

sample	$\beta(\text{cm/GW})$		
	at laser power density 63×10^{-3} (GW cm^{-2})	At laser power density 88×10^{-3} (GW cm^{-2})	At laser power density 113×10^{-3} (GW cm^{-2})
70 TeO ₂ :30 ZnO	1215	888	673
70TeO ₂ :29ZnO:1Eu ₂ O ₃	478	329	265
70TeO ₂ :27ZnO:3Eu ₂ O ₃	427	320	226
70TeO ₂ :25ZnO:5Eu ₂ O ₃	278	251	206

5.7 Summary and Conclusions

In this chapter we present linear and nonlinear optical studies on rare earth doped zinc tellurite glasses. Low phonon energy environment fits rare earth ions in zinc tellurite glass network.

- ❖ In zinc tellurite glasses, the incorporation of lanthanides increases the conversion of structural units and FTIR spectra indicate its formation. NBO ions are created with creation of dangling bonds.
- ❖ Glass transition is found to increase with Lanthanide ions in zinc tellurite glasses. Modifiers create localized states decreasing the band gap thereby increasing the density and refractive index of the glass network.

- ❖ Crystal field parameters are sensitive to the electrostatic interactions between the anions and cations. Fluorescence is observed from band states and tail states.
- ❖ Non linear optical properties of rare earth doped zinc tellurite glasses shows saturation of absorption. Saturation absorption is due to the accumulation of molecules in the singlet excited state leading to depletion of the ground state . Thus, the intensity at the focus is highly reduced whereby high transmittance is exhibited. The absorption process in europium doped glass is essentially in respect of the rare earth ion, showing SA. A switch over from RSA to SA shows that the presence of europium ion changes the nonlinear component of refractive index negative. At higher concentrations there is a possibility of aggregation thereby modifying the lifetimes of the excited states influencing the nonlinear absorption behavior.

References

- [1] Edmund paweł golis, manuela reben, jan wasylak, jacek filipecki, “*Investigations of tellurite glasses for optoelectronics devices*”, *Optica applicata*, Xxxviii, 1, (2008).
- [2] Hagemuller p. [ed.], “*inorganic solid fluorides, chemistry and physics*”, academic press, new York (1985).
- [3] wasylak j., ozga k., kityk i.v., kucharski j., “*optical limiting in europium and thulium doped Oxide glasses*”, *Infrared phys. and tech.* 45(4), 253–63, (2004).
- [4] Aidong Zhang, Aoxiang Lin, Jau-Sheng Wang and Jean Toulouse “*Multistage etching process for microscopically smooth tellurite glass surfaces in optical fibers*” *J. Vac. Sci. Technol. B* 28,4, (2010).
- [5] X. Feng *et al.*, “*Single-mode tellurite glass holey fiber with extremely large mode area for infrared nonlinear applications*”, *Opt. Express* 16 (18), 13651 (2008).
- [6] M. D. O’Donnell *et al* “*Tellurite and Fluorotellurite Glasses for Fiberoptic Raman Amplifiers: Glass Characterization, Optical Properties, Raman Gain, Preliminary Fiberization, and Fiber Characterization*”, *J. Am. Ceram. Soc.* 90, 1448, (2007).
- [7] J. S. Wang, E. M. Vogel, and E. Snitzer, “*Tellurite glass: a new candidate for fiber devices*”, *Opt. Mater. Amsterdam, Neth.*3, 187, (1994).
- [8] J. S. Wang, E. M. Vogel, E. Snitzer, J. L. Jackel, V. L. Da Silva, and Y. Silberberg, “*1.3 μm emission of neodymium and praseodymium in tellurite-based glasses*”, *J. Non-Cryst. Solids* 178, 109, (1994).
- [9] J. S. Wang, D. P. Machewirth, F. Wu, E. Snitzer, and E. M. Vogel, “*Neodymium-doped tellurite single-mode fiber laser*”, *Opt.Lett.* 19, 1448, (1994).
- [10] P. Joshi, S. Shen, and A. Jha, “*Er³⁺-doped boro-tellurite glass for optical amplification in the 1530–1580 nm*”, *J. Appl. Phys.* 103, 083543,(2008).
- [11] Maiman, T. H. “*The first experimental LASER: Stimulated optical emission in Ruby*” *Nat.*, 187, 493, (1960).
- [12] L. W. Tutt and T. F. Boggess, “*A review of optical limiting mechanisms and devices using organics, fullerenes, semiconductors and other materials*”, *Prog. Quantum Electron.* 17, 299 (1993).
- [13] Kumar, G.R.; Rajgara, F.A., “*Z scan studies and optical limiting in a mode locking dye*” *Appl. Phys. Lett.*, 67, 3871, (1995).
- [14] B. K. Garside and T. K. Lim, “*Laser mode locking using saturable absorbers*”, *J. Appl. Phys.* 44 (5), 2335 (1973).

- [15] T. Brabec *et al.*, “Kerr lens mode locking”, *Opt. Lett.* 17 (18), 1292 (1992).
- [16] U. Keller *et al.*, “Semiconductor saturable absorber mirrors (SESAMs) for femtosecond to nanosecond pulse generation in solid-state lasers”, *IEEE J. Sel. Top. Quantum Electron.* 2, 435 (1996).
- [17] Sennaroglu, “Continuous wave thermal loading in saturable absorbers: theory and experiment”, *Appl. Opt.* 36 (36), 9528 (1997).
- [18] B Erariah, “Optical properties of Lead-tellurite glasses doped with samarium trioxide”, *Bull. Mater Sci* 33, 391–394(2010).
- [19] R. El-Mallawany a, M. Dirar Abdalla b, I. Abbas Ahmedc, “New tellurite glass: Optical properties”, *Mater. Chem. and Phys.* 109, 291–296(2008).
- [20] Raouf A. H. El-Mallawany, “Tellurite glasses Hand book-Physical properties and data”, CRC press LLC, pp17-164, pp370-480(2002).
- [21] A.J. Kenyon, “Recent developments in rare-earth doped materials for optoelectronics”, *Prog. in Quant. Electron.* 26 (2002) 225–284
- [22] Burger H, Kneipp K, Hobert H, VogelW, “Glass formation, properties and structure of glasses in the TeO₂-ZnO system”, *J Non-Cryst Solids* 151,134-142, (1992).
- [23] R. A. Street, “Luminescence in amorphous semiconductors”, *Advan. In Phys.*,25, 397-454 (1976).
- [24] Munetoshi Seki, Kan Hachiya, Katsukuni Yoshida, “Photoluminescence excitation process and optical absorption in Ge-S chalcogenide glasses”, *J. of Non-Cryst. Solids.*, 324, 127–132 (2003).
- [25] S.G. Bishop and D.L. Mitchell, “Photoluminescence excitation spectra in chalcogenide glass”, *Phys. Rev. B.*, 8, 5696-5701 (1973).
- [26] J.H. Song, J. Heo, “Effect of CsBr addition on the emission properties of Tm³⁺ ion in Ge-Ga-S glass ” *J. Mater. Res.* 21, 2323(2006).
- [27] Y.B. Shin, J. Heo, H.S. Kim, “Enhancement of the 1.31 μ m ... with the addition of alkali halides,” *J. Mater. Res.* 16 (5) (2001) 1318.
- [28] P. Nachimuthu, R. Jagannathan, “Absorption and emission spectral studies of Eu³⁺ doped PbO-PbF₂ glass system”. *Proc. Ind. Acad. Sci.* 107, 59 (1995).
- [29] Mansoor Sheike Bahe, AliA. Said, Tai-Huei Wei, David J Hagan, E.W. Van Stryland, “Sensitive measurement of optical non linearities usin a single beam”, *IEE J. of Quantum Electron.*,26, 4(1990).
- [30] L. Irimpan, V. P. N. Nampoori, and P. Radhakrishnan, “Spectral and nonlinear optical characteristics of nanocomposites of ZnO–CdS”, *J. Appl. Phys.* 103,094914 (2008).

- [31] Rose Leena Thomas, Vasuja, Misha Hari, B. Nithyaja, S. Mathew, I.Rejeena, Sheenu Thomas, V. P. N. Nampoori and P. Radhakrishnan, “*Optical Limiting In TeO₂-ZnO Glass From Z-Scan Technique*”, JNOPM, 20, 3, 351-356(2010).
- [32] Zainab S. Sadik1, Dhia H. Al-Amiedy2, Amal F. Jaffar, “*Third Order Optical Nonlinearities of C450 Doped Polymer Thin Film Investigated by the Z-Scan*”, Advan. in Mater. Phys. and Chem., 2, 43-49 (2012).
- [33] L. C. Oliveira and S. C. Zilio, “*Chromium-Doped Saturable Absorbers Investigated by the Z-Scan*,” Braz. J. of Phys., 24, 2, 498-501(1994).
- [34] S. Venugopal Rao1, P. Prem Kiran, L. Giribabu, M. Ferrari, G. Kurumurthy, B. M. Krishna, H. Sekhar and D. Narayana Rao, “*Anomalous Nonlinear Absorption Behavior in an Unsymmetrical Phthalocyanine Studied Near 800 nm using Femtosecond and Picosecond Pulses*”, Nonlinear Opt. and Quant. Opti., 40, 183–191
- [35] N. K. M. Naga Srinivas, S. Venugopal Rao and D. Narayana Rao, “*Saturable and Reverse Saturable Absorption of Rhodamine B in Methanol and Water*,” J. of Opt. Soc. Am. B, 20, 12, 2470- 2479, (2003).
- [36] P. Prem Kiran, D. Raghunath Reddy, A.K. Dharmadhikari, Bhaskar G. Maiya, G. Ravindra Kumar, D. Narayana Rao, “*Contribution of two-photon and excited state absorption in axial-bonding type hybrid porphyrin arrays under resonant electronic excitation*”, Chem. Phys. Lett. 418, 442–447, (2006).
- [37] S Surendra babu, Kiwan jang, Eun jin cho, Hoseop lee, C K Jayasankar, “*Thermal, structural and optical properties of Eu³⁺-doped zinc-tellurite glasses*” J Phys.D:Appl.Phys, 40(2007).



LASER INDUCED FLUORESCENCE STUDIES ON EUROPIUM DOPED ZINC TELLURITE GLASSES

Present chapter reports the laser induced fluorescence spectroscopy of europium doped zinc tellurite glasses. The low phonon energy based emission spectroscopy is an important field in various applications like optical amplifiers, phosphors, fibers, lasers etc. Europium oxide is found to be efficient in fluorescing in the visible wavelength with laser excitation. The present chapter also gives some space to explain the concentration effect of europium and glass former (tellurium dioxide)/ modifier (zinc oxide) on fluorescence.

6.1 Introduction

In recent years there has been special interest to study the properties and applications of rare earth doped tellurite glasses. Lanthanide ions in glasses play an important role, especially by retaining their emission capabilities, in the host matrix. Photoluminescence from rare earth doped tellurite glasses are of major interest in the area of optoelectronic device applications like phosphors, display monitors, lasers and amplifiers for communication systems etc. Tellurite glasses exhibit high rare earth ion solubility and low phonon energy environment ^[1-10]. Low vibrational frequencies of these glasses allow enough non-radiative transitions from the excited states of dopant ions.

Literature indicates that the current interest of researchers on tellurite glasses is because of their optical characteristics such as high refractive index, broad IR transparency and low phonon energy ^[1-10]. Structural studies

are ongoing, to shed light on the short range order of tellurite glasses, based on different combinations^[11-14]. The structure of binary tellurite glasses reveals that its binary structural units are TeO_4 (Trigonal Bipyramid) subunits. As modifier ions are added it increases /decreases its density depending on the modifier used, by conversion of TeO_4 to TeO_3 along with the formation of non bridging oxygen (NBO) ions^[10]. When rare earth ions are doped in zinc tellurite glasses they exhibit linear and nonlinear optical properties useful in various optoelectronic applications. Zinc tellurite glasses are stable in such a way that rare earth ions experience low crystal fields when compared with other oxide glasses^[15].

Recent studies reveal that the large refractive index of tellurite glasses makes them a better non linear material^[17]. There are a few reports on visible fluorescence in rare earth doped tellurite glasses^[15, 16]. In this chapter we present data on laser induced fluorescence studies using 355 nm and 532 nm excitation wavelengths of Quanta Ray Q-switched Nd: YAG laser.

6.2 Fluorescence spectroscopy of europium doped zinc tellurite glasses

The linear fluorescence of europium doped zinc tellurite glass is examined using spectrofluorometer. The emission study reveals that it has a prominent emission between 530-610 nm region, when excited from 370 nm- 450 nm (Figure 6.1). In one of our previous studies, we have focused on the luminescence spectra of zinc oxide doped tellurite glasses by varying ZnO concentration. Blue emission was the major one and a weak band of emission was also observed at the green region. The luminescence intensity was found to be proportional to the TeO_2 content. In the present work we have incorporated europium ions in the zinc tellurite glass network to study the effect of the ions in the fluorescence behaviour of the glass.

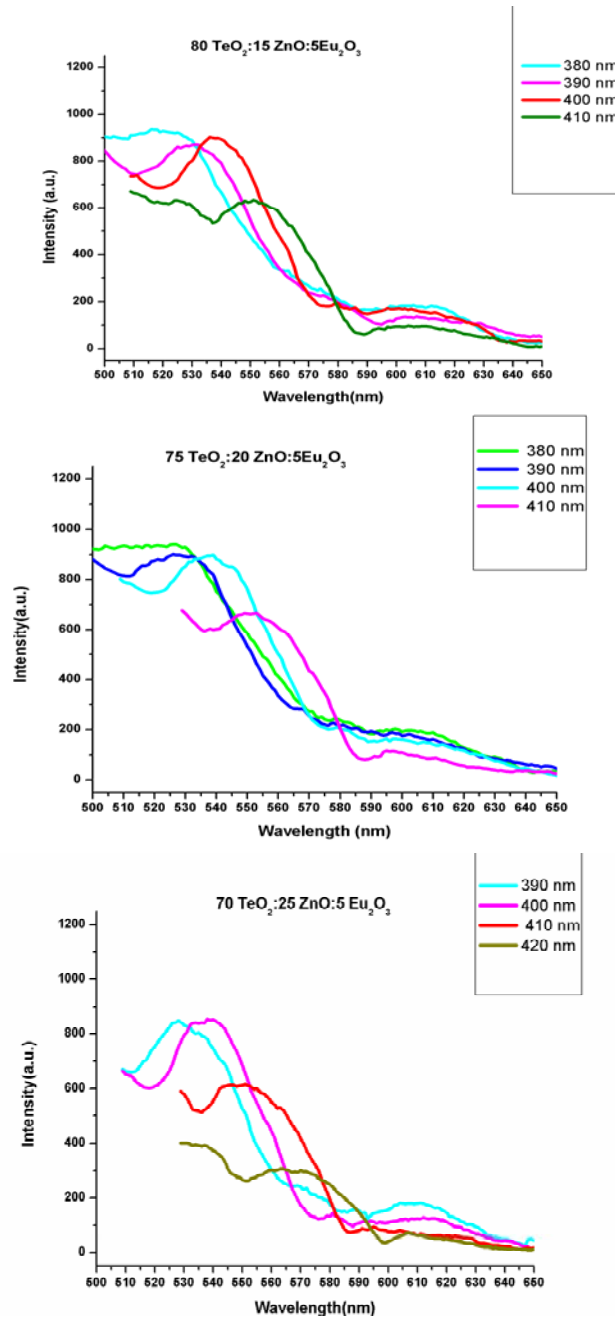


Figure 6.1: Linear Fluorescence spectra of europium doped zinc tellurite glasses recorded using spectrofluorometer

Emission intensity for three different compositions for the same excitation wavelength remains a constant, in the presence of europium ions in zinc tellurite glasses. There is also a shift in the emission peak with the excitation wavelength, from green to red. All these are some of the evidences for the high influence of europium ions on the tellurite glass structure. The europium ions occupy the trap sites like interstitials in the tellurite glass matrix. Thus the emission is originated either from transitions between trap states or that between trap states and band states.

Concentration effect of europium

The fluorescence intensity for the samples 70 TeO₂:29 ZnO: 1 Eu₂O₃, 70 TeO₂:27 ZnO: 3 Eu₂O₃ and 70 TeO₂:25 ZnO: 5 Eu₂O₃ are compared in this section of the thesis. The fluorescence intensity is found to be proportional to the europium content as observed in the figure below[Figure 6.2].

The observed emission bands arise from transitions involving defect states. Rare earth doped zinc tellurite glasses do not show any major emission arising from the band states. The present glass samples are modified with zinc oxide as well as rare earth ions. Thus the emission character is found to be confined to the localized state transitions. The crystal field symmetry at the rare earth ion site is such that it allows certain level of broadening of emission spectra as observed.

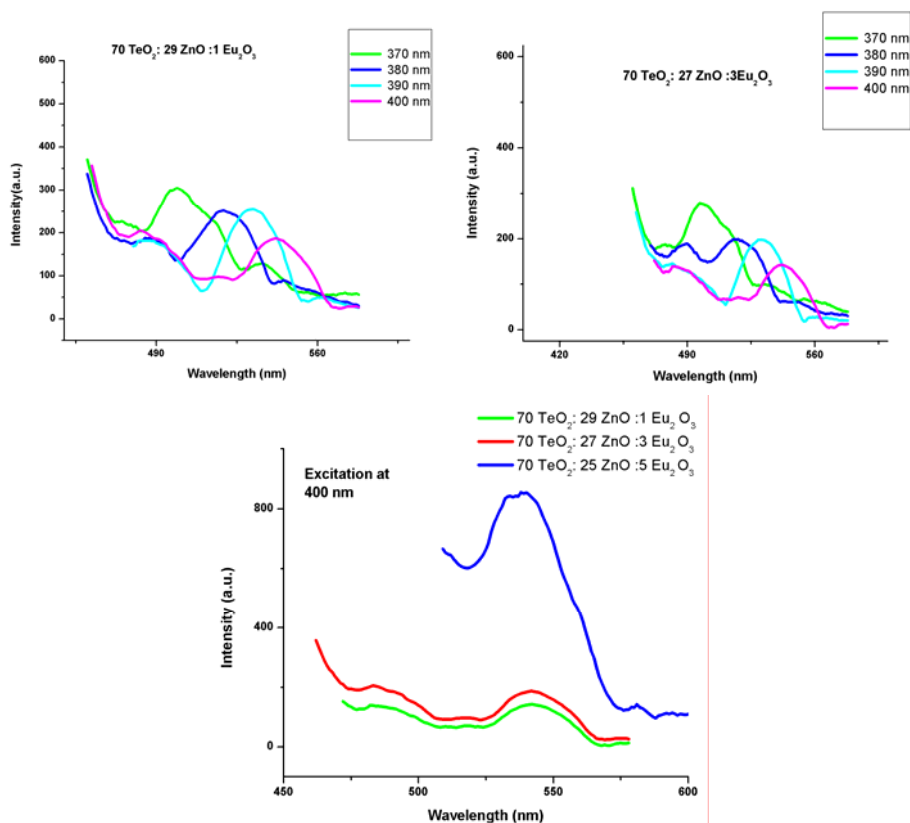


Figure 6.2: Fluorescence spectra recorded by varying europium concentration

6.3 Laser induced fluorescence spectroscopy of zinc tellurite glass

6.3.1 Introduction

Laser induced photoluminescence is spontaneous emission from atoms or molecules that have been excited by laser radiation. Two radiative transitions are involved in the Laser induced photoluminescence process. First, absorption takes place, followed by a photon-emission step. Laser induced photoluminescence has a large range of applications in spectroscopy. Laser induced photoluminescence is a dominant laser spectroscopic technique in the probing of unimolecular and bimolecular chemical reactions. This technique

serves as a sensitive monitor for the absorption of laser photons in fluorescence excitation spectroscopy. Emission studies using rare earths are of great importance with the arrival of Erbium doped tellurite glass amplifiers. The low phonon energy^[1-10] that the tellurite glass can supply towards the dopant ions value much in dealing with these emission performances.

6.3.2 Experiment

Laser induced fluorescence spectroscopy helps us to gain information on molecular states if the fluorescence spectrum excited by a laser on a selected absorption transition is dispersed by a monochromator. The pump beam is taken from a Quanta Ray Q-switched Nd: YAG laser which emits pulses of 7 ns duration at 532 nm and at a repetition rate of 10 Hz^[18]. The prepared bulk samples polished to 1.4 mm were used for the laser induced fluorescence measurement. A cylindrical lens is used to focus the pump beam in the shape of a stripe on the sample. In the present case it is adjusted to a pump beam width of 7 mm. The output is collected from the edge of the front surface of the bulk glass sample using an optical fiber in a direction normal to the pump beam. The emission spectra are recorded with Acton monochromator attached with a CCD camera. Princeton Instruments

NTE/CCD air cooled detectors have three distinct sections^[19]. The front vacuum enclosure contains the CCD array seated on a cold finger. This finger is in turn seated on a four-stage Peltier thermoelectric cooler. The back enclosure contains the heat exchanger. An internal fan cools the heat exchanger and the heat exits the unit through openings in the housing. The CCD array used is Roper Scientific NTE/CCD-1340/100-EM. The electronics enclosure contains the preamplifier and array driver board. This

keeps all signal leads to the preamplifier as short as possible, and also provides RF shielding. The SPEC-10 controller of Princeton Instruments controls the CCD. SpectraPro-500i is a 500 mm focal length monochromator/spectrograph. It features an astigmatism-corrected optical system, triple indexable gratings and triple grating turret. The SpectraPro-500i includes a direct digital grating scan mechanism with full wavelength scanning capabilities, plus built-in RS232 and IEEE488 computer interfaces. The 1200 grooves/mm grating has an aperture ratio f/6.5. The scan range is 0 to 1400 nm (mechanical range) and an operating range of 185 nm to the far IR and a resolution of 0.05 nm at 435.8 nm. WinSpec, the spectroscopic software, of Princeton Instruments^[20] is used for collecting, storing and processing data from the Roper Scientific system.

6.3.3 Results

6.3.3.1 Laser induced fluorescence spectroscopy of 80 TeO₂:15 ZnO: 5 Eu₂O₃ glass

Laser induced fluorescence spectroscopy of 80 TeO₂:15 ZnO: 5 Eu₂O₃ glass sample for five different powers are plotted below (Figure 6.3(a) and (b)). As the input power increases emission of the sample is also found to increase. We have analysed the fluorescence intensities by exciting the sample with 355 nm and 532 nm. It is found that for 355 nm excitation fluorescence intensity increases up to 16000 units. But for 532 nm, the fluorescence intensity is almost above 30000 units. Thus the fluorescence intensity is getting doubled in the second data.

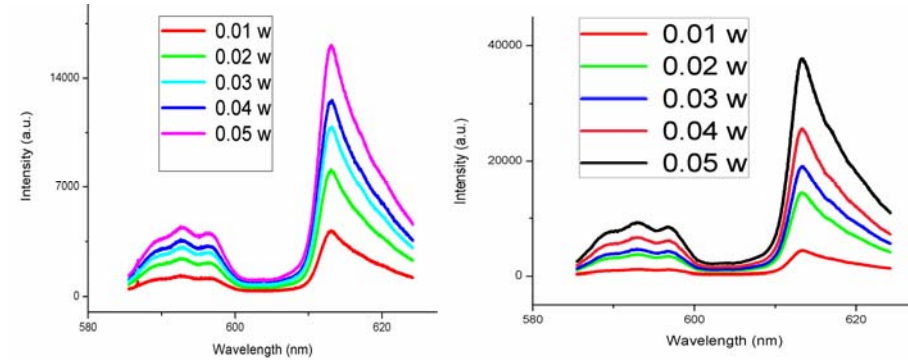


Figure 6.3 (a): Laser induced fluorescence of 80 TeO₂:15 ZnO: 5 Eu₂O₃ glass when excited with 355 nm

Figure 6.3(b): Laser induced fluorescence of 80 TeO₂:15 ZnO: 5 Eu₂O₃ glass when excited with 532 nm

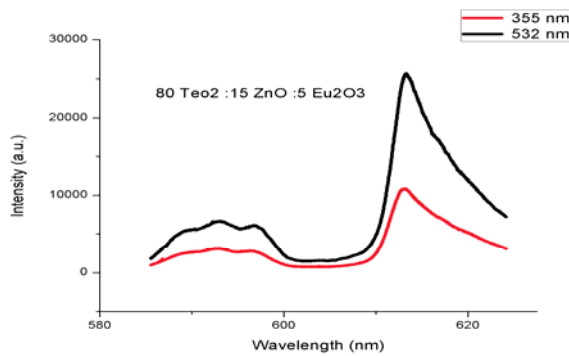


Figure 6.3(c): Laser induced fluorescence of 80 TeO₂:15 ZnO: 5 Eu₂O₃ glass: comparison of excitation wavelengths

A graph is also plotted to show this large increase in fluorescence intensity exhibited by 80 TeO₂:15 ZnO: 5 Eu₂O₃ glass sample, when excitation is changed from 355 nm to 532 nm (Figure 6.3(c)). A table (Table 6.1) listing out the fluorescence intensities of the sample, for 355 nm and 532 nm excitation is also shown below for comparison of the data.

Table 6.1: Laser induced fluorescence output of 80 TeO₂:15 ZnO: 5 Eu₂O₃ glass with laser power

Laser power (Watt)	Intensity when Excited with 355 nm(a.u.)	Intensity when Excited with 532 nm(a.u.)
0.01	4214	4405
0.02	8137	14215
0.03	10880	19156
0.04	12605	25596
0.05	16123	37748

6.3.3.2 Laser induced fluorescence spectroscopy of 75 TeO₂:20 ZnO: 5 Eu₂O₃ glass

The prepared bulk samples polished to 1.4 mm were used for the laser induced fluorescence measurement. The sample excited with second and third harmonics of Nd: YAG 1064 nm laser. The emission spectra obtained were proportional to the increase in laser power as shown below(Figure 6.4).

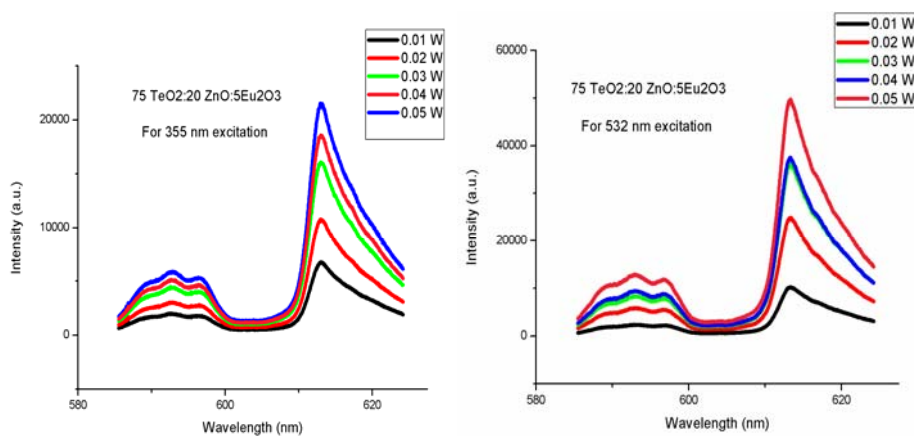


Figure 6.4: Laser induced fluorescence of 75 TeO₂:20 ZnO: 5 Eu₂O₃ glass with laser power

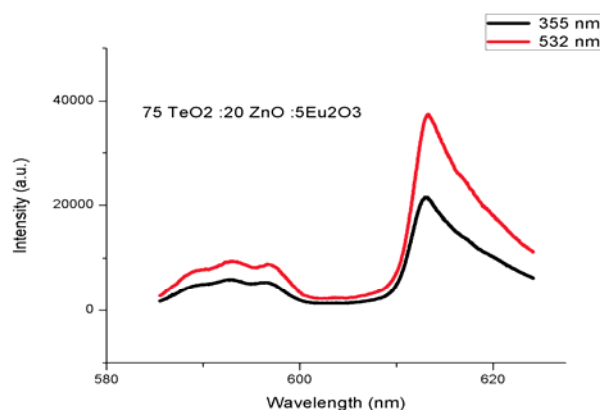


Figure 6.5: Laser induced fluorescence of 75 TeO₂:20 ZnO: 5 Eu₂O₃ glass: comparison of excitation wavelengths

On comparing the emission intensities, it is clear that the emission after exciting with 532 nm is very much increased than that when excited with 355 nm. The graphical representation of comparison of fluorescence intensities is shown in figure 6.5.

The table (Table 6.2) shown list out the fluorescence intensity values of 75 TeO₂:20 ZnO: 5 Eu₂O₃ glass, for both 355 nm and 532 nm excitations at various laser powers.

Table 6.2: Laser induced fluorescence output of 75 TeO₂:20 ZnO: 5 Eu₂O₃ glass with laser power

Laser power (Watt)	Intensity when Excited with 355 nm(a.u.)	Intensity when Excited with 532 nm(a.u.)
0.01	6761	10237
0.02	10779	24868
0.03	16098	36063
0.04	18580	37470
0.05	21501	49786

6.3.3.3 Laser induced fluorescence spectroscopy of 70 TeO₂:25 ZnO: 5 Eu₂O₃ glass

The study of laser induced fluorescence become more important, while dealing with a sample containing more ZnO content. The band gap is lowest for this sample comparing with the previous ones, due to the density of localized states present in them. The response to laser excitation is more prominent in the sample, compared to the previous ones. The obtained results with different laser powers are shown in the graphs figure 6.6 below. A graph is also plotted showing the intensity variation when the excitation wavelength is changed from 355 nm to 532 nm for 70 TeO₂:25 ZnO: 5 Eu₂O₃ glass sample.

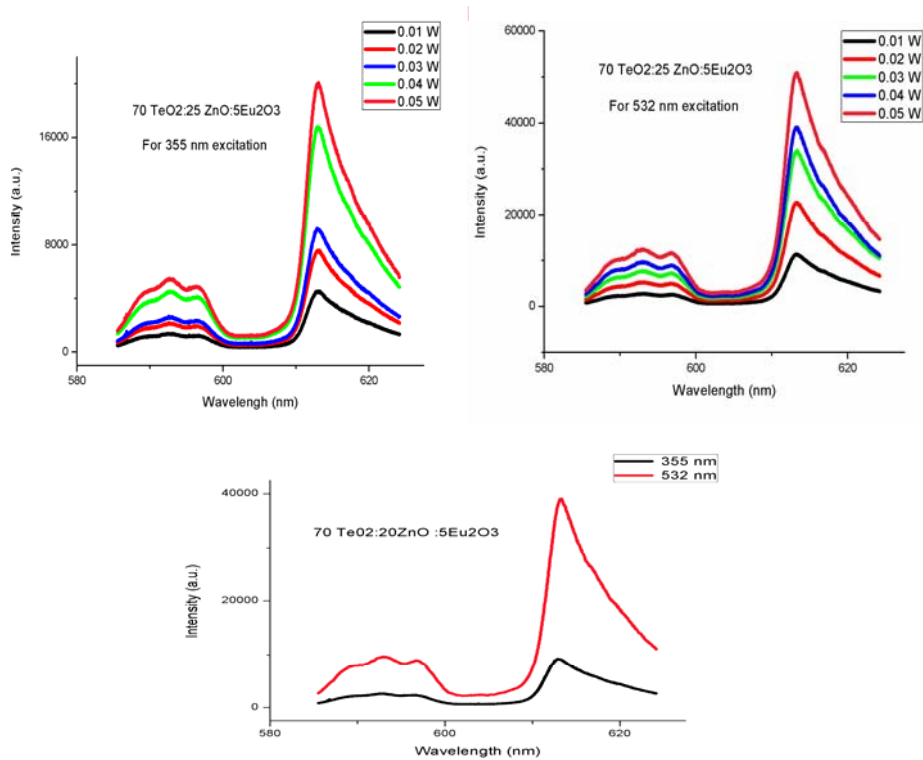


Figure 6.6: Laser induced fluorescence of 70 TeO₂:25 ZnO: 5 Eu₂O₃ glass with laser power

Table 6.3: Laser induced fluorescence output of 70 TeO₂:25 ZnO: 5 Eu₂O₃ glass with laser power

Laser power (Watt)	Intensity when Excited with 355 nm(a.u.)	Intensity when Excited with 532 nm(a.u.)
0.01	4542	11220
0.02	7574	22720
0.03	9239	33981
0.04	16813	39065
0.05	20068	50907

The table (Table 6.3) above shows fluorescence outputs of the sample for the two different wavelengths of excitation. Recollecting the corresponding outputs for the previous two samples, it is evident that the modification supported by zinc oxide also helps in creating a favourable crystal field environment for rare earth ions in tellurite glasses.

6.34 Discussion

The low phonon energy of tellurite glasses ($\sim 750 \text{ cm}^{-1}$)^[1-10], make them flexible to accommodate rare earth ions in their network. The absorption bands originating from the ground $7F_0$ level to higher energy level of europium ions, in zinc tellurite glasses are shown in the Figure 6.7 given below^[15, 16].

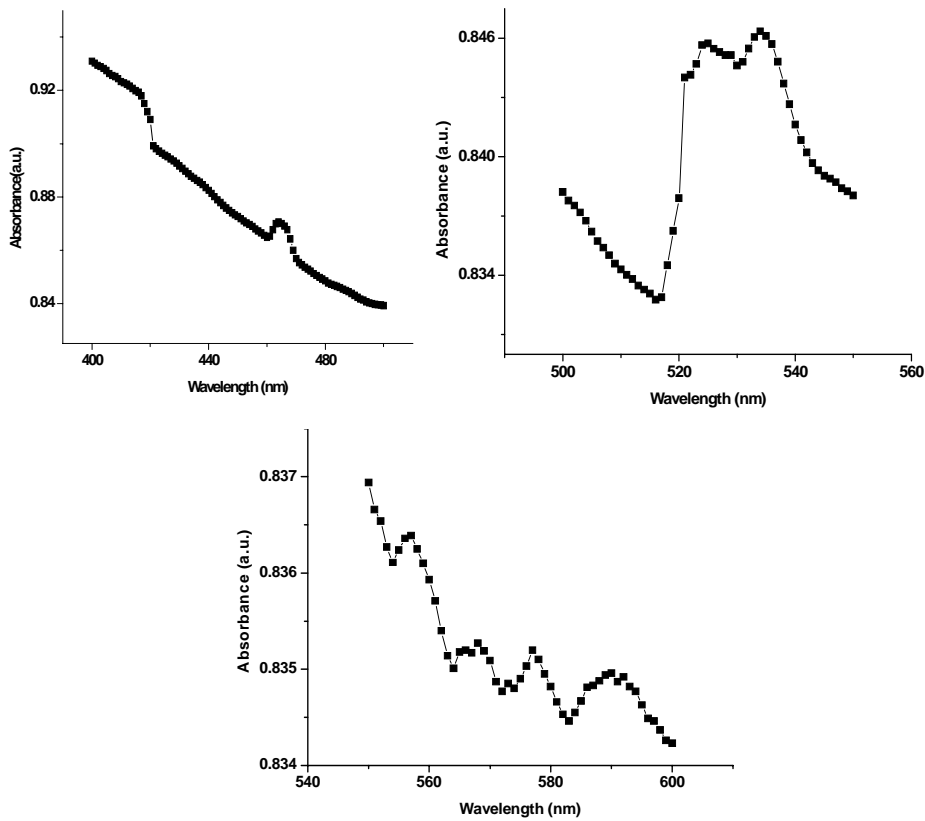


Figure 6.7: Absorbance of europium doped zinc tellurite glasses

It is reported that band gap of most of the binary tellurite glasses increases with increase in TeO_2 content and decreases with the amount of ZnO . The action of rare earth ions in tellurite glasses depends on its composition. Increase in band gap of rare earth doped tellurite glasses is attributed to the larger size of rare earth ions.

In 1992, Burger et al ^[11] reported that in zinc tellurite glasses band gap increases/decreases with TeO_2/ZnO contents and a major influence is with the tellurium content, which is due to the decrease in nonbridging oxygen

ions. The absorption edge of rare earth doped glasses becomes sharper in the UV region, due to the UV absorption of rare earth ions.

These sharp bands are caused by forbidden transitions involving the $4f$ levels, and these $4f$ orbits are very effectively shielded from interaction with external fields of the hosts by $5s^2$ and $5p^6$ shells. Hence, the states arising from the various $4f^n$ configurations are only slightly affected by the surrounding ions and remain practically invariant for a given ion in various compounds. The rare-earth ions in tellurite glasses occupy the center of a distorted cube, which is made of a four tetrahedral of phosphate, silicate, borate, and germanate glasses. Each tetrahedron contributes two oxygen atoms to the coordination of the rare-earth ions. The overall coordination number is 8, the most common coordination number of the rare-earth oxides^[1]. But a decrease in TeO_2 content and/or an increase in ZnO content helps rare earth doped zinc tellurite glasses to increase its nonbridging oxygen ions and increase its density, since the europium content is kept constant. This can be attributed to the formation of dangling bonds due to the rare earth ions along with ZnO added to the glass network.

Judd-Ofelt theory suggests that the radiative transition probability depends on the refractive index of the material^[15]. Therefore zinc tellurite glasses having large refractive index allows large radiative transition for all emission levels of Eu^{3+} .

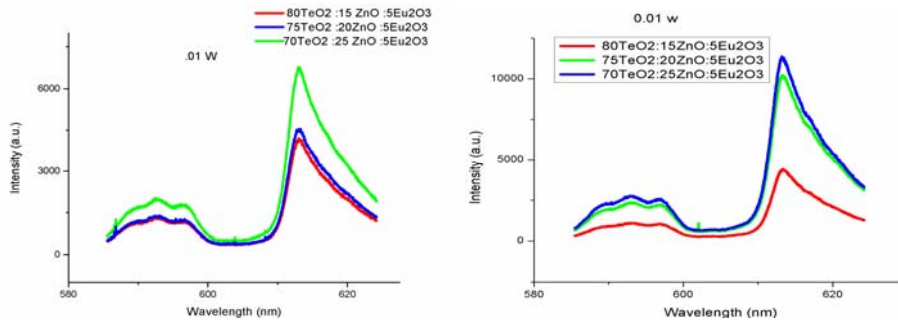


Figure 6.8: Laser induced fluorescence of tellurite glasses by varying ZnO (a) excited with 355 nm and (b) excited with 532 nm.

Our focus is on europium dioxide, which is capable of producing a laser induced red emission with tellurite glasses. We have studied laser induced fluorescence emission under two different excitation wavelengths namely, 355 nm and 532 nm (Figure 6.8). Variation of fluorescence intensity as a function of excitation intensity show different behavior in the case of both these excitation wavelengths. The intensity of emission in 532 excitation is much greater than that of 355 nm excitation. The energy level diagram of europium ions showing the transition corresponding to 615 nm emission is shown below (Figure 6.9).

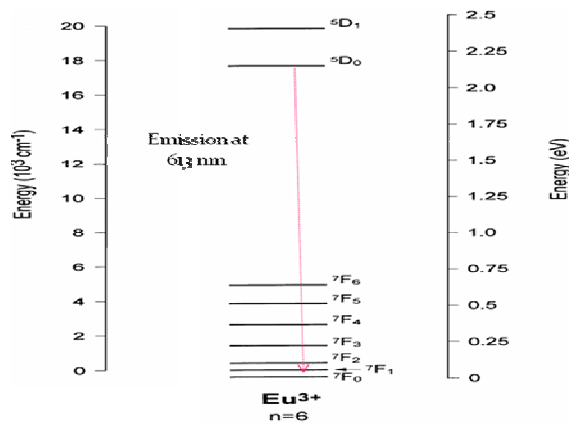


Figure 6.9: Emission bands of europium ion.

Both 355 nm and 532 nm excitations show the downconverted emission, but among them the 532 nm excited emission is found to be the efficient one at all compositions we have used for the study. The ground and first excited states of Eu³⁺ ions (⁷F₀, ⁷F₁ and ⁵D₀, ⁵D₁) allow red emission in tellurite glass. It is reported by Surendra et al, that ⁵D₀ → ⁷F₁ (595 nm) transition intensity is independent of host matrix and is magnetic – dipole allowed. ⁵D₀ → ⁷F₂ (613 nm) transition is electric dipole allowed and depends intensively on the local symmetry around the europium ions. The earlier works also show that the radial integral part of the f- orbital of europium ions is unaffected even with the variation of glass compositions. This is due to the strong shielding of the 4f shell by the 5s² and 5p⁶ orbitals.

In order to study the possibility of multiphoton processes, we have analyzed the log-log plot of fluorescence intensity as a function of input intensity, in the case of both laser excitations. In the case of 355 nm excitation the variation is linear as indicated by the slope of the graph (Figure 6.10).

Log-log plot of 532 nm excitation showing the signature of Two Photon Excitation along with One Photon excitation as evidenced by the slope 1.7 in the below graph. The plot showing a comparison of fluorescence emission (Figure 6.10) shows four times enhancement in the fluorescence emission of 532 nm excitation than that of 355 nm excitation. The study reveal that 532 nm excites both one photon induced fluorescence emission as well as two photon induced fluorescence emission. Thus the enhancement in the 532 nm excited fluorescence is more than the 355 nm excited fluorescence.

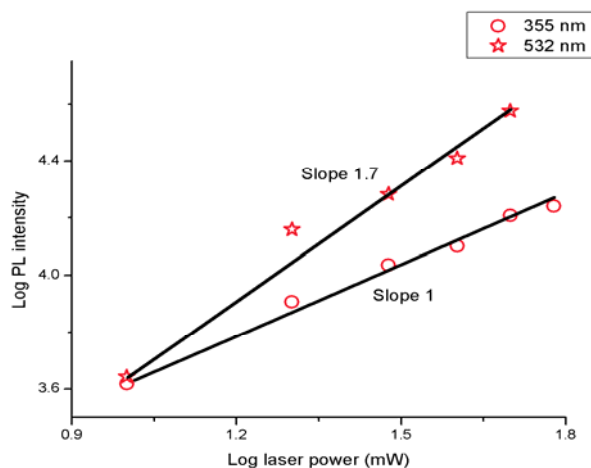


Figure 6.10: Log-log plot of photoluminescence intensity, for 355 nm and 532 nm excitation

Two Photon Absorption among the samples increases in order 80 TeO₂:15 ZnO: 5 Eu₂O₃<75 TeO₂:20 ZnO: 5 Eu₂O₃ <70 TeO₂:25 ZnO: 5 Eu₂O₃. This indicates that the band gap reduction helps in the enhancement of Two Photon Excited fluorescence spectra in zinc tellurite glasses. The above explanation points out that ⁵D₀ → ⁷F₂ (613 nm) transition is electric dipole allowed and depends intensively on the local symmetry around the europium ions. ZnO and rare earth ions produce dopant or defect sites in the tellurite glass matrix. The occurrence of other mechanisms like excited state absorption also can be assumed to be taking place in zinc tellurite glasses along with Two Photon Absorption, resulting in to such a good emission performance, when excited with 532 nm. Thus the obtained downconversion highly depend on the local symmetry of rare earth ions provided by zinc tellurite glass.

6.4 Concentration effect of europium on Laser induced fluorescence spectroscopy of zinc tellurite glasses

We have studied the fluorescence output of zinc tellurite glasses by varying europium oxide variation. The amount of variation is fixed from 0% -5%, by analyzing the literature. The results as shown in the graphs (figures 6.11(a),(b) and(c)) below shows that the fluorescence intensity is proportional to the europium oxide content.

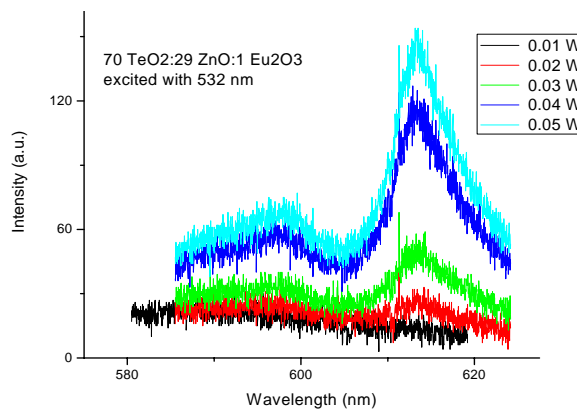


Figure 6.11(a): Laser induced fluorescence of 1% europium doped zinc tellurite glass

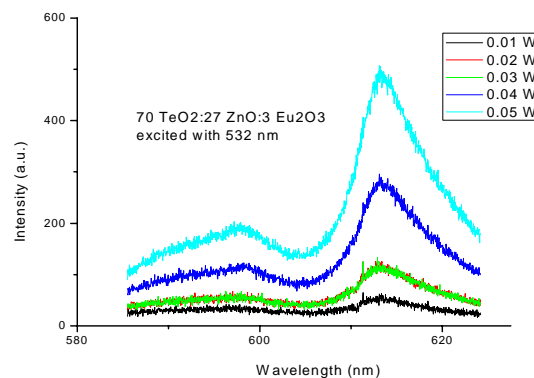


Figure 6.11(b): Laser induced fluorescence of 3% europium doped zinc tellurite glass

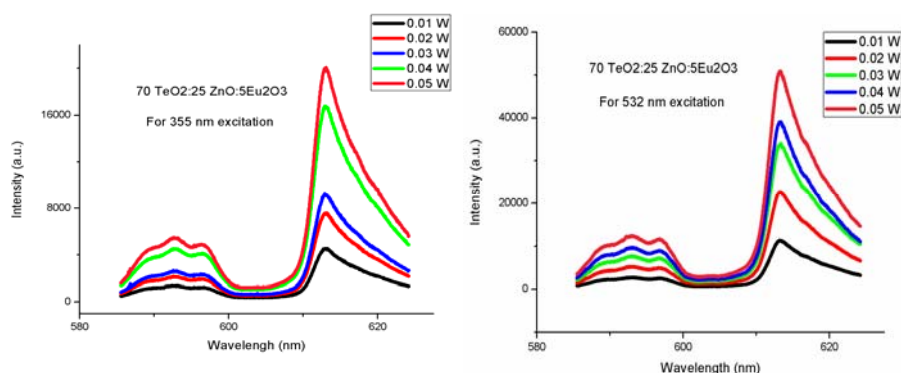


Figure 6.11(c): Laser induced fluorescence of 5% europium doped zinc tellurite glass

Table 6.4(a): Laser induced fluorescence output of zinc tellurite glass when excited with 355 nm: Concentration effect of europium

Laser power (Watt)	Intensity when Excited with 355 nm(a.u.)		
	70TeO ₂ :29ZnO:1Eu ₂ O ₃	70TeO ₂ :27ZnO:3Eu ₂ O ₃	70TeO ₂ :25ZnO:5Eu ₂ O ₃
0.01	14	18	4542
0.02	20	24	7574
0.03	19	22	9239
0.04	20	23	16813
0.05	20	26	20068

Table 6.4(b): Laser induced fluorescence output of zinc tellurite glass when excited with 532 nm: Concentration effect of europium

Laser power (Watt)	Intensity when Excited with 532 nm(a.u.)		
	70TeO ₂ :29ZnO:1Eu ₂ O ₃	70TeO ₂ :27ZnO:3Eu ₂ O ₃	70TeO ₂ :25ZnO:5Eu ₂ O ₃
0.01	22	63	11220
0.02	25	124	22720
0.03	59	133	33981
0.04	124	296	39065
0.05	153	495	50907

The output of 355 nm excitation doesn't show much output in samples having lower concentrations of europium oxide. The data makes it clear that 532 nm is the efficient excitation wavelength for lower concentrations. The intensity increase is tremendous as we move from 3% to 5% of europium content for both the wavelengths of excitations. Comparison of output intensities shows that Two Photon induced fluorescence is the basic mechanism involved behind the fluorescence output of the samples. This is the reason for such a good downconverted emission taking place in europium doped zinc tellurite glasses. The output intensities shown in the tables above (tables 6.4 (a) and (b)) give a detailed variation with laser power, giving a clear picture of the Two Photon induced fluorescence in europium doped zinc tellurite glass samples.

6.5 Summary and Conclusions

This chapter deals with the study of laser induced fluorescence emission under two different excitation wavelengths namely, 355 nm and 532 nm, in zinc tellurite glasses. The europium doped zinc tellurite glasses show a down converted emission in the red region. The intensity of emission in 532 excitation is much greater than that of 355 nm excitation. The ground and first excited states of Eu^{3+} ions (${}^7\text{F}_0$, ${}^7\text{F}_1$ and ${}^5\text{D}_0$, ${}^5\text{D}_1$) allow red emission in tellurite glass. ${}^5\text{D}_0 \rightarrow {}^7\text{F}_2$ (615 nm) transition is electric dipole allowed and depends intensively on the local symmetry around the europium ions. On comparing the emission intensities for both 355 nm and 532 nm excitations, it is evident that there is a signature of two photon excitation along with one photon excitation in laser induced fluorescence of europium doped zinc tellurite glasses. Europium doped tellurite glasses exhibiting visible fluorescence find applications as storage phosphors for imaging.

References

- [1] Raouf H. El-Mallawany, “*Tellurite glasses Hand book-Physical properties and data*”, CRC press LLC, (2002).
- [2] Sidebottom DL, Hruschka MA, Potter BG, Brow RK, “*Structure and Optical Properties of Rare Earth-Doped Zinc Oxyhalide Tellurite Glasses*”, J Non-Cryst Solids 222,282(1997).
- [3] Sun K, “*In: Preparation and characterization of rare earth glasses*”, Thesis, Brown University (1988).
- [4] B Erariah, “*Optical properties of Lead-tellurite glasses doped with samarium trioxide*”, Bull. Mater Sci 33, 391–394(2010).
- [5] R. El-Mallawany, M. Dirar Abdalla, I. Abbas Ahmed, “*New tellurite glass: Optical properties*”, Mater. Chem. and Phys. 109, 291–296(2008).
- [6] H. Lin, S.Tanabe, L. Lin, D.L. Yang, K. Liu, W.H. Wong, J.Y. Yu, E.Y.B. Pun, “*Infrequent blue and green emission transitions from Eu³⁺ in heavy metal tellurite glasses with low phonon energy*”, Phys. Lett. A, 358, 5-6, 474-477, (2006).
- [7] Akshay Kumar, D.K. Rai and S.B. Rai, “*Optical properties of Er³⁺ doped oxyfluoroborate glass*”, Spectrochim. Acta A 58, 3067 (2002).
- [8] W.A. Pisarski, J. Pisarska, G. Dominiak-Dzik, M. Maczka, W. Ryba-Romanowski, “*Compositional - dependent lead borate based glasses doped with Eu³⁺ ions: Synthesis and spectroscopic properties*”, J. of Physics and Chem. of Solids 67, 2452-2457 (2006).
- [9] W.A. Pisarski, J. Pisarska, M. Maczka, W. Ryba-Romanowski “*Europium-doped lead fluoroborate glasses: structural, thermal and optical investigations*”, J. of Mol. Struct., 792, 207-211(2006).
- [10] A.A. Sidek, S. Rosmawati, Z.A. Talib, M.K. Halimah and W.M. Daud, “*Synthesis and Optical Properties of ZnO-TeO₂ Glass System*”, Am. J. Applied Sci. 6 (8), 1489-1494(2009).
- [11] Burger H, Kneipp K, Hobert H, VogelW, “*Glass formation, properties and structure of glasses in the TeO₂-ZnO system*”, J Non-Cryst Solids 151,134-142, (1992).
- [12] D. L. Sidebottom, M. A. Hruschka, B. G. Potter, and R. K. Brow, “*Increased Radiative Lifetime of Rare Earth-Doped Zinc Oxyhalide Tellurite Glasses*”, Appl. Phys. Lett. 71[14] 1963-65 (1997).
- [13] F. Vetrone, J. C. Boyer, J. A. Capobianco, A. Speghini and M. Bettinelli, “*980 nm Upconversion in an Er - doped ZnO-TeO₂ Glass*”, Appl. Phys. Lett., 80; 1752-1754 (2002).

- [14] J. C. Boyer, F. Vetrone, J. A. Capobianco, A. Speghini and M. Bettinelli, “*Optical Transitions and Upconversion Properties of a Ho³⁺ Doped ZnO-TeO₂ Glass*”, J. Appl. Phys., 93; 9460-9465 (2003).
- [15] S Surendra Babu, Kiwan Jang, Eun Jin Cho, Hoseop Lee, C K Jayasankar, “*Thermal, structural and optical properties of Eu³⁺-doped zinc-tellurite glasses*”, J. Phys. D: Appl. Phys. 40, 5767–5774(2007).
- [16] Raffaella Rolli, Karl Gatterer, Mario Wachtler, Marco Bettinelli, Adolfo Speghini, David Ajo, “*Optical spectroscopy of lanthanide ions in ZnO–TeO₂ glasses*”, Spectrochim. Acta A, 57, 2009–2017(2001).
- [17] Rose Leena Thomas, Vasuja, Misha Hari V P N Nampoori P Radhakrishnan Sheenu Thomas, “*Optical non-linearity in ZnO doped TeO₂ glasses*”, JOAM, 13, 5, 523.
- [18] Quanta-Ray, Pulsed Nd: YAG lasers User’s manual GCR-100 series, Spectra-Physics, USA (1997).
- [19] Princeton Instruments NTE/CCD, Manual, Roper Scientific, Inc. USA, (2001).
- [20] WinSpec, “*spectroscopic software of Princeton Instruments*”, Roper Scientific, USA (2001).



CONCLUSIONS AND FUTURE PROSPECTS

This chapter concludes the major findings of the thesis along with the outline of the future works that can be done based on the results obtained.

Tellurite glasses are photonic materials of special interest to the branch of optoelectronic and communication, due to its important optical properties such as high refractive index, broad IR transmittance, low phonon energy etc. Tellurite glasses are solutions to the search of potential candidates for nonlinear optical devices. Low phonon energy makes it an efficient host for dopant ions like rare earths, allowing a better environment for radiative transitions. The dopant ions maintain majority of their individual properties in the glass matrix. Tellurites are less toxic than chalcogenides which is another class of nonlinear amorphous solids, chemically and thermally stable which makes them a highly suitable fiber material for nonlinear applications in the mid-infrared and they are of increased research interest in applications like laser, amplifier, sensor etc. Low melting point and glass transition temperature helps tellurite glass preparation easier than other glass families.

In order to probe into the versatility of tellurite glasses in optoelectronic industry; we have synthesized and undertaken various optical studies on tellurite glasses in the present thesis. Tellurium dioxide (TeO_2) is the most stable oxide of tellurium (Te). Tellurites differ from silicates in that their structure is not tetrahedral but a distorted octahedron/trigonal

bipiramid. The basic unit of a tellurium oxide is a trigonal bipyramidal structure. There exist band states and tail states where the band states correspond to the bonding states in the valence band / the antibonding states in the conduction band and the tail states correspond to the defects such as dangling bonds. The addition of modifier oxides generally creates nonbridging oxygens (NBOs) which are bonded ionically to the modifier ions. Breaking up the covalent network structure (depolymerization) creates mobile ion species in the material and tellurite structural units of the form TeO_3 / TeO_{3+1} are created. The role of modifier atoms in tuning the optical properties of Zinc tellurite glasses whereby making them potential candidates for photonic device applications are taken up in this thesis,

- ❖ In the present work melt quench method were used to prepare zinc tellurite glasses of compositions 80 TeO_2 :20 ZnO , 75 TeO_2 :25 ZnO and 70 TeO_2 :30 ZnO . Structural study using XRD reveals that the prepared material is amorphous in nature due to the absence of crystallization peaks. FTIR also contains information regarding the structural units TeO_4 and TeO_3 in the zinc tellurite glass network .DSC were used for thermal analysis of tellurite glasses and it is observed that the Glass transition increases with ZnO content.
- ❖ The absorption, transmission and reflectance measurements using UV/VIS/NIR Spectrophotometer reveal that the modifiers incorporated in the TeO_2 network create NBO ions affecting the band gap due to the creation of dangling bonds. Band gap decreases with increase in ZnO content whereby increasing the refractive index.

- ❖ Optical fluorescence studies of glasses carried out using Cary Eclipse Fluorescence spectrophotometer shows a blue fluorescence emission, where the intensity was found to be proportional to the tellurium content.
- ❖ Non linear optical properties of zinc tellurite glasses determined using z scan technique reveal reverse saturable absorption which makes it useful for optical limiting applications. Non linear absorption is found to increase with ZnO content. The observed nonlinear absorption has been explained through two photon absorption (TPA). The band gap red shift with increase in ZnO content is found to enhance two photon absorption. Two photon absorption coefficients are also found to be fluence dependent. From the closed aperture Z scan technique, which is sensitive to both nonlinear absorption and refraction, it is observed that these glasses exhibit positive nonlinear refraction.
- ❖ Thermal poling was done to tune the linear and non linear optical properties of zinc tellurite glasses. Since second-order nonlinear (SON) optical properties are forbidden in glasses which exhibit inversion symmetry on a macroscopic scale, it is possible to induce a second-order nonlinear susceptibility in bulk glass using specific treatment like optically assisted poling or thermal poling. The purpose of thermal poling in this work was to investigate its effect on the optical properties of zinc tellurite glass samples. Heating increases the mobility of the ions present in the glass and very large electric field causes orientation of tellurite structural units with nonbridging oxygen atoms that possess permanent electric dipoles. Dipoles are formed

in the medium due to induced polarization of the dopant .During the thermal poling process, an increase in the quantity of dipoles per volume occurs which can be aligned in the direction of electrical field. Network structure increases the defect states giving rise to a decrease in the band gap which is observed from the band gap measurements that we have undertaken. Electrochemical reaction under the large dc field may convert the tellurite glass structural from the TeO_4 to the deformed TeO_3 .Structural rearrangement reduces the molar volume and thereby increases the density of the zinc tellurite glass network.

- ❖ Non linear optical properties of zinc tellurite glasses exhibits reverse saturable absorption after thermal poling. Two photon absorption is found to increase with ZnO content and an enhancement of two photon absorption is also observed after thermal poling. Hence the band gap red shift enhances two photon absorption. The interesting results are that thermal poling leads to the tuning of optical properties such as band gap, refractive index and enhancement of Two Photon Absorption in the glass.
- ❖ The influence of lanthanide ions in the zinc tellurite glass matrix has been undertaken. We have incorporated oxides of lanthanum, samarium, europium and holmium in the study because of their capability in modifying the linear and nonlinear optical properties in the tellurite vitreous network. All of the lanthanide ions doped in the zinc tellurite glasses, exhibit their characteristic absorption bands in the absorption spectra. Study reveal that Lanthanides increases the conversion of structural units.FTIR spectra recorded indicates the formation of new

structural units. DSC analysis shows an increase in Glass transition with Lanthanides.

- ❖ Switching of optical nonlinearities from Reverse Saturable Absorption to Saturable Absorption is observed in zinc tellurite glasses without and with rare earth content respectively. Saturation absorption is due to the accumulation of molecules in the singlet excited state leading to depletion of the ground state and the intensity at the focus is highly reduced thereby exhibiting high transmittance. Change from RSA to SA shows that the presence of europium ion changes the nonlinear component of refractive index negative. At higher concentrations there is a possibility of aggregation thereby modifying the lifetimes of the excited states influencing the nonlinear absorption behavior. Our studies reveal that the Two Photon Absorption gets enhanced in the rare earth doped zinc tellurite glasses in the decreasing order of atomic number.
- ❖ Laser induced fluorescence spectroscopy of europium doped zinc tellurite glasses has also been undertaken using the pump beam taken from a Quanta Ray Q-switched Nd: YAG laser which emits pulses of 7 ns duration at 532 nm and 355 nm, at a repetition rate of 10 Hz. The low phonon energy based emission spectroscopy is an important field in various applications like optical amplifiers, phosphors, fibers, lasers etc. Europium oxide is found to be efficient in fluorescing in the visible wavelength with laser excitation. The europium doped zinc tellurite glasses show a down converted emission in the red region. The intensity of emission in 532 nm excitation is much greater than that of 355 nm excitation. On comparing the emission intensities for

both 355 nm and 532 nm excitations, it is evident that there is a signature of two photon excitation along with one photon excitation in the laser induced fluorescence of europium doped zinc tellurite glasses.

Future prospects

- ❖ Preparation and characterization of mixed chalcogenide - tellurite glass for non-linear applications.
- ❖ Preparation and characterization of tellurite glass based nano composite by solution casting for photonic applications.
- ❖ Non linear optical studies of tellurite glass based nano composite for photonic applications.
- ❖ Preparation of sol gel based tellurite glasses.
- ❖ Non linear optical studies of sol gel based tellurite glasses for photonic applications.
- ❖ Second harmonic generation from thermally poled zinc tellurite glasses.
- ❖ Preparation of tellurite glass based waveguides for optoelectronic applications
- ❖ Preparation of tellurite glass based fibers for optoelectronic communication.



Curriculum Vitae

Rose Leena Thomas

Kathanakute house
Kanankkary P.O
Kottayam
Kerala - 686632
roseleenat@cusat.ac.in
roseleenat@gmail.com



Rose Leena Thomas was born on 25th September 1982 at Mavida, Kerala, India, completed her schooling in 1998 at St. Mary's Girls' High School Pala. She entered St. George's College Aruvithura, affiliated to Mahatma Gandhi University and took her Masters degree in Physics in 2003. She completed her Bachelors degree in Education from St. Joseph's Training College, Mannanam affiliated to Mahatma Gandhi University in 2005 and Qualified SET 2006. For a couple of years, she served as a teacher in St.Thomas Higher Secondary School, Kumily and St. Antony's Higher Secondary School, Anakkal, Kanjirappilly. She joined at the International School of Photonics as a full time research scholar under UGC-RFSMS scheme on 24th June 2009 under the supervision of Dr. Sheenu Thomas. She is herewith submitting her thesis entitled "Synthesis and characterization of Tellurium oxide glasses for photonic applications" in March 2013.

